2014

Effect of Forced Flow Oscillation on Churn and Annular Flow in Vertical Wellbores

Catalina Posada
Louisiana State University and Agricultural and Mechanical College

EFFECT OF FORCED FLOW OSCILLATION ON CHURN AND ANNULAR FLOW IN VERTICAL WELLBORES

A Thesis

Submitted to the Graduate Faculty of the
Louisiana State University and
Agricultural and Mechanical College
in partial fulfillment of the
requirements for the degree of
Master of Science

in

The Department of Petroleum Engineering

by
Catalina Posada
B.S., University of Los Andes, Colombia, 2010
December 2014

ACKNOWLEDGEMENTS

I would like to express my sincere gratitude to my advisor Dr. Paulo Waltrich for believing in me and giving me the opportunity to conduct this research. His continued support and guidance have been essential to my success in this project.

I am grateful to my committee members, Dr. Mayank Tyagi, and Dr. Richard Hughes for their support throughout my entire graduate studies. Numerous times I have sought their advice and guidance on matters involving this project and classwork.

I would also like to extend my gratitude to the Louisiana State University and the faculty in the Craft and Hawkins Department of Petroleum Engineering in particular for giving me the opportunity to continue my academic career and attain this degree.

Thanks to all my friends that have spent the past years with me. You have always been the best guides for a memorable student life in Baton Rouge.

My profound gratitude goes to my family for believing in me and supporting every decision that I have made. Thanks for all the advice and love you give me. None of my accomplishments would be possible without them.

I would like to thank God for bringing me to this school and giving me the opportunity to have this life changing experience over the last two and a half years.

I would like to express my special gratitude to John Whitehead who since the first day has made part of this incredible experience. Your personal care in every aspect of my life and support has given me the strength and perseverance to pursue this challenge. I wish you all the success in life.

TABLE OF CONTENTS

LIST OF TABLES

LIST OF FIGURES

LIST OF NOMENCLATURE

$\overline{\delta_u}$ - Average upper structure layer thickness [mm, in]

δ_k - Instantaneous film thickness [mm, in]

$\overline{\delta}$ – Average film thickness [mm, in]

fw - wave frequency [Hz]

U_{ls} - superficial liquid velocity [m/s, ft/s]

U_{gs}- superficial gas velocity [m/s, ft/s]

U_m - mixture velocity [m/s, ft/h]

D - pipe diameter [m, in]

St_l - liquid Strouhal number

St_g – gas Strouhal number

X - Lockharte-Martinelli number

ρ_l – density of the liquid [kg/m^3, lbm/ ft^3]

ρ_g,- density of the gas [kg/m^3, lbm/ ft^3]

ρ_m - mixture density [kg/m^3, lbm/ft^3]

Fr_g Froude numbers

E_o – Eötvös number

Re – Reynolds number

σ – surface tension [N/m, dyn/cm]

μ_l – liquid viscosity [cP]

g – acceleration of gravity [m/s^2, ft/s^2]

θ – angle of well deviation [degree °]

f - two-phase friction factor

p – pressure [Pa, psi]

z – elevation [m, ft]

ABSTRACT

Producing oil and gas from marginal hydrocarbon reservoirs and mature fields present particular challenges. One of the challenges for these types of fields is flow instability. Pipeline risers and artificial gas-lift systems experience instabilities, which cause significant reductions in production among others operational drawbacks. Different types of instabilities (static and dynamic) have been identified affecting those systems. However, there is still a lack of systematic investigations associated with the understanding of dynamic instabilities (periodic oscillations) and their impact in production systems.

A systematic investigation of the effects of periodic forced oscillations on gas-liquid flows in a 42 m (140-ft) long, 0.04859 m (2-in) ID vertical pipe system has been carried out in the present study. The main objective of this investigation is to characterize the effect of oscillations on two-phase flow in vertical pipes to better understand this phenomenon. The time variation of liquid holdup, pressure drop and pressure gradient were analyzed under two superficial liquid velocities (U_{ls}= 0.017 and 0.3 m/s), and three superficial gas velocities ranges of oscillation (U_{gs}=3-9, 9.5-14, and 8.5-21.5 m/s), as well as the impact in the flow regimes.

For the range of conditions tested, it is possible to conclude that the axial variation of liquid holdup is directly affected by the periodic forced oscillations of the inlet gas flow rate, depending on the superficial liquid velocity.

Additionally, experimental data under oscillatory and steady-state conditions were compared for similar superficial liquid and gas velocities. From the experimental results was observed that the pressure gradient was lower for oscillatory conditions than for steady-state conditions, for superficial gas velocity in between 4.0 and 9.0 m/s and superficial liquid velocity

of 0.017 m/s. This behavior was correlated to the influence of the forced oscillated gas flow rate on the liquid holdup under those conditions.

The experimental results of liquid holdup and pressure gradient were also compared with different two-phase flow models to evaluate its performance under steady-state and oscillatory conditions. Beggs and Brill (1973) was found to be the best fit for the steady-state conditions tested. Among all models tested, the empirical correlation developed in this work (which was obtained from the steady-state data) showed the best agreement for the oscillatory experiments.

CHAPTER 1: INTRODUCTION

1.1 Instabilities in the Oil and Gas Industry

In the oil and gas industry, the access to conventional reservoirs is increasingly becoming more difficult over the past decades. New alternatives such as reservoirs in remote areas, known as marginal reservoirs are now the focus of many companies (Abili, Kara, and Ohanyere 2014). The geographical location of marginal hydrocarbon reserves makes their production and operation exceedingly difficult. Another type of field with similar challenges are mature fields. The oil industry is increasingly producing from mature reservoirs located all around the world (Thais McComb 2013). The challenge faced by engineers in marginal and mature fields is to maximize the hydrocarbon recovery over the field life and maintain economically viability. Therefore, optimal production is the ultimate goal.

Marginal and mature fields experience many difficulties. As an example, mature reservoirs are close to reaching their economic limits. Further, the facilities and technology are old, which increasingly complicate the engineer's job. In marginal reservoirs, it is necessary to implement advanced solutions because conventional practices do not make them profitable. However, when the investment decisions have been made and the installation of new technology completed, these reservoirs still exhibit unstable production. Unstable production in multiphase systems has been identified as an undesired phenomenon because wells that are unstable are difficult to operate efficiently (Hu 2005, Lozada et al. 2011). There are different causes of instabilities in production systems. Ideally, engineers should be able to recognize them prior to implementing remediation techniques.

Ideally, the flow rates of oil, gas and water coming from the reservoir the reservoir can be considered constant. However, in practice it is easy to show that the fluid flow in the reservoirs will always experience some level of oscillation while flowing:

- Most reservoirs (if not all) will have some variation on its physical properties. For instance, changes in porosity, permeability and fluid viscosity in all three coordinates can be found in most reservoirs. Hence, some levels of oscillations are expected to be always present on the flow rate of oil, gas and water coming from the reservoir.
- Even if we assume steady fluid flow coming from the reservoir in the bottom of the well, multiphase flow in wellbores are never completely steady flows. Multiphase flow in pipes always presents some level of pressure oscillations, even if the flow rates of gas and liquid are kept constant at the pipe inlet. Since the flow coming from the reservoir is directly proportional to the bottomhole pressure, the flow rates of oil, gas and water will consequently oscillate.

Unstable flow phenomena in vertical pipes are commonly found in completions of deepwater and mature fields. In offshore wells, severe slugging typically occurs in multiphase flow on riser systems and it is characterized by oscillations in pressure, flow rate and liquid holdup. Most of these riser systems are characterized by a horizontal or inclined flowline portion connected to a vertical pipe (riser). Severe slugging is less likely to occur if fluids are flowing through horizontal/inclined or vertical pipe only.

Slugging occurs when large amounts of liquid accumulate in certain regions of the subsea riser, especially when the riser is inclined. When the pressure behind the liquid column has increased enough, the liquid slug will move upwards at a high momentum followed by a substantial amount of gas. To mitigate this problem, different techniques have been

implemented. These techniques include passive or active choking at the top of the riser and artificial gas lift systems (Seim et al. 2011). Gas lift has also been widely used in mature wells suffering from this slugging phenomenon occurring in the production tubing when the reservoir pressure has declined significantly.

Due to the applicability of gas lift systems in the industry, recent investigations have focused their attention in the instabilities of such systems, while identifying two types of instabilities:

i. *Local Instabilities (microscopic)* – occur locally at the liquid gas interface (Kakac 2009) (e.g. Kelvin-Helmoltz instabilities (Brennen 2005))
ii. *Systematic Instabilities (macroscopic)* – affect the complete two-phase system and are classified in two sub-categories (Kakac 2009):
    a) Static instability- the system experiences a static instability when the flow conditions are modified by small step from the initial steady-state conditions and it is not possible to go back to the original state (Xu and Golan 1989). An example of this type of instability is casing heading, which has been widely studied (Eikrem et al. 2008, Torre et al. 1987, Fairuzov et al. 2004, Hu 2005).
    b) Dynamic instability- the system experiences dynamic instabilities when the inertia and other effect give feed back to the fluctuations generating periodic oscillations in the flow around the initial state (Yüncü and Kakaç 1988). For instance, density wave oscillation, which has been study to a lesser extent (Hu 2005, Jahanshahi et al. 2008)).

In Alhanati's et al. (1993) investigation, it was pointed out that this density wave (or dynamic instability) was present in some of the wells and the only source that could explain them was associated "to vertical two-phase flow in pipes under certain conditions." This phenomenon

captured the attention of these investigators and reaffirmed that the analysis and design of two-phase flow systems needs a complete understanding of this physical phenomenon.

Some terms and definitions related to two-phase flow instabilities in pipes are introduced at the beginning of this investigation to avoid any misinterpretation related to the terminology used along the study. Some of the terms may not have the same meaning that other investigators have use in previous studies.

Steady flow: is one in which the system parameters are function of the space variables only. A stable flow is present in two-phase flow systems when new operating conditions tend toward the original conditions asymptotically after suffered certain type of perturbation (Yüncü and Kakaç 1988).

Flow instabilities: are created when perturbations in the flow happen. These fluctuations take their energy from the mean flow (flow pattern transition) or externally supplied by the boundaries of the system such as changes in inlet pressure, inlet mass flow rate, inlet enthalpy or power input. The fluctuations can disturb the flow at small scale and the flow can be considered stable. However, if the fluctuations generate large scale disturbance the flow become unstable (Yüncü and Kakaç 1988).

Density wave oscillations: are part of the dynamic instabilities. The difference in density between the fluid entering and the fluid exiting or being injected (low density two-phase mixture) triggers delays in the transient distribution of pressure drops along the tube, which may induce self-sustained oscillations. When density wave oscillations are being experienced, fluid waves of alternative higher and lower density mixtures travel through the system (Papini et al. 2011, Hu 2005).

Steady state forced oscillation: the flow oscillations are called forced if the flow is subjected to an external periodic influence whose effect on the system can be expressed by a separate term, a periodic function of the time, in the differential equation of motion. During some time after the external force has been activated, the transient natural oscillations inevitably damp out. Since only these oscillations depend on the initial conditions, it is possible to say figuratively that the oscillator eventually "forgets" its initial state, and its forced oscillations become steady.

1.2 Motivation

The increasing energy demand has made the oil and gas industry look for alternatives that can increase production. Many times, these alternatives have commonly been associated with marginal and unconventional reservoirs, but occasionally to mature reservoirs. As previously mentioned, producing oil and gas from deepwater and offshore fields have being the interest among many oil companies. However, to make production of such fields economical, mitigation of instabilities caused by either multiphase flow phenomenon or induced by the technology implemented to produce from these wells can play an important role on completions design, flow assurance problems and production forecast.

Some numerical studies have been carried out on flow instabilities in vertical pipes (Hu 2005, Jahanshahi et al. 2008). However, an experimental investigation of dynamic instabilities was not found in the open literature. Due to this lack of information on dynamic instabilities, this research aims to experimentally characterize instabilities in two-phase flow in vertical pipes.

1.3 Objectives

Gas-liquid two-phase flow in pipes has been extensively studied under steady-state conditions. However, the behavior of two-phase in pipe is always transient in nature. When the pipe inlet conditions are kept steady, these natural flow oscillations are periodic and steady, and the flow is assumed to be in steady-state. Depending on the inlet conditions, these natural oscillations can be larger or smaller. Pipe inclination can also significantly alter the amplitude and frequency of these natural oscillations. Therefore, when pipe segments with completely different inclinations are connected to each other, forced flow oscillations are introduced in the flow downstream from the point of severe inclination change. For instance, in deepwater riser systems, horizontal or near horizontal flowlines are connected to vertical pipe risers. The natural flow oscillations from two-phase of near-horizontal pipes are significantly different for horizontal and vertical pipe under the same flowing conditions. Hence, unnatural (or forced) oscillations are introduced in the base of the riser, originated from the natural flow oscillations of the horizontal flowline portion. The introduction of flow instabilities or oscillations is not created only by variation in pipe inclination, but also by the addition of other types of completion equipment, such as gas lift valves or downhole pumps. These types of equipment generate considerable oscillations to the flow, which consequently create significant instabilities to the two-phase flow in the wellbore.

Based on the presence of forced instabilities and oscillations on two-phase flow in pipes, the primary objective of this study is to analyze and characterize the effects of forced oscillations on two-phase flow in vertical pipes. This study will investigate the effect of forced oscillations of gas flow rate on the time variations of flow regimes, pressure gradient and liquid holdup. All the

experimental data used to achieve this goal was obtained by a previous investigation carried out by Waltrich (2012).

In order to accomplish the primary goal of the present work, the following secondary objectives were defined:

1. To analyze the behavior of pressure gradient, flow regimes, and liquid holdup while under forced oscillations of the inlet gas flow rate.
2. To carry out a comparison between steady-state and oscillatory experimental data.
3. To compare and verify the performance of two-phase flow correlations with steady-state and oscillatory data. Different multiphase flow correlations have been developed to predict two-phase flow in pipes under steady-state and transient conditions. Therefore, the evaluation of these models with respect to steady-state and oscillatory data is carried out.

1.4 Outline of Thesis

This thesis is divided into six chapters. A brief description of each chapter is given below.

Chapter 1 briefly introduces the problem and the importance of this research, in addition to the objectives.

Chapter 2 presents the fundamentals of multiphase flow in vertical pipes, some basic concepts of pressure drop and several correlations widely used in the oil and gas industry to calculate liquid holdup and pressure gradient for two-phase flow in vertical pipes. In addition, the review of some investigations related to instabilities on two-phase flow in vertical pipes and where these instabilities are found in field operations.

Chapter 3 describes the experimental facility, the procedure, and the characteristics of the experimental data. It also includes the effects of inlet conditions on two-phase flow in vertical pipe as a function of time.

Chapter 4 presents the results of the comparison between experimental data for steady-state and oscillatory conditions. The evaluation of pressure gradient and liquid hold up for similar pressure and flow rate conditions is presented. Also, flow regimes and frequency of the waves are analyzed.

Chapter 5 shows the outcomes of the comparison between multiphase flow correlations and the experimental data for the different conditions. Further, the efficiency of these correlations to predict the pressure gradient and the liquid holdup under steady-state and oscillatory conditions are discussed.

Chapter 6 presents the conclusion obtained from this investigation and the recommendations for future work.

CHAPTER 2: LITERATURE REVIEW

In the petroleum industry, two-phase flows can be found in wells, risers and pipelines. The appropriate understanding of these types of flows is crucial for proper completions design and optimization of production. Therefore, a study of the fundamentals in multiphase flow in vertical pipes is presented in this section covering the concepts of flow regimes, waves and liquid film characteristics, pressure drop, two-phase flow instabilities and where these instabilities can be found in the petroleum industry. In addition, the basic equations and the most commonly used empirical correlations for numerical prediction of for two-phase flow in vertical pipes are presented.

2.1 Multiphase Flow

During the production of oil and gas, multiphase flow takes place along the wellbore and flowlines. Multiphase flow is defined when more than one phase or component are flowing through a tube. These different phases or components flow with different configurations or arrangement depending of the flowing conditions. These flowing patterns are known in multiphase flow as flow regimes or flow patterns. Therefore, a brief overview of the flow regimes that occur in vertical gas-liquid pipes is presented.

2.1.1 Flow Regimes

When the gas and liquid are flowing upward at the same time, these gas and liquid phases circulate through the pipe in different flow patterns, or flow regimes. These flow regimes are defined as the geometrical arrangement and shape of these two phases in the pipe (Shoham 2006). This geometry can alter the interfacial area presented for mass, momentum, or energy exchange between the phases (Brennen 2005). Therefore, the prediction of flow regimes is crucial for proper characterization of these types of flows.

Flow regimes have been experimentally characterized by different methods such as wavelet transforms (differential pressure fluctuations) (Elperin and Klochko 2002), liquid holdup PDF distributions (Waltrich 2012), and visual observations, (Waltrich 2012, Shoham 2006). Considering a vertical tube, five flow patterns can be encountered as shown in Figure 2.1. These flow regimes are: bubble flow, slug flow, churn flow, annular flow, and dispersed-bubble flow (Taitel et al. 1980).

The flow pattern transitions or boundaries between different flow regimes occur when a particular flow regime becomes unstable as the boundary is approached, and the increase of the instability induces the transition to another flow pattern (Brennen 2005). The multiphase transitions are most of the time not sudden changes in flow behavior, but smooth transition from one flow regime to another. Due to this smooth transition, is very difficult in practice to define the exact conditions for these transitions.

For multiphase flow in vertical pipe with low upward gas velocity and the liquid phase velocity is kept constant, if the gas velocity is increased, the flow patterns evolve from bubble flow to annular flow. In the literature other flow patterns have been identified depending on the inclination angles. Since the present work discuss mainly about upward two-phase flow in vertical pipes, a brief description of the five flow regimes encountered in vertical pipes only is presented next.

Bubble flow: the liquid-phase is the predominant and continuous phase. It is distributed homogeneously in the pipe. The gas-phase is present in small bubbles which are dispersed and travel towards the surface through the liquid-phase. This flow regime is found for low gas velocity and high liquid velocities.

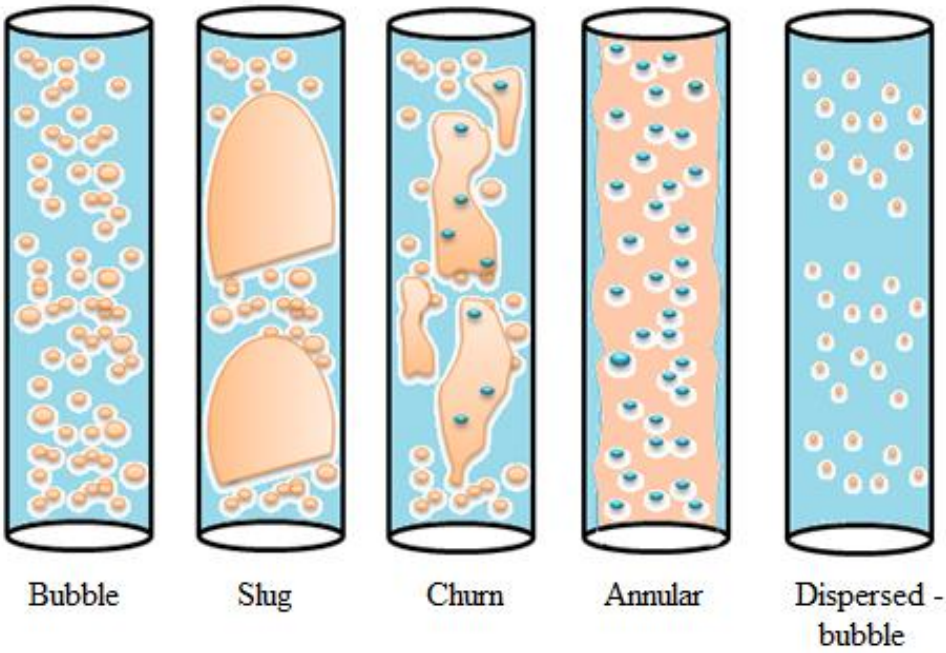

Figure 2.1 Flow patterns in a two-phase flow system for vertical pipes (Taitel et al. 1980).

Slug flow: This flow is determined by an increase in the gas-phase fraction, where the bubbles of gas are very close to one another. The proximity between bubbles causes them to coalesce, forming larger bubbles called Taylor-Bubbles. These types of bubbles have a size of almost the diameter of the pipe and travel upwards. Only a thin liquid film that flows downward separates these bubbles from the wall of the tube. This flow is characterized by a sequence of Taylor-Bubbles and liquid slugs. The slugs may contain small bubbles. This is an intermittent flow.

Churn Flow: In this flow regime, the Taylor -Bubbles dissipate due to higher gas flow rate. However, the gas phase is present in form of huge waves with a chaotic upward flowing behavior. The liquid-phase presents oscillatory waves traveling up and down which generate no

definite limits between the two phases. It is also an intermittent flow. This flow is presented in more detail in the following section.

Annular flow: In the annular flow, the gas-phase is the predominant and continues phase. It travels in the core of the pipe at high velocities. The liquid-phase is presented in liquid droplets localized in the core of the tube flowing with the gas-phase, and also creates a uniform thin film around the pipe which may contain gas bubbles. Annular flow is characterized by the formation of waves at the gas-liquid interface. These waves are usually large with high amplitude, and they are related to the formation of the entrained liquid droplets.

Dispersed bubble flow: In this flow regime, the continuous liquid-phase transports small dispersed bubbles uniformly through the tube. This flow is developed under high liquid rates. As a consequence, the two phases have the same velocity. It is considered a homogeneous flow.

It is worth mentioning that when a well is producing, it can experience all the flow regimes mentioned above during its life. That happens because the velocity is a parameter that depends on the area and density. Different flow regimes can also be encountered in the pipeline when the well is producing due to changes in pressure, temperature or pipe diameter and inclination.

Because of the importance of flow regimes in multiphase flow and its applications in different industries (nuclear, oil and gas, chemical and process, geothermal), several researchers have created empirical transition models under certain range of conditions to predict them. These transition models are called flow regime maps.

The flow regimes have been determined through experimentation where visual observations are the main method of characterization. Experimental data was then used to create

maps on a two dimensional plot. These maps were generated to determine the dependency of the flow regimes on fluid properties (surface tension, density, viscosity), on phase volume fluxes, or phase volume fractions. Flow pattern maps allow for the prediction of the flow regimes and the transition boundaries between the different regimes.

A variety of maps have been developed from many investigators. The main differences between their maps are the inclination of the pipe (horizontal (Beggs and Brill 1973, Baker 1954) or vertical (Hewitt and Roberts 1969, Duns and Ros 1963)), and the coordinates system such as dimensional coordinates (Taitel et al. 1980) (superficial velocities, mass flow rate or momentum fluxes) or dimensionless coordinates (Aziz and Govier 1972, Beggs and Brill 1973, Hewitt and Roberts 1969), which generally use Reynolds and Froude numbers, gas volumetric ratio, liquid and gas flow rate ratio, or a combination of parameters. These empirical maps are expected to be applied with confidence only when they are used to characterize flow regimes under comparable conditions. Two examples of flow regimes maps are shown in Figure 2.2.

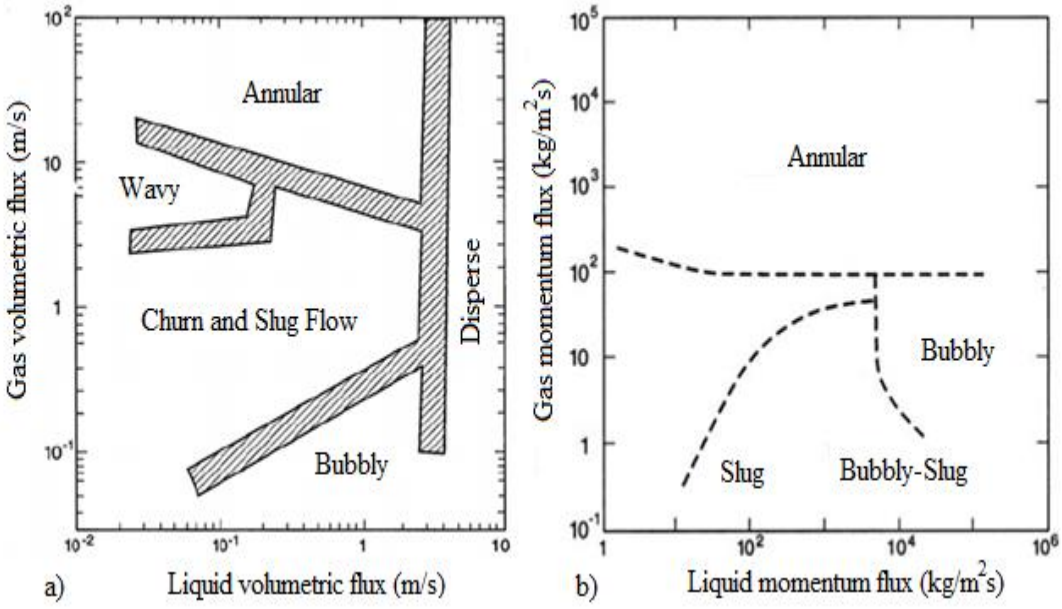

Figure 2.2 Flow regime maps for air and water in vertical pipes a) (Weisman 1983), b) (Hewitt and Roberts 1969)

Both flow pattern maps were developed experimentally for air and water mixtures, in vertical pipes, and relatively small diameters. In Figure 2.2 a) the pipe diameter was 2.5 cm, and gray areas represent the transition zone between flow regimes (Weisman 1983). In part b), a 3.2 cm diameter tube was used to run experiments at atmospheric pressure as well as steam and air at high pressure. In this map, the lines represent the boundaries for the flow regimes (Hewitt and Roberts 1969).

A more recent comparison between experimental data and some of the most common transition models was carried out by (Waltrich et al. 2013).This experiment was carried out in a long vertical pipe (42-m log), using air and water as the gas and liquid phase. Slug, churn, and annular flow were the flow regimes of interest in that investigation. The regimes were characterized by three different methods: visual observation, differential pressure, and liquid holdup. A flow regime map was created with dimensional coordinates and superficial velocities as presented in Figure 2.3.

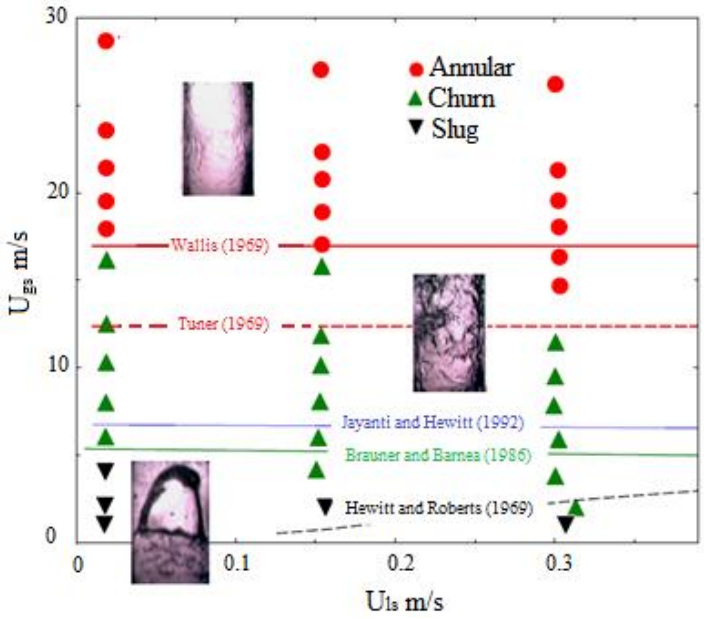

Figure 2.3 Comparison between experimental data and common flow regime transition models (Waltrich et al. 2013)

2.1.2 Churn Flow

The churn flow is a typical flow regime shown only in gas–liquid two phase flow, in vertical or near vertical pipes. The characteristics of this flow regime have not been extensively investigated due to a confusion in the literature when the term 'churn' was used as a developing slug flow (Taitel et al. 1980) and 'churn turbulent' as a bubbly flow regime (Zuber and Findlay 1965). Finally, Hewitt and Roberts (1969) recommended a new intermittent flow regime that occurs between slug and annular flow, when the slug flow is disaggregated due to an increase in gas velocity. This is called churn flow. One of the main problems characterizing this flow regime is the similarities with annular flow. However, the main differences between these two flow regimes have been determined in more recent study (Barbosa et al. 2002)

As mentioned above, churn flow is an intermittent and unstable flow regime. The transition from slug flow to churn flow comes with a formation of huge waves that flow upwards, and a liquid film that travels up and down (Wang et al. 2013a). Thus, churn flow is characterized by a thicker oscillatory liquid film that is in between the huge waves, and a number of liquid droplets carried in the center of the tube (Azzopardi and Wren 2004). The study of these parameters is essential in understanding the behavior of this flow regime.

Waves in Churn Flow

In churn flow, one type of wave has been identified, named huge waves. These waves are faster than the disturbance waves of annular flow but slower than those present in slug flow. Huge waves have been characterized to have a near linear relationship between velocity and width (Azzopardi and Wren 2004).

The velocity of the waves has been related to the transition between flow regimes. The transition between slug and churn, or between churn and annular are examples of them. Sekoguchi and Mori (Azzopardi and Wren 2004) defined the transition phenomenon between slug and churn flow when the wave frequency of the emerging slug and huge waves are equal. Similarly, the churn to annular transition appears when the frequency of huge waves and disturbance waves are equal.

Few studies have been carried out trying to understand the behavior of churn flow. (Barbosa et al. 2002), focused his studies on understanding the behavior of churn flow at the inlet. The study measured the frequency of the waves and their velocities, and the results were consistent when compared with a previous study. Also, a theoretical model of wave growth was developed based on a mass, momentum, and force balance assuming sinusoidal wave shape. This model predicts the velocity and the distance travelled by the waves. Barbosa found that the wave frequency increases with either an increase in liquid or gas flow. If the liquid flow increases the waves form faster. Further, if the gas flow rate increases the critical amplitude –defined as the amplitude at which the wave starts moving upwards- is smaller, resulting in faster appearance of waves.

The evolution of huge waves in churn flow was recently investigated (Wang et al. 2012). In this study a mathematical model was designed with the objective to better understand the transition from churn to annular flow. Fortunately, this type of study may also be implemented in mechanistic models to predict pressure drop in pipes. The investigation begins from some of the Barbosa et al. (2002) assumptions, such as the sinusoidal wave shape, for simplification, and the forces acting on the waves. It was found that the appearance of liquid oscillations were due to wave reversal, and gravity. Also, it was determined that the oscillation of the falling liquid film

was influenced by other factors such as interfacial shear stress variations, surface tension, inertial effects and viscosity, when the transitions from churn flow to annular flow was close or at low gas superficial velocity. Wave amplitude was analyzed and found to increase with an increase in tubing size, and decrease with an increase in gas superficial velocity. One of the most pertinent conclusions was that gas pressure was the most relevant factor affecting the wave behavior. However, the studies of Wang et al. (2012) and Barbosa et al. (2002) were focused only in the near inlet regions and did not the behavior away from the pipe entrance.

Waltrich et al. (2013) then analyzed in a long vertical pipe (42-m long) the frequency of disturbance and huge waves with respect to dimensionless superficial gas velocity and different axial positions. The later author used a model developed by Hazuku et al. (2008) to automatically count the frequency of waves based on time-series measurements of liquid holdup. This technique calculates the number of large liquid structures in vertical annular flow. Hazuku et al. (2008) defined the liquid flow structure (waves) when the wave has a peak that is greater than the average film thickness of upper waves and the thickness of the both extremities smaller than the average film thickness. The average upper structure was determined using the following equation (Hazuku et al. 2008):

$$\overline{\delta_u} = \frac{1}{n}\sum_{k=1}^{n} \delta_k \ (\delta_n > \delta) \tag{1}$$

Where $\overline{\delta_u}$ was the average upper structure layer thickness, δ_k instantaneous film thickness, and $\bar{\delta}$ is the average film thickness. This method was applied by Waltrich et al. (2013) to slug, churn, and annular flow regimes. Waltrich et al. (2013) found that the wave frequency does not have a considerable change with axial position.

2.1.3 Annular Flow

Upward annular flow in vertical pipes is characterized by a gas core that flows in the center of the pipe and a liquid film that is located along the pipe wall. The gas core flows upwards at high velocities with some liquid droplets created by the process of liquid entrainment. The liquid film contains some gas entrainment and it travels in the same direction as the gas core but at a lower velocity. The interface between the gas and the liquid creates some large disturbance waves and ripple waves (Han et al. 2006). In Figure 2.4, the main properties of annular flow are presented.

The liquid entrainment in annular flow can be defined as a mass transfer mechanism that happens from the continuous liquid velocity field into the droplet field (NI 2007). The liquid-gas relative velocity generates surface instabilities on the film. These instabilities result in the formation of droplets and their entrainment. Due to the complexity of the gas-liquid interfacial structure, several mechanisms of droplet entrainment have been characterized. One of the most accepted mechanism describing the formation of droplets for low viscous fluids (such as water) was explained in (Okawa et al. 2002). In the roll wave mechanism, the drops are formed at the gas-liquid interface when the wave crest reaches the turbulent gas flow. This turbulent gas flow can create small atomized droplets because the tips of the waves have been elongated enough for an interaction between interfacial shear forces and surface tension forces.

Waves and liquid film thickness are the two main properties in annular flow related to the accumulation of liquid. Recently, Berna et al. (2014) has carried out an extensive literature review and comparison of the main properties related to droplet entrainment. They purposed new equations for liquid film thickness, wave celerity and frequency. Their comparison covered vertical and horizontal pipes and a large range of liquid and gas velocities.

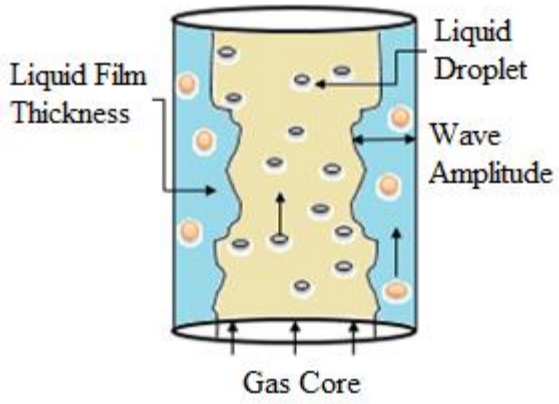

Figure 2.4 Schematic illustration of gas and liquid phase distribution in annular flow.

Waves in Annular Flow

Waves in annular flow play an important role in the process of liquid entrainment. There are two types of waves' disturbance and ripple waves. A comparison of the main characteristics between the two types of waves is shown in Table 2.1.

Table 2.1 Characteristics of waves in annular flow

	Waves	
	Disturbance	*Ripples*
Amplitude	Large (relatively to the mean film thickness)	Small(relatively to the mean film thickness)
Life time	Long	Short
Occurrence	Large liquid flow rate	Low liquid flow rates
Liquid mass	Carry Liquid	Do not carry liquid
Velocity	Fast	Slow
Distribution on vertical pipe (small diameter)	Uniformly around the pipe circumference	Do not occupy the total circumference

The disturbance waves are what carry the liquid mass along the pipe, influence the flow pressure drop, dominate the mixing properties of the liquid film thickness, and the properties distributed uniformly around the pipe (Berna et al. 2014). It has been found that the waves transport between 60-80% of the total liquid mass (Han et al. 2006). Therefore, it is essential to understand and evaluate some of its properties.

- Wave amplitude describes the distance between the wave base height (base film thickness) and the peak of the wave. For upward co-current annular flow, Holowach et al. (2002) proposed a model for droplet entrainment transient two-phase flow that integrates a wave amplitude equation.

- Wave frequency is the number of waves formed in a certain interval of time. This parameter increases when the liquid and gas flow rate are larger. The wave frequency was found to be a function of the gas mass flux, and that the frequency increases in the range of 23-47 kg/m^2s (Han et al. 2006). One of the most common correlations to calculate wave frequency was proposed by Azzopardi (2006). His model is based on a correlation between the dimensionless Lockharte-Martinelli number and the liquid Strouhal number (Azzopardi 2006). However, in a recent investigation the wave frequency was analyzed in annular flow under oscillatory flow conditions (Okawa et al. 2010) also using Sekoguchi's correlation. The later correlation was developed for multiple pipe diameters 8-26mm with liquid superficial velocity range from 0.04-0.14 m/s and gas superficial velocities between 20-50 m/s predicting the experimental results with +/- 10% deviation. It was also validated using air-water fluids in a 11mm pipe diameter by (Hazuku et al. 2008), obtaining a good match of their experimental data in a range of +/- 25% deviation. Okawa et al. (2010) found that the wave frequency associated

with the annular flow increased when the oscillation period was decreased. The main two correlations for the wave frequency are presented here.

Azzopardi's correlation:

$$f_w = \frac{St_l U_l}{D} \tag{2}$$

Where *fw* is the wave frequency, *Ul* the liquid superficial velocity, D the pipe diameter, and *Stl* liquid Strouhal number defined as:

$$St_l = 0.25X^{-1.2} \tag{3}$$

And *X* is Lockharte-Martinelli number.

$$X = \sqrt{\frac{\rho_l U_l^2}{\rho_g U_g^2}} \tag{4}$$

Where *ρl, ρg, Ul,* and *Ug* are density of the liquid, density of the gas, liquid superficial velocity, and gas superficial velocity respectively.

Sekoguchi's correlation:

$$f_w = \frac{St_g U_g}{D} \tag{5}$$

$$St_g = f_1(E_o) f_2\left(Re_l Fr_g\right) \tag{6}$$

WhereE_o, Re_l, Fr_g are Eötvös, Reynolds, and Froude numbers, defined as

$$E_o = \frac{gD^2\left(\rho_l - \rho_g\right)}{\sigma} \tag{7}$$

Where *g* is the gravity acceleration and *σ* is the surface tension.

$$Re_l = \frac{\rho_l U_l D}{\mu_l} \tag{8}$$

Where μ_l is the liquid viscosity.

$$Fr_g = \frac{U_g}{\sqrt{gD}} \tag{9}$$

$$f_1(E_o) = E_o^{-0.5}[0.5\ ln(E_o) - 0.47] \tag{10}$$

$$f_2\left(Re_l Fr_g\right) = 0.0076\ ln\left(\frac{Re_l^{2.5}}{Fr_g}\right) - 0.051 \tag{11}$$

Liquid Film Thickness in Annular Flow

The liquid film thickness is defined as the amount of liquid between the pipe wall and the mean height of the waves formed in the gas-liquid interface. In annular flow under steady-state conditions, when the gas flow rate is high, the liquid film travels upwards and there is a thin film. If there is a reduction in the gas flow rate or an increment in liquid flow rate, the liquid film increases, which lowers the gas-liquid interfacial friction (Han et al. 2006). As a consequence, the liquid film velocity decreases because the effect of gravity begins to govern the flow, as illustrated in Figure 2.5. Different experiments were carried out to better characterize this feature as a function of position in the pipe (Waltrich et al. 2013, Hazuku et al. 2008). The liquid film varies in the axial direction resulting from the pressure drop along the pipe. Consequently, the gas flow rate and interfacial shear stress also increase in the vertical direction.

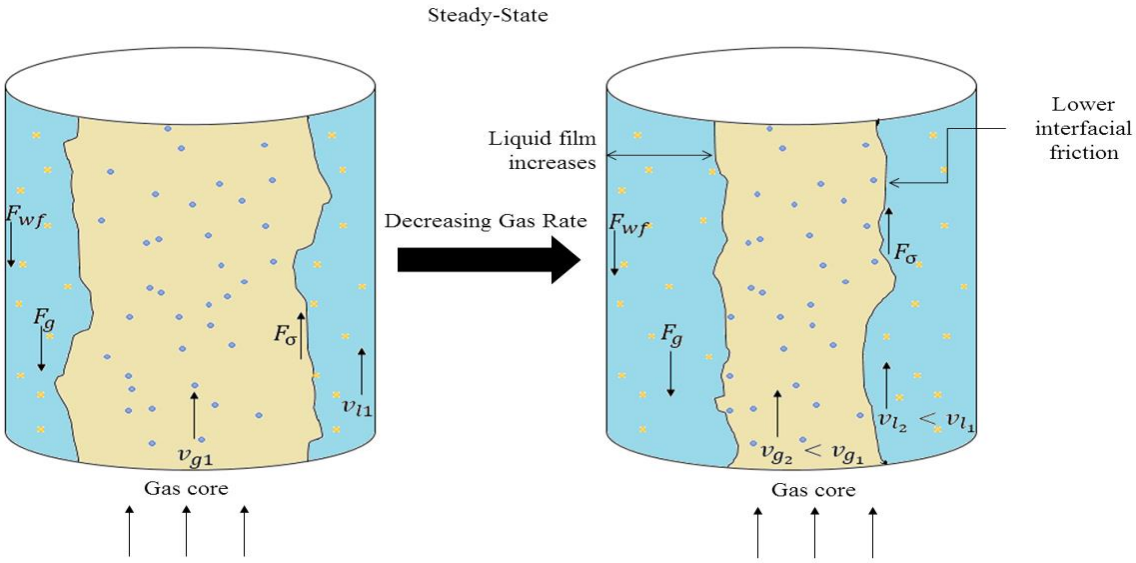

Figure 2.5. Representation of liquid film behavior in steady-state.

The liquid film was also studied under sinusoidal forced oscillations of the inlet flow rate (Okawa, 2010). It was seen that this parameter oscillates at the same period as the inlet mass flux. Furthermore, the mean film thickness tends to increase when there is a diminution in the oscillation period.

After studying multiphase flow and the main features of the flow regimes, it appears there is a correlation between the flow regimes and the pressure drop that the wellbore experiences. The gas and liquid velocities also appear to be a function of the gas-liquid interaction. Additionally, the waves have been identified as one of the properties that carry the liquid phase upwards. Hence, the amount of liquid present in a certain section of the pipe (liquid holdup) is related to flow regime, size, velocity and wave frequency. Parameters such as the velocity and the liquid hold up are used to estimate the pressure drop across the tube.

2.2 Pressure Gradient

Pressure gradient is defined as the sum of variations of potential energy in the fluid (elevation), the variation of pressure due to friction, and the change in kinetic energy of the fluid (acceleration). Considering the fluids as a homogenous mixture, an energy balance equation can be used to a pipe segment to obtain the total pressure gradient (Brill and Mukherjee 1999).

$$\left(\frac{dp}{dz}\right)_T = \left(\frac{dp}{dz}\right)_{el} + \left(\frac{dp}{dz}\right)_f + \left(\frac{dp}{dz}\right)_{ac} \tag{12}$$

$$\frac{dp}{dz} = \frac{\rho_m g sin\theta}{g_c} + \frac{f\rho\, U_m^2}{2g_c D} + \frac{\rho_m U_m}{g_c}\frac{dv}{dz} \tag{13}$$

For vertical pipes θ=90°, f is a two-phase friction factor, and the ρ and ν are mixture density and velocity, respectively. These parameters can be obtained from different empirical correlations or models available in the literature. The acceleration component in Eq. 12 is usually neglected due to its small contribution to the total pressure gradient. However, for high flow velocities or for changes in flowing area, the acceleration term should be considered.

A graphical representation of equation 13 is presented in Figure 2.6. This curve is most commonly known in petroleum engineering as the Tubing Performance Relationship (TPR). It is used to estimate the flowing pressure and flow rate for a particular well when it is combined with the Inflow Performance Curve (IPR) (Economides et al. 2013). The TPR illustrates that for a constant liquid rate low levels of gas rate, the pressure gradient is dominated by the elevation component in equation 13. As the gas rate increases, the pressure gradient begins to decrease since the amount of liquid in the pipe is reduced, as a consequence of large interfacial shear stresses between liquid a gas phases. If the gas rate continues to increase, the curve reaches its

minimum point. Then, with a further increase in gas rate, the pressure gradient increases as a result of increasing in the friction component.

The two main flow regimes (named annular and churn flow regimes) studied in this investigation can be related to this curve. The pressure gradient for churn flow conditions is generally found to the left of the minimum point of the TPR. On the other hand, the pressure gradient under annular flow is usually found to the right of this point.

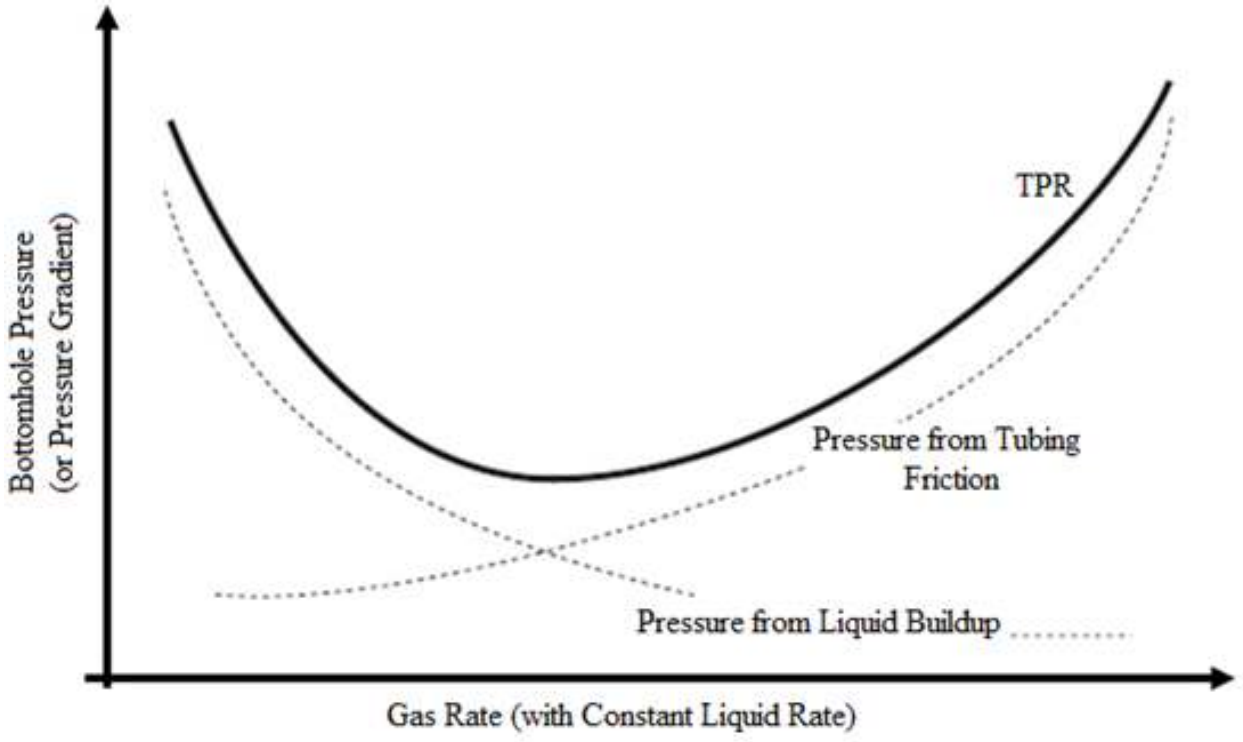

Figure 2.6 Steady-state pressure gradient behavior for multiphase flow in vertical pipes (Lea et al. 2011)

The pressure gradient is one of the most important parameter to be characterized during the design and optimization of production systems in petroleum engineering. Therefore, several correlations have been developed to determine the pressure gradient in multiphase flow in pipes. There are different types of approaches to evaluated pressure gradient in multiphase flow in

pipes such as empirical correlations and mechanistic models. Some of these models will be briefly described in the next section.

2.2.1 Multiphase Flow Correlations to Predict Pressure Gradient

Many empirical correlations have been developed to predict pressure gradient of multiphase flow in pipes. The main advantages of empirical correlations are the simplicity to implement and a minimum knowledge of the system's characteristics are required. One disadvantage is that these correlations are considered only accurate on the range of conditions that it was developed. Therefore; there is not a single correlation that can be applied for all cases. This investigation uses four empirical correlations to compare with the experimental data. These correlations are: Hagedorn and Brown (1965), Gray (1974), and Beggs and Brill (1973) and Duns and Ros (1963). A brief description of each of these correlations is discussed next.

Hagedorn and Brown

This is one of the most commonly used correlations for wellbores because of its performance. This correlation was developed by obtaining experimental pressured drop and flow rate data. The experiment was conducted on a vertical well of length 457.2 m (1500 ft). The fluids used were water and crude oils as the liquids and air as the gas. The oil viscosities were 0.01, 0.035, and 0.11 Pa*s (10, 35, and 110 cp) at stock tank conditions. The experiments were run using three different tubing sizes, 2.54, 3.17 and 3.81 cm (1.00, 1.25, and 1.50 in). It is worth mentioning that the pressure gradient and liquid holdup were back calculated from the measurements after assuming a friction factor correlation.

Gray

The Gray correlation was developed using 108 well test data sets. It is mainly used to calculate the pressure gradient in vertical gas wells producing condensates or water. The tubing size used was 8.89 cm (3.50 in). The limitations are of these correlation is that the flow velocity must be lower than 15.24 m/s (50 ft/s), the diameter less than the tubing size used, and the condensate and water ratio cannot exceed 50 bbl/MMcf and 5 bbl/MMcf respectively.

Beggs and Brill

This correlation was developed in a small scale test facility. The pipe length was 27.43 m (90 ft). The pipe material was acrylic in order to visually characterize flow regimes. The pipe diameter range was 2.54-3.81 cm (1.00-1.50 in). Air was used as the gas phase and water as the liquid phase. The gas and liquid rates were varied to observe and characterize the flow regimes under horizontal conditions. This process was completed for each pipe size. The liquid holdup and pressure gradient was measured for different inclinations and the liquid holdup was corrected based on the angle. As a result, this correlation is applicable to any pipe inclination and flow direction, but it is not recommended to be used for pipes near vertical orientation. The range of applicability for gas flow rates is between 0-0.1 m^3/s (0-300 MSCF/d), for liquid flow rates within 0-0.0018 m^3/s (0-1029 bbl/d), pressure between 241-655 Kpa (35-95 psia), pressure gradient 18.1 Kpa/m (0-0.8 psi/ft), liquid holdup 0-0.87 and the angle variation -90/+90.

Duns and Ros

This method introduced the first dimensional analysis of two-phase flow in pipes. The laboratory facility was a vertical loop with a transparent section that allowed visual characterization of the flow patterns. The height of th test section was 56 m (185 ft) and the pipe

diameter tested was in the range of 3.20-14.22 cm (1.26-5.60 in). Two annular configurations were used and the system pressure was nearly atmospheric. The fluids used were air for the gas phase, and viscous oils and water for the liquid phase. This correlation was developed measuring the liquid holdup and the pressure gradient for a total of 20,000 data points.

In summary, these four correlations were selected in this investigation in order to compare its performance against steady-state and oscillatory experimental data. The performance of these correlations have been evaluated taking into account their characteristics and range of applications. Hagedorn and Brown correlation was selected due to its performance in previous comparisons, especially in vertical wellbores. Gray correlation was selected due to its application in gas wells. Beggs and Brill correlation is not recommended for vertical upward flow; however, it was selected because both the fluids and pipe diameter are similar to this study. Finally, the Duns and Ros method was selected since their flow loop characteristics are similar to this study, and also predicts liquid holdup and pressure gradient depending on the flow regime.

After reviewing some basic concepts of pressure gradient prediction under steady-state conditions, it is also important to review some of the previous investigations related to pressure instabilities and oscillations in multiphase flow in pipe.

2.2.2 Instabilities and Oscillations in Multiphase Flow in Pipes

Pressure and flow oscillations are usually created by the flow instabilities. The flow instabilities have been widely studied in the nuclear field because those phenomena occur in multiples applications such as heat exchangers, boiling water reactors, fuel channels and refrigeration systems. The instabilities are found where gas-liquid phase-changes occur. Processes associated with multiphase flow have been categorized as one of the most complex

transport phenomena in the industry because besides the complexity of single phases, the motion of the gas-liquid interface and the interaction between the phases should be taken into account.

Hydrodynamic instabilities of two-phase flow in pipes have been studied by Fukuda and Kobori (1978). Their flow loop had a heated length of 3.7 m and an equivalent diameter of 0.97 cm. The fluid was water; the pressure range was 0-6860 Kpa, temperature range 0-50°C and flow rates between 0.5 and 17 kg/s. This study classified the hydrodynamic two-phase flow instabilities into three types of local instabilities (Ledinegg instabilities) and five types of density wave instabilities. For each type of instabilities, different pressure drop term governed the system. The experiment experienced two types of instabilities both attributed to density wave instability. The type I instability occurred when there was almost no steam coming out of the channel. The type II occurred under high steam conditions. The group concluded that for the unheated riser the gravitational pressure drop played a dominant role in the type I instability, while the type II instability was dominated by the frictional pressure drop. This test was performed under natural and forced circulation conditions; however, in the forced circulation test the pump was run to keep the total flow rate constant. The forced circulation implemented by Fukuda et al. was more similar to steady-state conditions; whereas, in the current investigation forced flow oscillations will be analyzed.

March-Leuba (1992) published a summary of the main problems related to density wave instabilities in boiling water reactors (BWR). The report discussed three primary sources of instabilities. However, just two of the causes of instabilities are mentioned here because of their similarity to scenarios found in the oil industry. The control system instability is associated to the action of regulators that, through actuators (typically valves), try to control some of the variables of the reactors including the pressure or the water level control. This type of instability produces

low frequency oscillations in either the water inlet, the water temperature, or in the reactor pressure, and has been reported as sinusoidal oscillations.

The other source of instabilities is called the channel thermohydraulic instability. This instability is encountered under heated channels where multiphase flow occurs. This instability has two subsets associated with it, static and dynamic. The static subset is usually described by steady-state laws where the existence of two equilibrium points is present and the system has a tendency to jump from one point to another. Examples of this type of instability include flow excursion and flow regime relaxation. The second subset, dynamic instability, requires the use of a dynamic conservation equation to be explained. Some examples of this instability are density wave oscillation, pressure drop oscillation, and flow regime induced instabilities. The most common instability in BWR is caused by the density wave mechanism, which governs the inlet flow feedback. A sinusoidal change in the inlet flow causes delays in the local pressure drop causing it to behave in a sinusoidal form.. An illustration of how the density wave mechanism influences the pressure drop is shown in Figure 2.7. This graph is an interpretation of the explanations and figures given by March-Leuba (1992).

The density wave mechanism was identified as the second cause of unstable gas-lift wells (Hu 2005). It has been recognized as the new phenomenon that is produced from depleted reservoir's located in the North Sea, generally deepwater wells. The gas injection at the bottom of the well changes the mixture density, and in turn causes a drop in hydrostatic pressure. The phase fraction variation at the bottom of the well makes the change in mixture density travel along the tubing as a density wave.

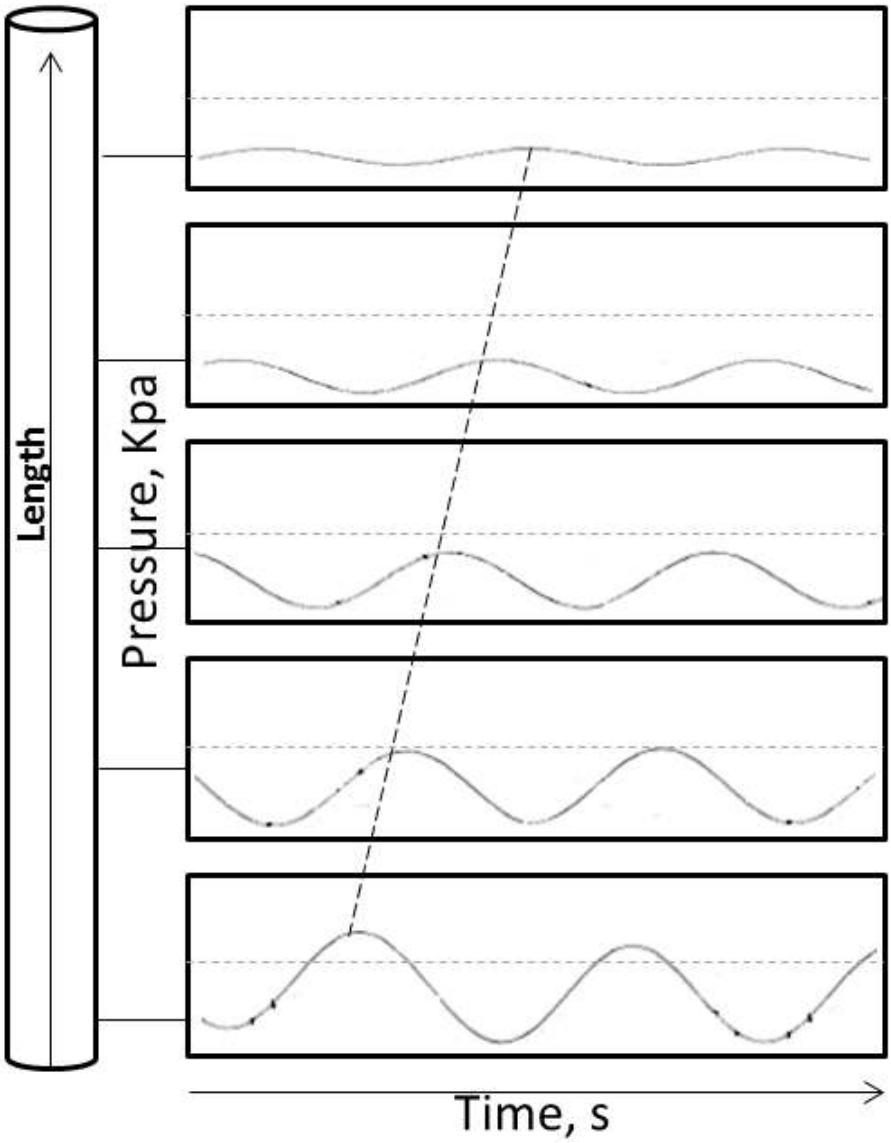

Figure 2.7 Local pressure drop delay introduced by the density-wave mechanism. Graph modified from (March-Leuba 1992).

A study of the physical principles of impulse pumping in single-phase was carried out by Pierre (2010) with emphasis on petroleum applications. Impulse pumping produces flow from the bottomhole to the surface through pressure waves created at the wellhead. The application of this type of system requires a scenario where pipes are fluid-filled, such as, water hammer phenomena in hydraulic pipelines. Pressure waves are disturbances that transmit energy and

momentum from one point to another through the medium, thus moving the fluid. The investigation focused on the performance of this method in terms of head, flow rates, and efficiency; while evaluating vertical, inclined and horizontal pipe arrangements. It was found that the parameters that influenced the impulse pumping system the most were the pressure wave amplitude, the wellhead pressure, lifting height, fluid compressibility and the fluid volume in the pipe. The experiments and simulations revealed that the fluid volume directly impacted the flow rate and the impulse pumping efficiency. Also a relationship between the pipe diameter and the flow rate was found. An increase in diameter produced a greater flow rate, but a larger volume required more energy to create a pressure wave in the wellhead. From this analysis, the study made some general conclusions. The efficiency of the system is inversely proportional to the square root of the diameter. The frequency of the waves only impacted the impulse pumping efficiency. An increment of 100 Kpa (14.50 psia) in the wellhead can displace 10 m of water height. Finally, that this method is only recommended for single-phase and shallow wells.

In the oil field, flow instabilities may occur under low gas-liquid superficial velocities. Riser configurations such as downward inclined; undulating pipe and other complex shapes may be the perfect scenario to create these instabilities. Often, these instabilities create much longer production cycles of slug than steady-state slugs, for which gas injectors are commonly implemented in order to remediate this problem. For example, a study of two-phase flow in large pipe diameter vertical riser published by Ali (2009) covered the flow instabilities in risers, and proposed gas injectors to combat these instabilities. Through pressure measurements, void fraction measurements, and visualization, this study affirmed that gas injectors achieved flow stability with a shrink in the slug size and eventually an alteration of the flow regime from slug to churn flow.

Two-phase flow instabilities have been studied since the ’60 due to their presence in many different industrial systems. They have been identified as one of the causes of flow and pressure oscillations in the pipes. Therefore, the identification of the type of instabilities occurring in the pipe seems to be relevant in the understanding of the flow behavior in the pipes.

2.3 Where Can Forced Flow Oscillation Conditions Be Found in the Petroleum Industry?

Natural Flow

In the petroleum industry, well cycling is the term used to define a regulated intermittent production. As mentioned in recent studies (Hu et al. 2010), the well cycling technique has been used as an alternative method to increase the well capacity before artificial lift systems are implemented, a low cost and quick solution. A typical regulated intermittent production cycle is shown in Figure 2.8. The initial stage in a production well is represented by the diagram on the left. In this stage, the well is producing both gas and liquid phases under stable conditions. Over time due to the reservoir depletion effect, the gas velocity decreases and liquids begins to accumulate, and thus the well must be shut in, as indicated in the top right of Figure 2.8. When the well is no longer producing, the bottomhole pressure begins to rise approaching the reservoir pressure, and some liquids in the well may return into the reservoir (referred to as fall back). After the bottomhole pressure has increased enough, the choke is reopened and the well now has enough energy to carry the liquids to the surface, and the cycle restarts. This technique allows production in wells which experience liquid loading for long periods of time. However, there are some wells that cannot be cycled, such as unfractured wells and those with solids fill (such as sand).

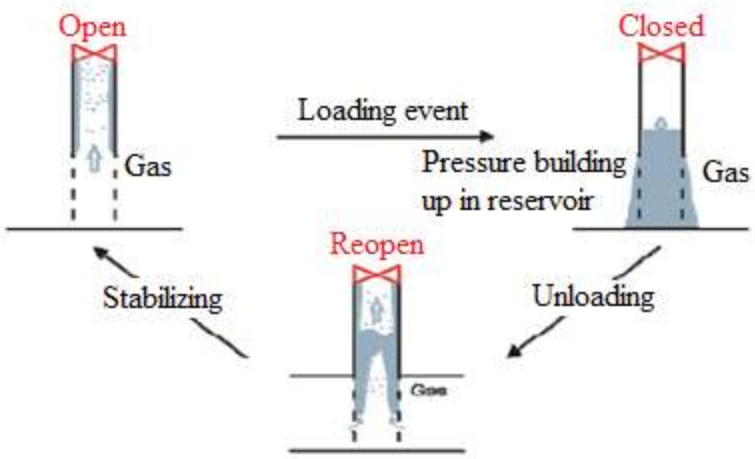

Figure 2.8 Regulated intermittent production cycle (Hu et al. 2010)

A study of the well cycling technique was carried out by Hu et al. (2010). Two models were combined to simulate the wellbore-reservoir dynamics. Well cycling involves a transient flow interaction between the reservoir near the wellbore and the wellbore itself. Due to the nature of this process, a transient three-phase gas-oil-water flow (OLGA) model was combined with a three-phase Darcy flow model in porous media (ROCX) (Sagen et al. 2011). In the simulation, the reservoir model computes a production rate sensitivity coefficient as a function of the wellbore pressure at each time. Then, this coefficient is used by the well model to get a new wellbore pressure. The first aspect of this research analyzed when the cycle should have begun, as in prior to the onset of liquid loading (60 days) or after (80 days) under the same conditions, gas flow rate of 85,000 sm3/d and a bottomhole pressure of 39.5 bar. For the first case, it was found that the well had a favorable cycling performance of 16 cycles and a cumulative gas production of 4.3E6 sm^3. However, the second case showed that the well did not produce with regularity in short time intervals and produced just 3.5E6sm^3 of gas. The differences in the cases were attributed to the amount of water each well accumulated at the bottomhole and near the

wellbore region. The second aspect investigated if different wells could be cycled. Nevertheless, they could not find constant parameters on the critical limit of well cycling.

The well cycling technique can be compared to a very well-known artificial lift system, plunger lift. This artificial system is frequently more effective than the intermittent natural flow, albeit an economic analysis will tell if the implementation of a plunger lift systems will increase the production sufficiently to justify the extra operating cost. If the liquid production is 1699 m^3/h (1000 ft^3/min) under well cycling operation, the use of artificial lift will not be warranted (Lea et al. 2011).

The necessity to find new technologies to develop and commercialize marginal fields is more important given the increasing number of fields. For offshore marginal fields, the subsea processing technology with an implementation of multiphase pumping was proposed as a method to develop these types of reservoirs.

Abili et al. (2014) studied two marginal reservoirs, one located in the North Sea and one in the Gulf of Guinea. The investigation implemented the multiphase pumping technology with the aim of increasing production through the remediation of slugging. The term slugging is defined as a variation and irregularity in the flow of liquid and gas across the production line. These oscillations can occur from two different sources. The gravity induced slugging that is caused by the irregular seabed and depth, and operational and transient slugging produced by an external origin, such as startup operation changes. The undesired effects of this oscillatory behavior can damage the equipment (separator, pumps) if severe slugging is not controlled. Furthermore, production line damage due to corrosion and fatigue are generated because of the liquid loading and variation of fluid velocity. As a consequence, there is a reduction in

production and an increment in cost because this requires a larger production facility to handle these oscillations.

The first scenario implemented in the Abili et al. (2014) study with OLGA was referred as the base case, implying the field was producing without the subsea processing technology; whereas, the second scenario implemented subsea processing by using a multiphase pump. The first scenario showed that both reservoirs were oscillating under natural conditions, meaning the producing flow regime was slug flow, the same as found in the production line. As a conclusion, this investigation determined that with subsea multiphase pumping it was possible to stabilize the flow rate for longer periods of time. The total time taken into account was 8 years. During this period it was possible to increase the productivity by 17% in both fields.

Flowline-risers

As mentioned above, slugging is an undesirable phenomenon due to the different problems generated by the fluctuations in flow rate and pressure. To mitigate this phenomenon several studies have been carried out with different approaches. These studies include different types of remediation: external bypass line, back pressure increase, subsea separation, choking, and gas lift (Ali 2009). In offshore fields, the production of oil and gas is carried out from the subsea to topside facilities through several pipelines called risers. In multiphase riser systems, a number of fluctuations are experienced. The internal hydrodynamic behavior of these pipelines is very complex because of the nature of multiphase flow and the fact that the facility is floating. As a result, unsteady cycle flow is created with larger liquid slugs causing instabilities to last long periods of time.

One of the methodologies to mitigate the fluctuations was to use an automatic control system designed to identify the slugs with flow rate, pressure, and temperature sensors, to reduce the amount of slugging through a choke valve controlled by software (Silva et al. 2013) fed by the sensors data. This control system was implemented on a test flow loop made of 10.16 cm (4 in) diameter PVC and acrylic pipes with a total length of 120 m, divided in three sections. This flow loop also includes an inclined pipe of 16 m, a vertical pipe with a height of 20 m, a riser-separator system, and the fluids were air and water. Two types of control were implemented:

i. Bottom control - it consisted of sensors and a control valve installed in the subsea wellhead (downstream to the inclined section)
ii. Platform control - it consisted of sensors and choke valve installed upstream the separator.

According to the results, the automatic bottom control reduced the pressure peaks by 57% due to a decrease in the flow rate peaks. Consequently, the average flow rate increased by 8% in comparison to no control system implemented. These results were justified by the systems capability to foresee the formation of the slug prior to arrival at the surface, and then control the flow rate. The results are presented in Figure 2.9 and Figure 2.10. These results show that the automatic control reduced the amplitude of the oscillations, but increased their period, influencing the average flow rate. This was interpreted as the average flow rate may be a function of the amplitude oscillations.

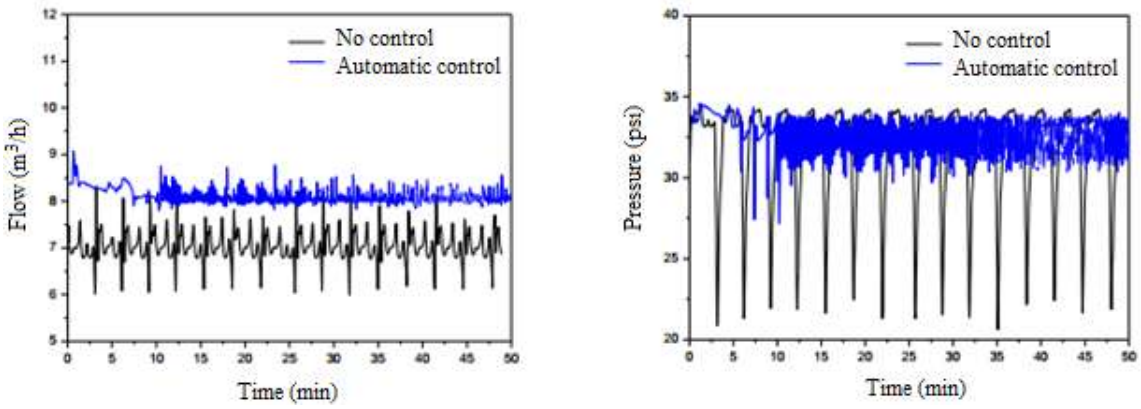

Figure 2.9 The graphs represent the natural and controlled oscillations. The left graph shows the flow rate variation and the right indicates the pressure variation both with respect to time (Silva et al. 2013).

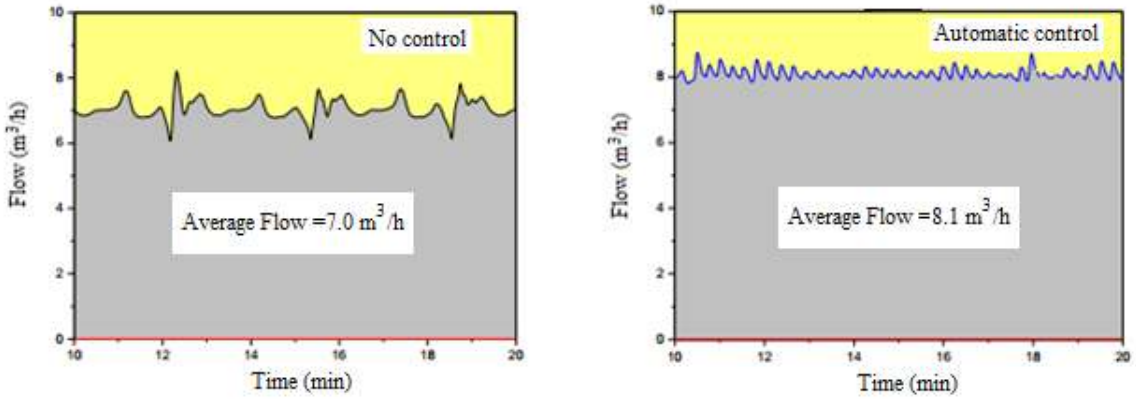

Figure 2.10 The graphs are a comparison between no control and automatic control of the average flow rate (Silva et al. 2013).

An experimental study in a flowline-riser system was also carried out in the Shell Technology Center located in Amsterdam to analyze the effect of gas lift in subsea riser systems (Seim et al. 2011). To achieve their objective three aspects were analyzed:

i. A study of slugs was carried out in the facility consisting of a 65 m horizontal pipe attached to a 35 m inclined pipe succeeded by a vertical riser of 15.5 m high. The riser is a transparent PVC pipe with a 45 mm ID. The maximum pressure was 6 bar and the

fluids were air and water. Three types of slugs were defined and identified: severe slugging type I (liquid slug length larger than the riser), severe slugging type II (liquid slug length smaller than the riser) and small scale slugs (created in the flowline). In order to better distinguish between the different slugs a stability map was developed as a function of liquid and gas superficial velocities.

ii. A comparison between the experiments and the OLGA simulator was done. The comparison was divided in two parts. First, the performance of OLGA predicting the three different types of slugs was investigated under the range of conditions tested. The results showed that OLGA predicted the severe slugging of type I and II, but it did not capture the behavior of the small scale slugs. This outcome was reflected in the under prediction of pressure drop. The second part of the comparison involved a transient analysis where lab experimental and field data was contrasted with OLGA. As a general conclusion, the simulator slightly over predicted the time period of the slugging cycle.

iii. The effect of gas-lift in the different types of slugs and transition zones and compare with the OLGA. In this aspect, experiments were run with and without gas lift. In general, OLGA matched the oscillatory pressure behavior when no gas was injected under severe slugging type I and II conditions, but with a few problems, such as under slugging type I, OLGA under predicted the pressure drop with an increment of gas injection Figure 2.11 a). Whereas, for slugging type II, OLGA did not match the amplitude of the pressure oscillation with the gas lift Figure 2.11b).

The most relevant conclusion of this study was that even if the gas lift decreased the hydrostatic pressure and lowered the frequency of the slugs, this method did not work as slug prevention unless annular flow was reached.

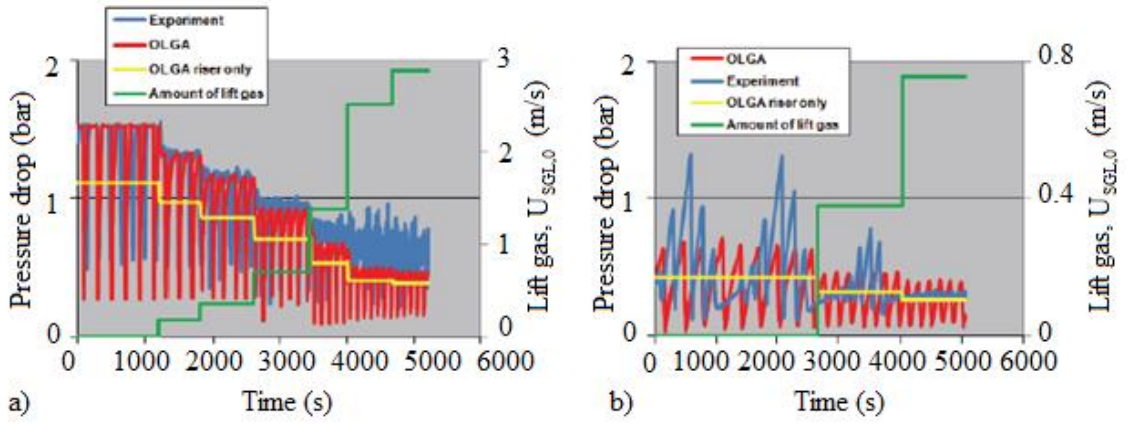

Figure 2.11 Effect of gas lift in pressure drop along the riser. Comparison between lab experimental data and OLGA for severe slugging type I a) and severe slugging type II b) (Seim et al. 2011).

Another experimental study developed by Shell in the Houston Technology Center investigated the feasibility of gas lift in large pipe diameter riser (Schoppa et al. 2013). The setup consisted of a transparent vertical riser 12.2 m (40 ft) high with an 27.94 cm (11 in) ID that was connected to a 7.62 m (25 ft) long flowline. The fluids were air and water. This investigation discussed that slug flow in large pipe diameters may not occur. Only one Taylor Bubble was observed located at the inlet of the gas injection at early times. Most of the runs were completed under churn flow conditions. It was found that the initial slug was responsible for removing the liquid, and after that the net liquid outflow was zero under churn flow conditions. The initial behavior was well captured by OLGA, but after that the simulator results predicted extra liquid carryover and continuously predicted slug flow. Under steady-state, the flow regimes observed were differed from the ones defined for smaller pipe diameter (ID < 100 mm). Also, the in-house models and OLGA under predicted the liquid holdup in steady-state. As a result, the pressure drop was over predicted by 30-60%. In base of these results, a Computational Fluid Dynamics (CFD) model was implemented. CFD and OLGA were compared giving between 15-50%

discrepancies with respect to the experimental data when predicting the pressure drop obtaining lower differences with CFD.

2.4 Conclusions

After the literature review compiled here, some evidences show that there is a lack of experimental investigations regarding the effects of the flow oscillations (instabilities) in different situations presented in the oil and gas industry. Basic design parameters such as pressure gradient and liquid holdup should be characterized in more details to better describe the mechanism behind this phenomenon. Moreover, the simulators available do not accurately predict the oscillatory behavior under certain conditions, with the largest discrepancies found when churn flow was present in the pipe flow. For these reasons, further investigations seem necessary to understand the effects of forced gas flow oscillations in pipes under churn and annular flow.

CHAPTER 3: CHARACTERIZATION OF ANNULAR AND CHURN FLOWS IN VERTICAL PIPE UNDER OSCILLATORY CONDITIONS

3.1 Introduction

In the petroleum industry, field data has shown that flow oscillations are more likely to be found in vertical wells with gas-lift systems or flow-line risers with "L" shape under specific conditions (Hu 2005, Kaasa et al. 2007, Pickering et al. 2001). The fact that most of the vertical wellbores and pipelines in the field are generally very long makes the study of this phenomenon more complex. Around the world, there are only a few facilities that meet the length requirements to be considered long (z/D>500) (Fernandez et al. 2010). With the objective of investigating the onset of liquid loading in gas wells, a large scale experimental facility was built in Texas A&M University (Waltrich 2012), the so-called TowerLab. The characteristics of the flow can change significantly in long pipes as a consequence of flow development. Therefore, it is essential to perform experimental investigations in long vertical test sections, which can reflect a more realistic scenario when they are compared to the field behavior.

A description of the main characteristics of the TowerLab design is presented in this section followed by an explanation of the procedure used to obtain the experimental data. Later in this chapter, analysis of effects of forced gas flow oscillation on the flow regimes, local liquid holdup, pressure variation, and pressure gradient with respect to time is also discussed.

3.2 Experimental Facility

The TowerLab is a vertical flow loop designed to perform air-water two-phase flow experiments. It is a large-scale vertical test section composed of a sequence of clear PVC pipe with 2-m long segments and 0.04859-m ID, creating a total length of 42 m (z/D=875). A schematic diagram of the experimental facility is shown in Figure 3.1

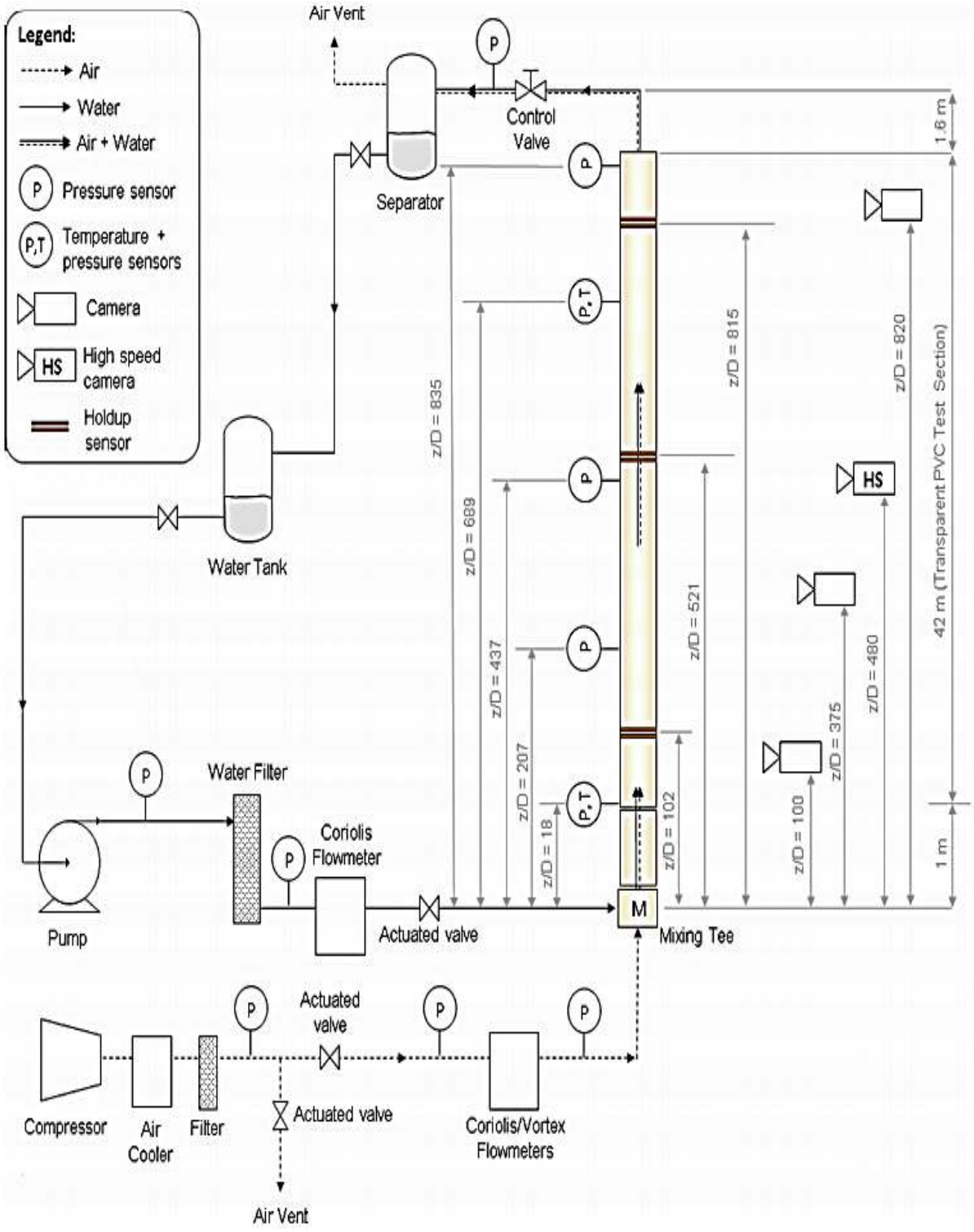

Figure 3.1 Schematic view of the experimental two-phase flow loop (Waltrich et al. 2013)

Water Circuit

The water is supplied from a 662 L water tank using a centrifugal pump. This water tank is fed by a separator. The water flow rate is controlled by a variable speed driver and an electronically-actuated valve, which is located downstream to the water pump. The water passes through a filter with a 10 μm pore size to avoid that impurities and solid particles circulate through the flow loop. The water flow rate is measured just upstream to the mixing tee using a Coriolis mass flow meter. The average uncertainty of the water flow rate is ±2 kg/h.

Air Supply

Compressed air is supplied by a screw compressor. The air flows through an air cooler and a filter, and the pressure and gas flow rate at the inlet of the test section is controlled by an electronically-actuated valve. The air flow rate is also measured just upstream the mixing point using a vortex meter and a Coriolis meter, depending of the level of flow rate. The average uncertainty of the air flow rate is ±2.5 kg/h.

Instrumentation of the Test Section

The water and air pipelines comingle in a tee, where the air and water are mixed. The mixing point is a tee with 0.0762 m pipe size that has a 0.0508 m perforated nipple within. The control of the pressure and flow rate in the system was by the actuated valves located in each pipeline and the control valve (0.0508 m ball actuated valve) at the outlet of the test section.

The vertical pipe (test section) was conditioned with a series of instruments that enabled the characterization of flow regimes and the measurement of pressure, temperature, liquid film and slug/wave frequency over a range of pressure and flow rates. In Figure 3.1, the location of

the flow monitoring instrumentation is indicated. Figure 3.1 represents all the lengths based on dimensionless axial position (z/D).

The two-phase flow regimes were identified by direct visualization through the clear pipe and cameras. To monitor different positions at the same time, high-speed and CCD (Charge-Couple Device) cameras were installed in four locations along the pipe from the mixing tee: 100D, 375D, 480D and 820D.

The absolute pressure was measured using pressure transducers at five different positions: 18D, 207D, 437D, 689D, and 835D from the mixing point. Strain-gauge transducers were installed to measure the static pressure. The transducers were connected to the test section via 6.25 mm ID nylon tubing filled with liquid (water) to avoid pressure signal dampening due to bubble trapping. The average uncertainty of the pressure is ±0.3 kPa. Temperature signals were taken using T-type thermocouple probes, inserted inside the nylon pressure line taps.

The liquid film was measured using two-wire conductivity probes which consist of two parallel wires mounted perpendicularly to the flow direction (Zabaras et al. 1986). The sensors were set at 102D, 521D and 815D from the mixing tee. More details about the probe characteristics and calibration can be found in Waltrich et al. (2013).

The methodology used to calculate the average uncertainty of the instrumentation implemented in this experimental set up can be found in Waltrich (2012). Table 3.1 lists the average expanded uncertainty for the experimental measurements.

Average uncertainties for experimental measurements associated to TowerLAB instrumentation.

Table 3.1 Average uncertainties for experimental measurements associated to TowerLAB instrumentation.

p (kPa)	$\Delta p/\Delta z$ (kPa/m)	T (K)	δ_f (mm)	h_l (-)	m_a (kg/h)	m_w (kg/h)
±0.3	±0.06	±1	±0.05	±0.02	±2.5	±2

3.3 Experimental Data

Two types of experimental data were used in this investigation. One type was steady-state experimental data, which was acquired from previous investigations where the main objective was to study the onset of liquid loading in gas wells (Waltrich et al. 2013). The other type was oscillatory experimental data obtained from the same experimental facility under similar pressure and flow rate conditions. The oscillatory experiments were run maintaining a constant liquid flow rate while the inlet gas flow rate was forced to periodically oscillate. Although the oscillatory data was run in the previous study of Waltrich (2012), it has been neither analyzed nor published. The current investigation is the first attempt to study and evaluate this type of experimental data and its applicability in the oil and gas industry.

3.3.1 Steady-State Experimental Data

Waltrich *et al* (2013) carried out 91 experiments, which were then divided by different levels of liquid flow rate and pressure. As a result, the study ended with seven sets of experiments. For each level of constant liquid rate and pressure, the gas rate was changing for each run. The current investigation only used two of the total experiments sets. The selection of the data sets was based on the similarity of the conditions including pressure and flow rates between the steady-state and oscillatory data. Table 3.2 indicates the main characteristics of the two data sets selected.

Table 3.2 Summary of the conditions used in the steady-state experiments (Waltrich 2012)

Sets	*Number of runs*	*Inlet Pressure range*	*Water mass flow rate*	*Air mass flow rate*	*Water velocity*	*Air velocity at z/D=18*
		Kpa	*kg/h*	*kg/h*	*m/s*	*m/s*
Low liquid content	11	124-181	124	4-276	0.019	8.5-26
High Liquid content	13	202-287	2016	14-362	0.3	0.6-20.3

3.3.2 Oscillatory Experimental Data

The purpose of the oscillatory experiments was to study certain instabilities and oscillations on two-phase flow in vertical pipes. Six experiments were run and categorized by the liquid flow rate. Figure 3.2 is a sample of the type of experimental runs that was analyzed in this investigation.

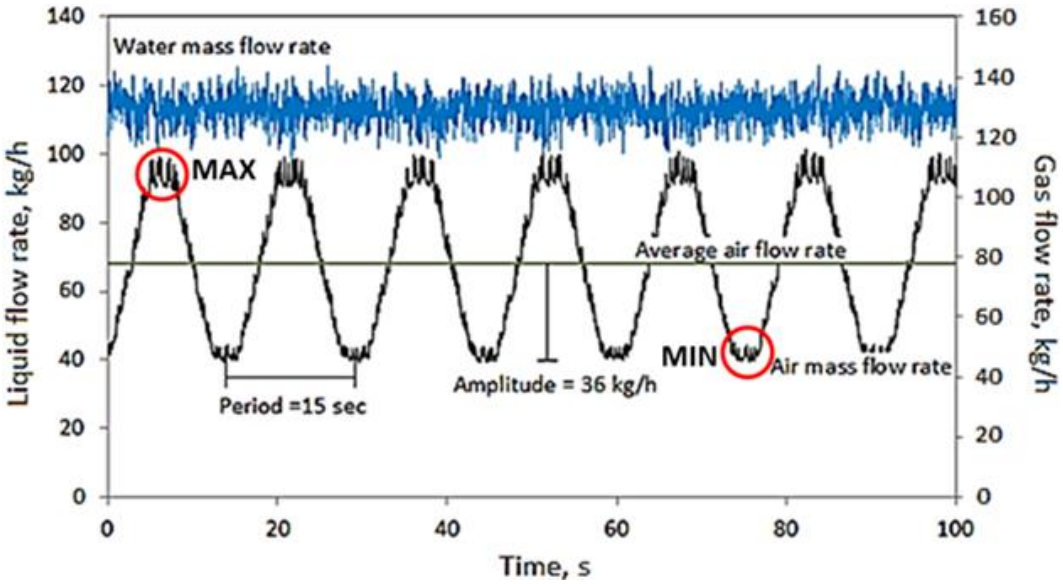

Figure 3.2 An example of the oscillatory data analyzed in this study. Water mass flow rate of 109 kg/h and air mass flow rate range of 44-116 kg/h, at 130 Kpa inlet pressure.

Two sets of data were obtained oscillating the inlet gas flow rate, while keeping the liquid flow rate constant. Three different range of gas flow rate were used with two levels of liquid rates. The gas flow rate was oscillated sinusoidallly at a frequency of 50 Hz. The experiments were recorded for a total of 180 seconds.

Table 3.3 shows the range of conditions of the oscillatory experiments which were running for the study of instabilities in wellbores and pipelines. Characteristics of the sinusoidal behavior of the gas flow rate such as velocities, period, and amplitude are also included.

Table 3.3 Summary of the conditions and features of the experimental runs under sinusoidal oscillations.

Sets	*Water mass flow rate average*	*Air mass flow rate range*	*Inlet Pressure*	*Water velocity*	*Air velocity z/D=18*	*Amplitude*	*Period*
Units	*(kg/h)*	*(kg/h)*	*(Kpa)*	*(m/s)*	*(m/s)*	*(kg/h)*	*(s)*
Low Liquid content	109	47-106	130	0.017	4.0-9.0	36	15
		114-142			12.0-14.0	24.5	10
		108-225			12.0-21.5	68	23
High Liquid content	2003	47-143	210	0.3	3.0-7.0	48	21.5
		133-214			9.5-12.0.	40	18
		120-297			8.5-16.5	88	46

3.3.3 Experimental Procedure

Two different procedures were followed when running the experiments in TowerLab. The steady-state procedure allowed for the characterization of important parameters such as pressure gradient, liquid holdup and flow regimes, whereas the oscillatory technique was used to capture the instabilities of the same parameters but under oscillatory conditions. The major objective of this experimental investigation was to measure two-phase flow pressure and liquid holdup, while characterizing the flow regimes at specific locations. The local pressure was

obtained directly from differential pressure transducers, the liquid holdup from the two-wire conductivity probes, and the flow regimes from the video recordings. All the measurements were made through a data acquisition system. A control system was also implemented to help manage operations such as controlling the opening of valves and monitoring the pressure gauges. The control and monitor computer software used was LabView.

Steady-State Runs

To run the steady-state experiments, a couple steps were followed. With the tubing free of liquid and the control valve located at the top of the test section completely open, the compressor and pump were turned on through the data acquisition control panel. This panel allowed the pump speed to vary. Next, the actuator valve for the gas line was opened allowing air in the mixing tee. After that, the liquid was injected in the mixing tee by opening the actuator valve. The actuator valves were adjusted until the desired flow rates were reached. The pressure was regulated using the control valve (choke vale) at the top of the test section. The flow was allowed to stabilize for a certain amount of time (approximately 5 minutes) to ensure proper that steady-state conditions were met. This stabilization period was defined to be accomplished when changes on the measurements of pressure where within three times the standard deviation for about one minute. Finally, the liquid and gas flow rates were kept steady and the experimental data was then recorded for approximately 3 minutes.

Oscillatory Runs

To run the oscillatory experiments, the same steps for steady-state were followed. The specific conditions selected were first treated as a steady-state experiment, and then maintained for 5 minutes. After that, the actuator valve located in the gas pipeline was forced to oscillate with a frequency of 50Hz. The period of the oscillations were controlled through the data

acquisition system. Data from these experiments were recorded for the oscillatory portion of the test for 3 minutes. This procedure was repeated for different ranges of gas flow rate and for two constant liquid flow rates.

3.4 Results and Discussions

The operating conditions in the petroleum industry are transient in nature. The transient phenomena in two-phase flow in pipes are generally slow and related to changes in the inlet flow rate, outlet pressure, or caused by opening and closing of valves (Shoham 2006). The transient behavior has generated certain types of oscillations in the wellbore due to the flow instabilities. The flow instabilities have been classified and studied analytically for gas-lift systems by Hu (2005). The types of oscillations present in this investigation have been categorized as steady-state forced oscillations. These oscillations have been related to dynamic instabilities, especially density wave oscillations where the flow instability is created by an external force. The investigation carried out by Hu (2005) confirmed that some gas-lift systems can experienced the density wave oscillations through the analytical modelling of the transient phenomenon. These oscillations are characterized for having a finite period and amplitude as shown in Figure 3.2. The dynamic instabilities were relevant for this investigation because the experiments were run under the specific conditions (external forced and differences in fluid densities) necessary to experience the density wave oscillations.

The next section introduces the results from the experiments carried out at TowerLab. The analysis was based on the behavior of flow regimes, liquid holdup, and pressure oscillations with respect to the position, gas and liquid flow rates.

Flow Regimes

The study of flow regimes under transient (or oscillatory) conditions has not been as widely studied as in steady-state conditions. Minami and Shoham (1995) was the only investigation found in the literature that developed a model to characterize flow regimes under oscillatory conditions. However, their investigation was carried out in a horizontal pipe then the model that they proposed could not be compared with the current investigation. Minami and Shoham (1995) tried to compare their results with some of the steady-state transition models, but the results did not satisfy the expectations. The models investigated were Taitel and Dukler (1976) and Kelvin-Helmholtz stability criterion. The transient simulator OLGA has implemented a model to predict the flow regimes under transient conditions. However, this model does not have defined churn flow and most of the experiments under steady state conditions were identified as churn flow. Thus, in this investigation the characterization of flow regimes under transient conditions was determined via visual observations.

The identification of flow regimes and liquid waves frequency in present study was based on the videos recorded during the experiments. Four cameras were synchronized and installed along the vertical test section pipe, and the behavior of the flow was captured at four different locations. For the conditions tested, the results show that there were no major changes in the flow regime characteristics with position. Since the flow regime was independent of location, the study chose to focus on the camera with the highest frame capture rate (10,000 frames per second), located at the third position (z/D=480, see Figure 3.1). This camera location would also allow a significant pipe length for axial development flow.

A description of the main parameters used to characterize the flow regimes under oscillatory conditions is presented:

- Annular flow behaved similarly to steady-state conditions, when both liquid film and gas phase were flowing upwards and some liquid drop traveling with the gas core upwards.
- Churn flow was identified similarly to steady-state: the gas core moves upward but was more difficult to be identified, and liquid phase behaved in a chaotic manner flowing upward and downward. However, the net-liquid flow in churn flow is upward. The liquid film was constantly undulated and some droplets were visualized falling downwards.
- Slug flow was observed under the lower gas flow rate range. The characterization of the slug flow was done using part of the definition mentioned in the literature review. In the videos it was impossible to clearly identify a Taylor bubble; however, the liquid film and the liquid slugs were observed. Therefore, in this investigation slug flow was defined as a flow regime where the liquid film flows only downward and liquid slugs flows only upwards along with entrained gas bubble. A possible explanation of why the Taylor bubble was not seen can be related to the size of the bubble. If the Taylor bubble was bigger than the focal length of the camera, the camera cannot capture it.

The oscillatory experimental data were shown as a function of the local liquid and gas superficial velocities. The local superficial gas velocities were calculated from instantaneous inlet gas flow rate and the local pressure at z/D=437. Based on gas flow rate variation for the oscillatory data, the analysis was carried out defining three different time periods for each test: maximum, minimum and average as is represented in Figure 3.2. These time periods were

correlated with the videos recordings and the flow regimes were characterized according to this criterion, as is shown in Figure 3.3 and Figure 3.4

For U_{ls}=0.017 m/s were characterized three flow regimes, slug, churn and annular flow, as is shown in Figure 3.3. The range of gas variations were selected to cover two flow regimes under steady-state conditions, annular and churn flow. However, for each range of gas variation two flow regimes were observed under oscillatory conditions at constant U_{ls}=0.017 m/s. This behavior can be explained by the influence of the gas variation because for experiments where the liquid content is low, small changes on local pressure can impact the liquid distribution on the pipe and this is directly related to the flow regimes.

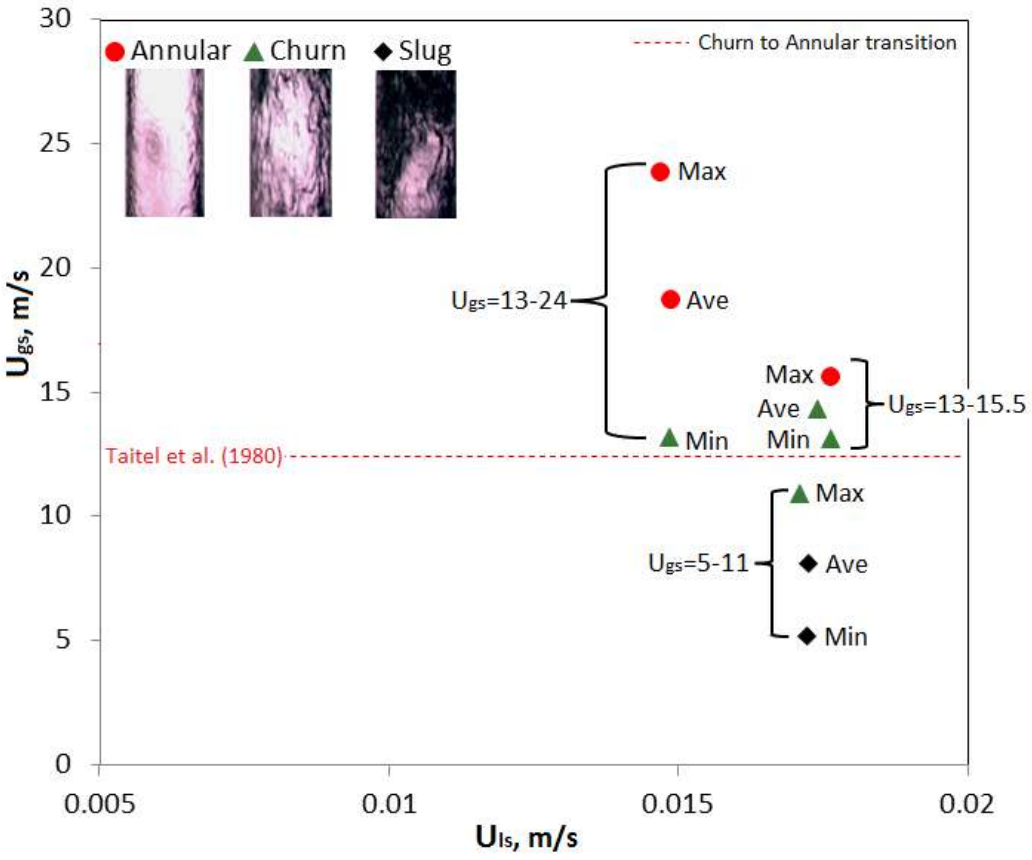

Figure 3.3 Flow regime characterization for low liquid content U_{ls}=0.017 m/s under oscillatory conditions at 130 Kpa. Maximum, minimum and average points for each gas flow rate range from the experimental observations were plotted.

For U_{ls}=0.3 m/s only two flow regimes were identified, slug and churn flow, see Figure3.4. Under U_{ls}=0.3 m/s only one flow regime was observed during each range of gas variation. One reason that can explain the differences on behavior between the two liquid velocities is that for U_{ls}=0.017 m/s the system requires less energy to reach the following flow regime due to the significant lower amount in liquid content. Also with the rapid variation of pressure and velocity in space and time due to the oscillation, for the U_{ls}=0.3 m/s may take more time to perceive the change in pressure and liquid holdup, therefore there are not changes in flow regime.

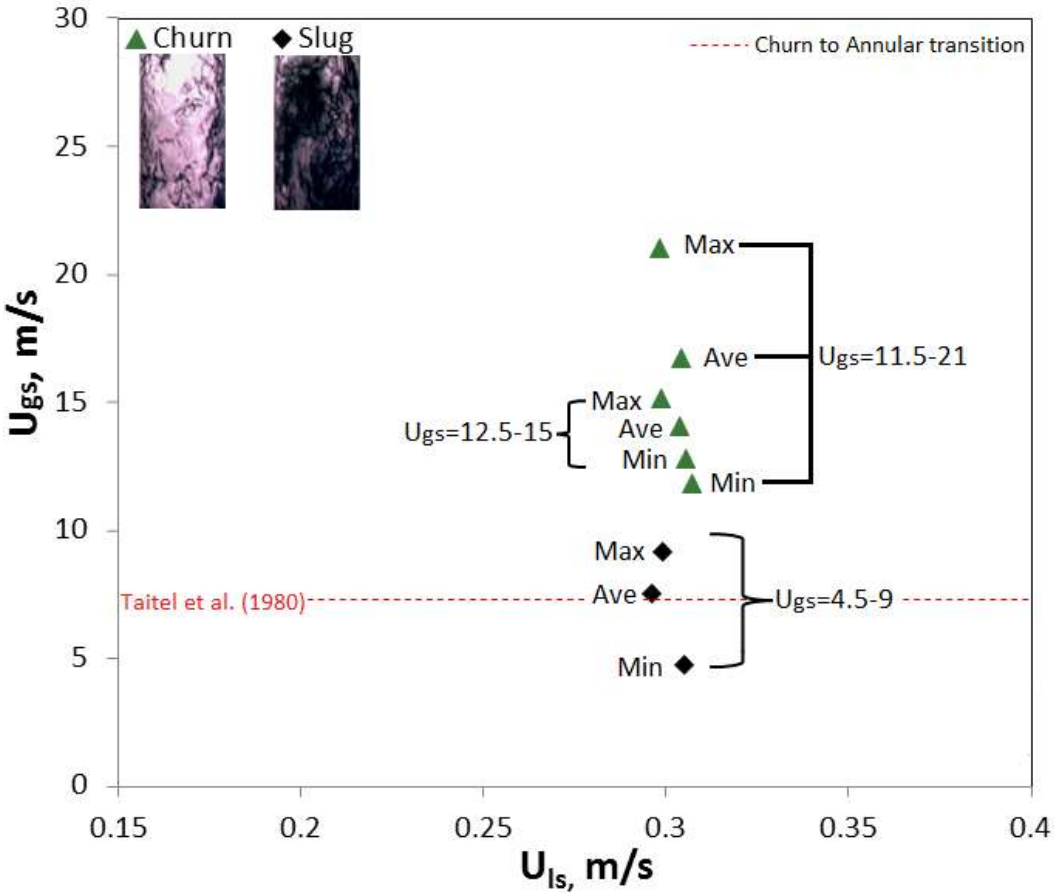

Figure 3.4 Flow regime characterization for high liquid content U_{ls}=0.3 m/s under oscillatory conditions at 210 Kpa. Maximum, minimum and average points for each gas flow rate range from the experimental observations were plotted.

A churn to annular transition model was included in each diagram to have a reference of steady state behavior. According to the results in Figure 3.3 and Figure 3.4, it was found that Tailet et al. (1980) did predict the transition zone between churn to annular flow for U_{ls}=0.017m/s taking into account that this model was developed for steady-state conditions and in this investigation it is being applied to predict transient conditions. The discrepancy between the model and the experiments for U_{ls}=0.3 m/s were much higher predicting annular flow for almost all the data. Minami and Shoham (1995) reported similar conclusions with respect to the lack of performance of the steady-state Taitel et al. (1980) model to predict flow regimes under oscillatory conditions for larger amount of liquid.

For the six different conditions analyzed in this investigation, three flow regimes were identified: slug, churn and annular flow. Table 3.4 summarizes the flow regimes found and the average liquid wave frequency in each scenario. The average liquid wave frequency was obtained from the analysis of 5.5 seconds videos. A wave structure was counted when a large liquid structure wave passed through the camera. The more details of such large liquid structures can be found in Waltrich et al. (2013). Annular flow is characterized for having two types of waves as was mentioned in the literature (disturbance and ripple waves). However, to calculate the frequency of the waves for annular flow, this study only took into account the disturbance waves as a flow structure. This approach was selected for two reasons. First, the disturbance waves are the responsible for carrying the liquid upward. Secondly, slug and churn flow regimes do not have two different types of waves.

Table 3.4 Summary of the observed flow regimes and wave frequency under oscillatory conditions.

Sets	*Water Velocity (m/s)*	*Air Velocity range (m/s) z/D=437*	*Flow regimes*	*Average liquid Wave Frequency Hz*
Low Liquid content	0.017	5-11	Slug-churn	1.7
		13-15.5	Churn-Annular	1.3
		13-24	Churn-Annular	1.5
High Liquid content	0.3	4.5-9	Slug	1.8
		12.5-15	Churn	2.8
		11.5-21	Churn	1.8

Liquid Holdup

The local liquid film thickness was measured for three different positions 102D, 521D and 815D under several transient gas flow rate conditions. The time variations of the local film thickness measured in oscillatory conditions were used to estimate the liquid holdup. The effect of forced gas flow oscillations on the liquid holdup was then analyzed.

It was observed from the experimental results that the local liquid holdup and the amplitude of the large liquid structure waves decreased with distance from the inlet. A typical behavior of the liquid holdup with respect to time and for different positions is shown in Figure 3.5. The decrease of the liquid holdup and wave frequency in the axial direction followed a similar trend also observed by other investigators for vertical two-phase flow systems (Waltrich et al. 2013, Hazuku et al. 2008, Okawa et al. 2010). The axial decrease in liquid holdup can be explained based on the increase of gas velocity and shear stress due to the pressure drop along the pipe. The high frequency fluctuations seen in Figure 3.5 are characteristic of the flow and are also present in steady-state.

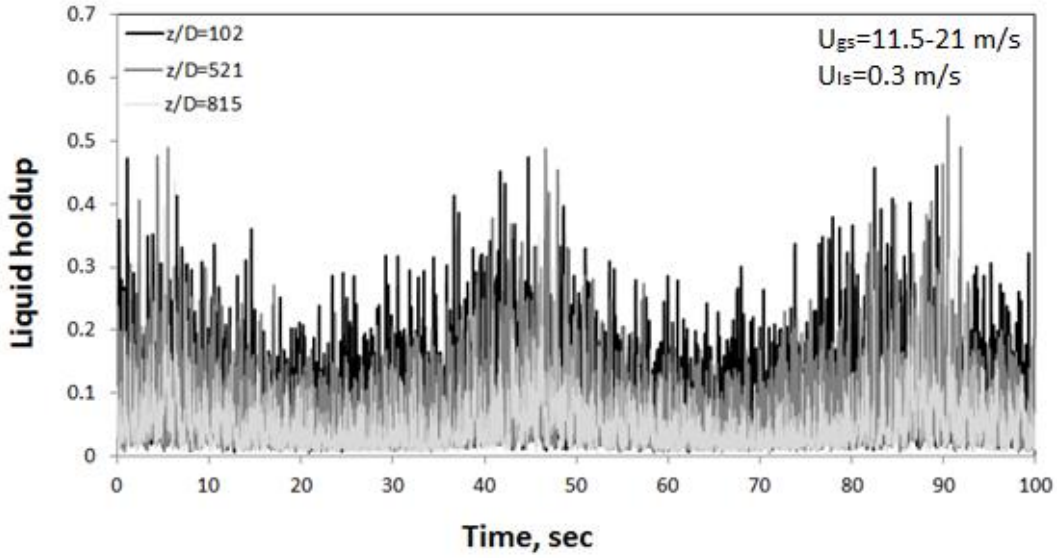

Figure 3.5 A typical time variation of liquid holdup under oscillatory conditions at 210Kpa.

Under steady-state conditions, the liquid holdup increases with a decrease in gas flow rate (as seen in Figure 2.5). Under oscillatory conditions, a similar behavior was expected when the gas flow rate reached the wave minima under a constant liquid rate. In this study the experimental results showed that, for U_{ls} = 0.3 m/s, the liquid holdup behaved similar to steady-state conditions. An example of this behavior is presented in Figure 3.6 *c* and was observed only at the first sensor (z/D=102). The liquid holdup decreased when the gas flow rate was increasing and it reached its maximum when the gas flow rate was lowered at its minimum. .Figure 3.6 *a* and *b* also shows the other two local measurements of liquid holdup along the pipe. These other two measurements of the liquid holdup did not exhibit a specific pattern, but they revealed a time delay in the waves with respect to the initial behavior.

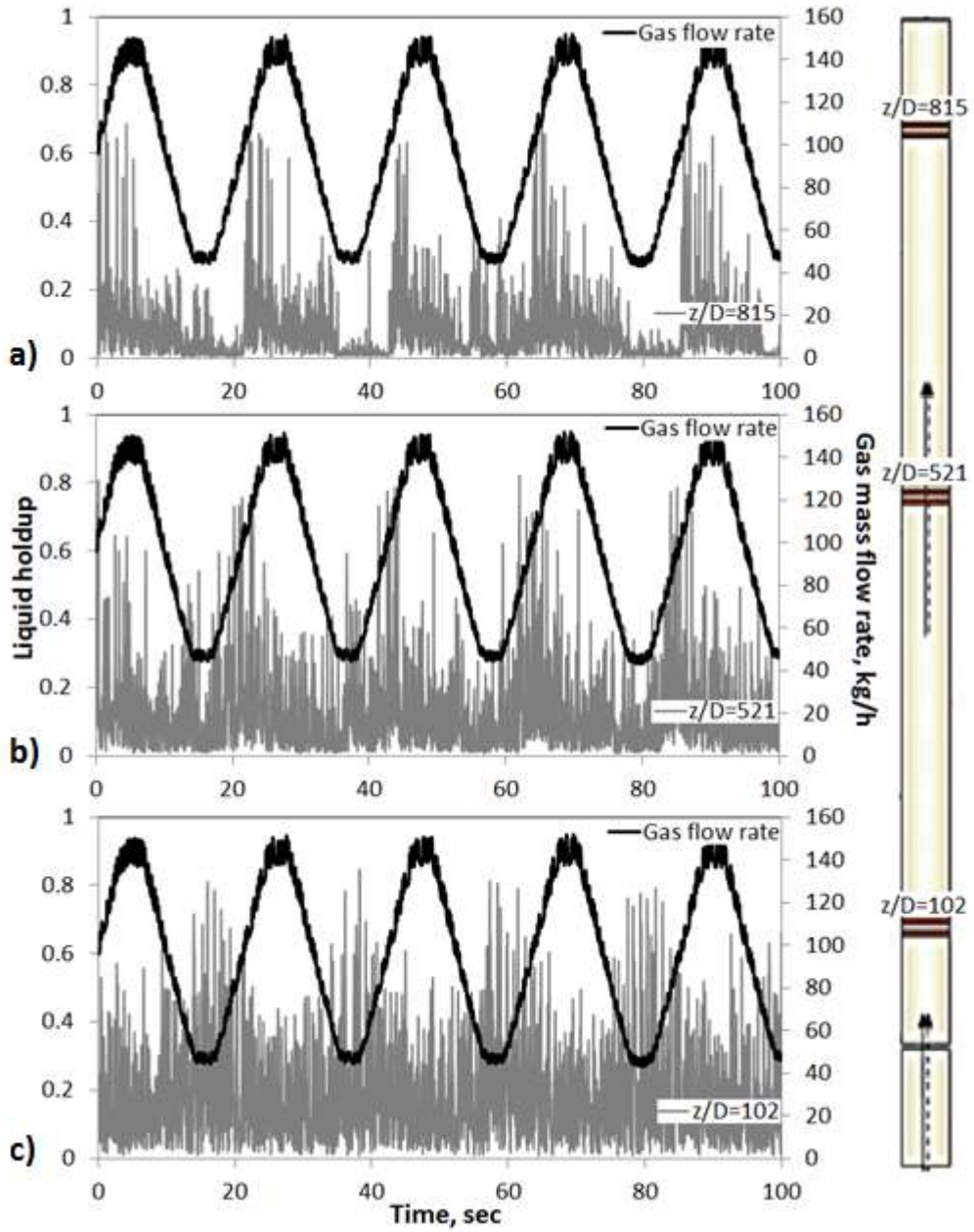

Figure 3.6 Representation of the liquid holdup time delay as a function of position under inlet gas flow oscillations.

This delay in the liquid holdup can be associated to the density wave oscillation mechanism. This mechanism involves interactions and delayed feedbacks between the inertial of the flow and compressibility of the two-phase mixture. Due to the nature of the present experiment where the gas flow rate was constantly changed at the inlet, the fluid waves were

alternative higher and lower density mixtures and traveled through the system, delaying the transient distribution of pressure drops along the tube (March-Leuba 1992). The time delay was characterized reading the approximate time when the liquid wave began to increase. The beginning of the wave formation was compared for each position with respect to time. Differences on time with respect to position were observed in the formation of the wave for all the gas variations at U_{ls} = 0.3 m/s. Figure 3.6 shows the time delay of the liquid holdup from the bottom to the top on the pipe for U_{ls} = 0.3 m/s and U_{gs} = 4.5-9 m/s. The time delay was estimated to be 6 seconds for those conditions. For U_{gs} = 12.5-15 m/s the time delay was approximately 5 seconds. To estimate the time delay of this last scenario a moving average trendline was applied with a frequency of 25 Hz. The trendline was implemented due to the difficulty of the reading caused by the high frequency oscillation characteristic of the two-phase flow behavior. For U_{gs} = 11.5-21 m/s the time delay observed was 5 seconds too.

Figure 3.7 presents the time variations of the local liquid holdup (z/D=102) and the forced oscillations in gas flow rate at a low and constant liquid rate (U_{ls} = 0.017 m/s). As can be seen from the figure, it was found that the local liquid holdup decreases while the gas flow rate is lowered for all three tests where the gas flow rate was changing. This behavior was the opposite of the steady-state response, as it was explained in the literature review (see), and also had a contrary respond compared with the oscillatory experiment for U_{ls} = 0.3 m/s. The fact that the liquid holdup is decreasing while the gas rate is being lowered was associated with the geometrical arrangement of the phases, and the expansion of the gas. This unexpected phenomenon in Figure 3.7 can be explained by the effect of the forced oscillations, as illustrated in Figure 3.8

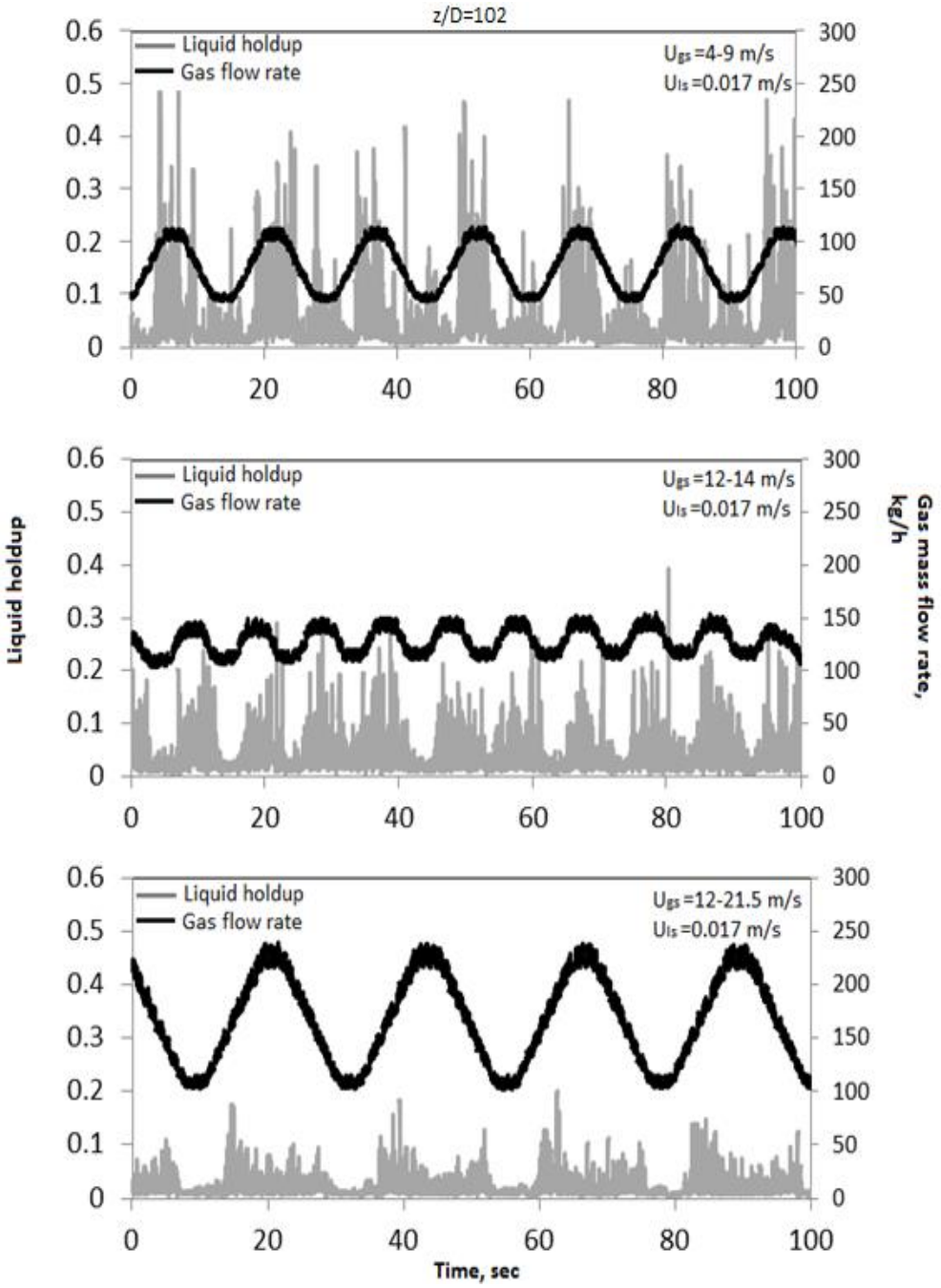

Figure 3.7 Time variation of the inlet gas mass flow rate and liquid holdup under oscillatory conditions at 130 Kpa and a constant liquid mass flow rate of 109 kg/h (U_{ls}=0.017m/s).

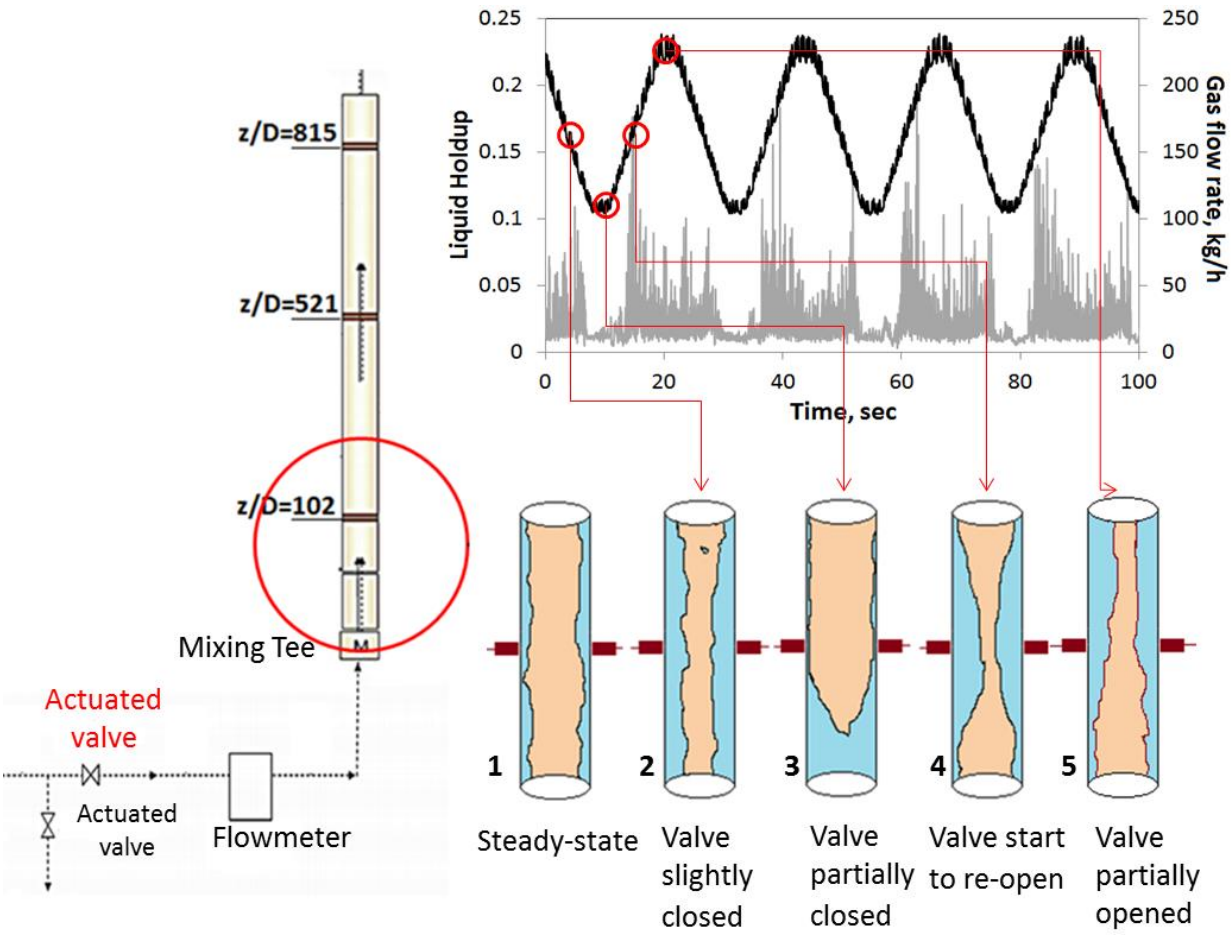

Figure 3.8 Time variations response of the liquid film thickness under low superficial liquid velocity conditions.

The experimental procedure of the oscillatory runs consisted of an initial steady-state period Figure 3.8-*1*, followed by an oscillatory period Figure3.8 *2-5*. The following steps described the liquid film respond at z/D=102 with respect to the gas variation.

1. The experiments were run first under steady-state conditions for at least five minutes under the assumption that after that amount of time the flow was fully developed.
2. For this particular case showed in Figure 3.8, the steady-state condition was run at the maximum of the gas flow rate of this gas variation range. When the valve was been slightly closed the sensor started to read a thicker liquid film because the liquid in the

pipe began to fall back due to a decrease in the gas velocity which lowered the gas-liquid interfacial friction.

3. In this step, the minimum valve opening was reached and the liquid that was falling started to accumulate in the bottom of the pipe under the sensor. The amount of liquid injected and accumulated in the bottom of the pipe was not enough to fill the length of the pipe until the first sensor. As a result, the liquid film read by the sensor was thinner when the gas flow rate was decreased.
4. When the valve began to reopen, the increase in the gas flow rate pushed the liquid accumulated in the pipe up creating a big wave or a liquid slug that passed by the first sensor. The liquid flowed upwards as a consequence of the increase in gas velocity and larger interfacial shear stress.
5. Finally, when the gas flow rate reached their maximum for the experiment, the sensor still read a thicker liquid film in comparison with the reading in third step, but lower than the fourth step. At that moment the liquid was still pushed up by the gas, but the energy given to the liquid when the gas velocity started to increase carried up a larger amount of liquid. The cycle began again.

Similar type of behavior has been found in the literature describing flooding mechanisms. Flooding may occur when liquid is found beyond the liquid inlet (Vijayan et al. 2001). Due to the nature of the current experiments where the liquid is already in the pipe before oscillations begin, flooding mechanisms are a reasonable explanation. Different types of flooding mechanism have been identified depending on forms of the liquid outlet (Govan et al. 1991) or tube diameter (Vijayan et al. 2001).The mechanism that most closely approximates the behavior of the liquid holdup has been called flooding, which occurs by upward transports of ring-types waves.

Vijayan et al. (2001) explains that at low air flow rates the air does not cause any disturbance to the liquid film and thus falls down due to gravity. If the air flow is increased, large amplitude waves are created on the interface around the pipe near the liquid outlet. In the current case, instead of the waves being formed close to the outlet, they are generated near the sensor. If the amplitude of the waves is large enough bridging may occur.

Pressure Variation

Typical time variations of the pressure drop measured under oscillatory conditions are shown in Figure 3.9 for U_{ls}=0.017 m/s and Figure 3.10 for U_{ls}=0.3 m/s. The results have shown that the pressure experienced two types of fluctuations, high and low frequency. The high frequency oscillation has been related to the nature of the flow and they are also present under steady-state conditions. For all the cases, the gas flow rate was oscillated sinusoidally. The low frequency of the pressure observed in the experiments has been associated to the effect of the inlet gas flow rate oscillation on the pressure. Figure 3.9 represents an example of the pressure oscillation for U_{ls}=0.017 m/s experiments. The graph shows that the low frequency component of the pressure in the pipe oscillates in phase with the inlet gas flow rate and it superimposes the high frequency oscillations. The sinusoidal behavior of the pressure indicates that the tubing pressure is governed by gas flow rate oscillations due to it oscillates at the same period that the gas flow rate. The graph also illustrates that both the pressure and the amplitude of the oscillation were a function of position, decreasing with an increase in length. Those behaviors were found for all the cases investigated.

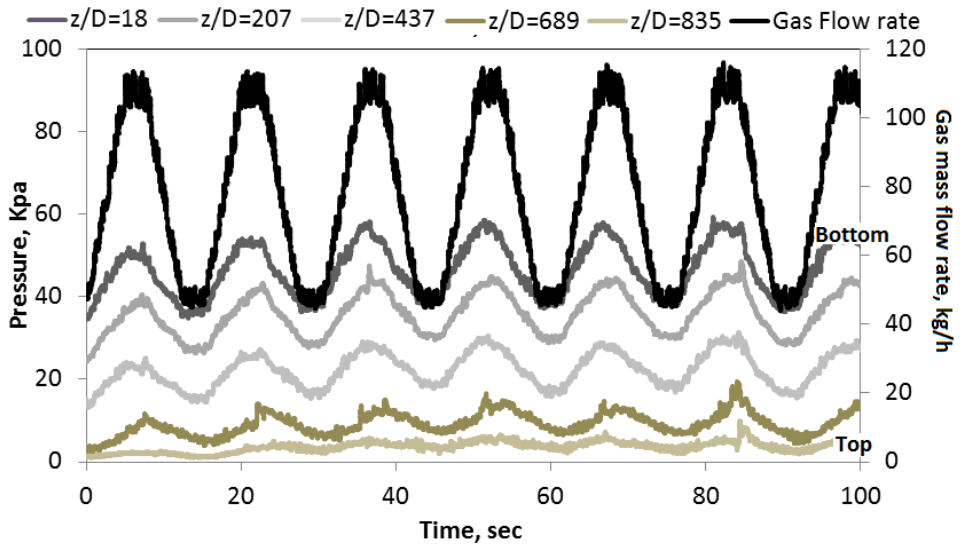

Figure 3.9 Time variations of the inlet gas flow rate and local pressure under oscillatory conditions at 130 Kpa, Q_L=109 kg/h (Uls=0.017m/s) and Qg=47-106 kg/h.

Figure 3.10 describes the typical influence of the gas variation on the local pressure for U_{ls}=0.3 m/s. Two of the three cases studied at this constant liquid were found to oscillate in phase with the gas flow rate, and on the other case (U_{gs}=11.5-21 m/s) the pressure oscillation was nearly in phase with the sinusoidal behavior of the gas. Besides the sinusoidal oscillation of the pressure induced by the gas, the high frequency oscillation observed on the experiment increased with position its amplitude and period with an increment in the gas flow rate, as is shown in Figure 3.10. The mechanism of the formation of the high frequency pressure oscillations is not completely understood. However, these oscillations may be associated with the passing of large air bubbles that coalesce and form big liquid waves or slugs. The liquid structure propagates downwards and again rises with the gas.

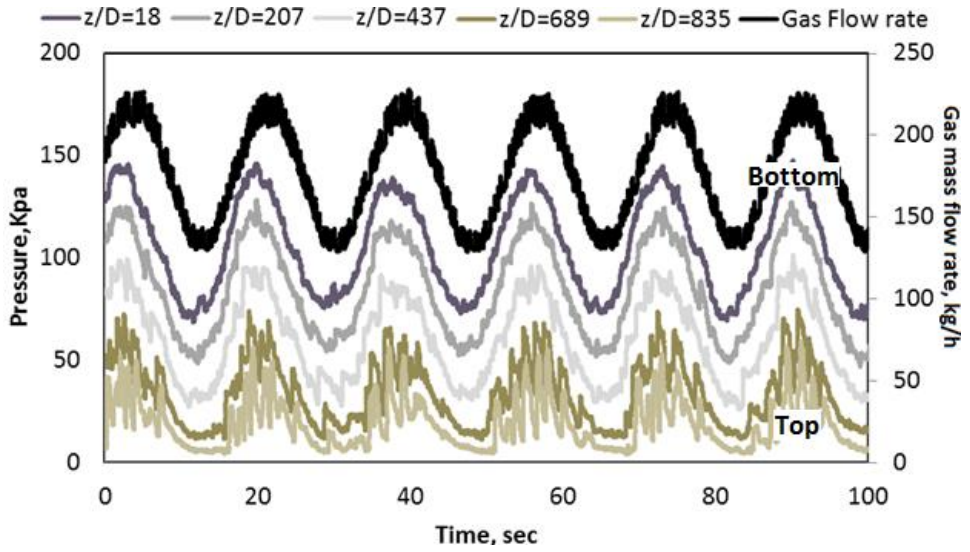

Figure 3.10 Time variations of the inlet gas flow rate and local pressure under oscillatory conditions at 210 Kpa, Q_L=2003 kg/h (Uls=0.3m/s) and Qg=133-214 kg/h.

3.5 Conclusions

The behavior of flow regimes, liquid holdup, and pressure drop were investigated under forced gas flow rate oscillations. From the analysis of the oscillatory experimental data the following conclusions were obtained:

- Slug, churn, and annular two-phase flow regimes flow were characterized under oscillatory condition through video recordings located at four axial positions (z/D= 100, 375, 480, and 820). The comparison between the flow regimes characterized in this investigation and the steady-state transition model Taitel et al. (1980) showed that for U_{ls}=0.017 m/s the model gave a reasonable prediction of the churn-annular flow transition zone, but it should not be used to predict flow regimes for U_{ls}=0.3 m/s.

- For U_{ls}=0.017 m/s it was found that there was a change in flow regime when the gas flow was oscillating, while only one flow regime was observed for U_{ls}=0.3m/s.
- Under oscillatory conditions, the local liquid holdup and the amplitude of its waves decreased with distance from the inlet. This behavior has been previously reported for steady-state experiments.
- For U_{ls}=0.3 m/s, the liquid holdup at position z/D = 102 increased while the gas flow rate was lowered at the first sensor, which is the same behavior under steady-state conditions. The measurements of liquid holdup also showed a delay with respect to the position associated to the density wave time delay created when there are changes in the inlet gas flow rate. In the other hand, for experiments with U_{ls}=0.017 m/s the liquid holdup at location z/D=102 decreased while the gas flow rate was lowered, which is the opposite behavior as in the steady-state conditions.
- The sinusoidal behavior of the pressure indicates that the tubing pressure is governed by gas flow rate oscillations.

CHAPTER 4: COMPARISON OF STEADY- STATE DATA WITH OSCILLATORY CONDITIONS

4.1 Introduction

In the petroleum industry, engineers consider steady-state conditions under the assumption that the magnitude, direction of flow and pressure remain constant over a certain time interval. What this assumption means is that the amount of liquid and gas obtained at the top of the production system should be the same as that coming from the reservoir. When these parameters change due to natural oscillations of gas-liquid flow in pipes, or variations during operations, these assumptions may no longer be considered. In these cases, engineers should begin to consider the system under transient conditions.

Multiphase flow in pipes is a transient phenomenon in nature. Even for constant flow rates of gas and liquid at the inlet of the pipe, periodic oscillations of pressure and liquid holdup will occur along the pipe. However, as these oscillations are steady-periodic variations while keeping the inlet flow rates constant, multiphase flow in pipes can be assumed under steady-state conditions. In the other hand, as described in the introduction, since pressure oscillations are always present in some degree in multiphase flow in pipes and the flow rate coming from the reservoir is proportional to the bottomhole pressure, truly steady-state flow in wellbores may never exist! One can argue that the pressure oscillations in the porous medium in the reservoir may damp the pressure variation from the multiphase flow in the wellbore. However, this subject is still not well understood. Therefore, the characterization of multiphase flow in pipes under some degree of oscillations is essential to evaluate the effect of using steady-state assumptions while analyzing multiphase flow in wells.

The aim of this chapter is to compare experimental data obtained under steady-state and with periodic oscillations of gas flow rate. This investigation considers that valuable information can be obtained from this type of analysis considering that steady-state data are often used to describe multiphase flow in wells that may have some degree of oscillations.

The experiment data for both steady-state and oscillatory conditions comes from the same experimental apparatus. This allows for a more accurate comparison between experimental data from identical setups under both steady-state and oscillatory conditions.

In this section, the comparison between steady-state and oscillatory data include analysis of flow regimes, liquid holdup, pressure gradient. Evaluation of models available in the literature for flow regime transitions and wave frequency analysis will also be discussed in this chapter.

4.2 Results and Discussions

Flow Regimes and Wave Frequency

Figure 4.1 and Figure 4.2 illustrate comparative results that were created to analyze the behavior of the flow regimes under steady-state and oscillatory conditions. The characterization of the flow regimes for steady-state conditions were taken from Waltrich et al. (2013) and plotted with the oscillatory experimental data previously characterized in *Chapter 3*. The minimum, average, and maximum flow rates described in *Chapter 3* were implemented in the graphs and compared with the steady state results. The data are shown as a function of the liquid and gas superficial velocities. Because the characterization of the flow regimes was obtained through videos using the camera located at z/D=437 (see Figure 3.1), the local superficial gas velocity was determined based on that specific location for each test run. The local superficial gas velocities were calculated using the instantaneous inlet gas flow rate and the estimated local

pressure for z/D=437. The linear behavior of the pressure with respect to the length allowed for the estimation of local pressure. Additionally, the graphs evaluated the performance of different models existing in the literature for flow regimes transition. Since only slug, churn and annular flow regimes were observed with this experimental data set, transition models for these regimes only were included in Figure 4.1 and Figure 4.2.

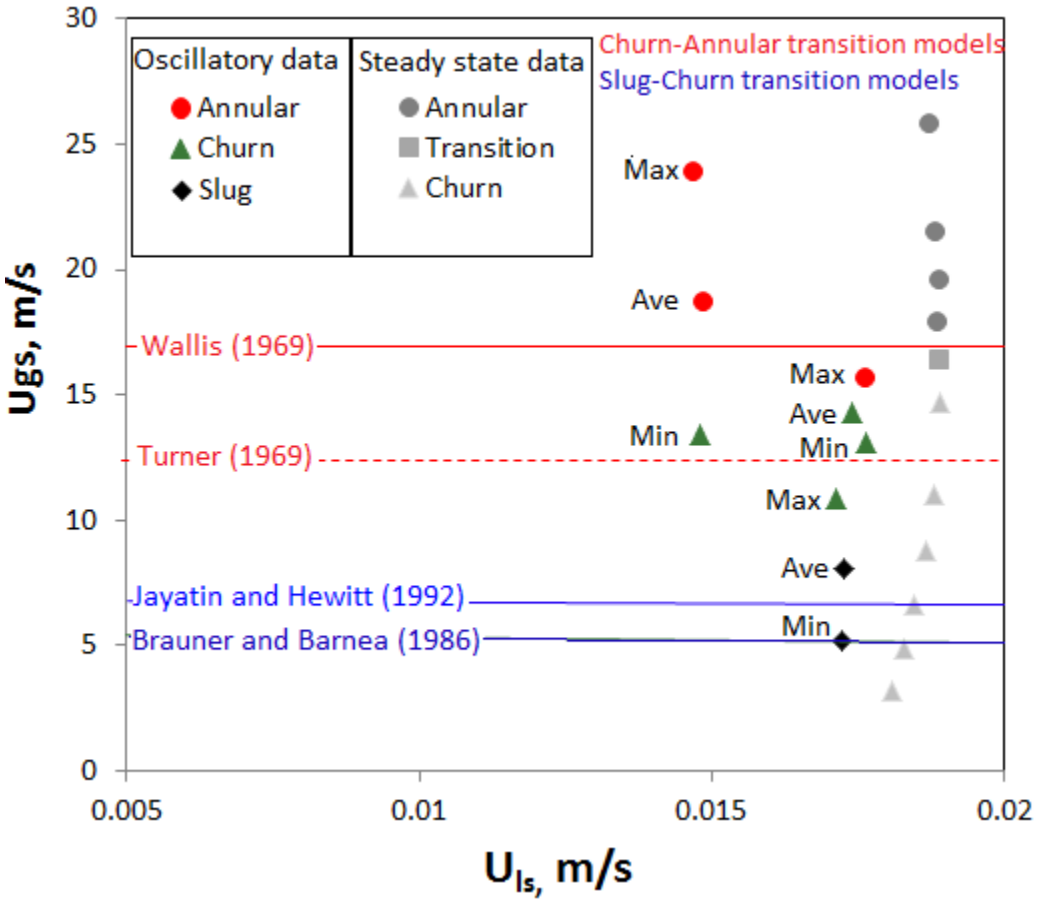

Figure 4.1 Flow regime comparison for steady-state, oscillatory data and transition models at 140 Kpa.

Figure 4.1 presents the comparison between steady-state and oscillatory flow regimes at 140 Kpa. The range of local superficial gas velocities for steady-state conditions was 4-29 m/s, while three different oscillatory ranges were used in the transient conditions including 5-11, 13-15.5, and 13-24 m/s. In this graph is possible to see some differences in between the flow

regimes under steady-state and oscillatory conditions. Under steady-state for the same range of liquid and gas conditions only two flow regimes (churn and annular flow) were identified. On the other hand, for oscillatory conditions three flow regimes were observed in the experiments (slug, churn and annular flow). The differences in behavior seemed to be related to the oscillation of the gas at the inlet, being this the reason of the formation of the slug flow under oscillatory conditions. This conclusion was based on the responds of the liquid holdup under U_{ls}=0.017 m/s were the liquid slug were formed due to an accumulation of the liquid when the gas flow rate was decreased (chapter 3). Therefore, it may be possible to conclude from these experimental results that periodic oscillations of gas flow rate may create slug flow regimes for significant larger superficial gas velocities than in steady-state flow conditions, and shrink the superficial gas velocity range where churn flow can form.

Figure 4.1 also shows the comparison between steady-state, oscillatory data and different transition models at 140 kPa. For the churn to annular transition, two models were implemented: Wallis (1969) and Turner (1969). Wallis criterion had a much better agreement with both steady-state and oscillatory conditions than Turner's model. Taking into account that the models are represented in the graphs by a line when they are actually more like a zone, the Tuner's models can still be considered as a good approximation of churn-annular flow transition model for the current steady-state and oscillatory conditions. For the transition between slug and churn flow, Brauner and Barnea (1986) and Jayanti and Hewitt (1992) were considered. However, none of them matched the steady-state experimental data. On the other hand, both of the models seem to give a reasonable agreement with the oscillatory experimental data, being Jayanti and Hewitt (1992) closer to the transition zone given by the experiments.

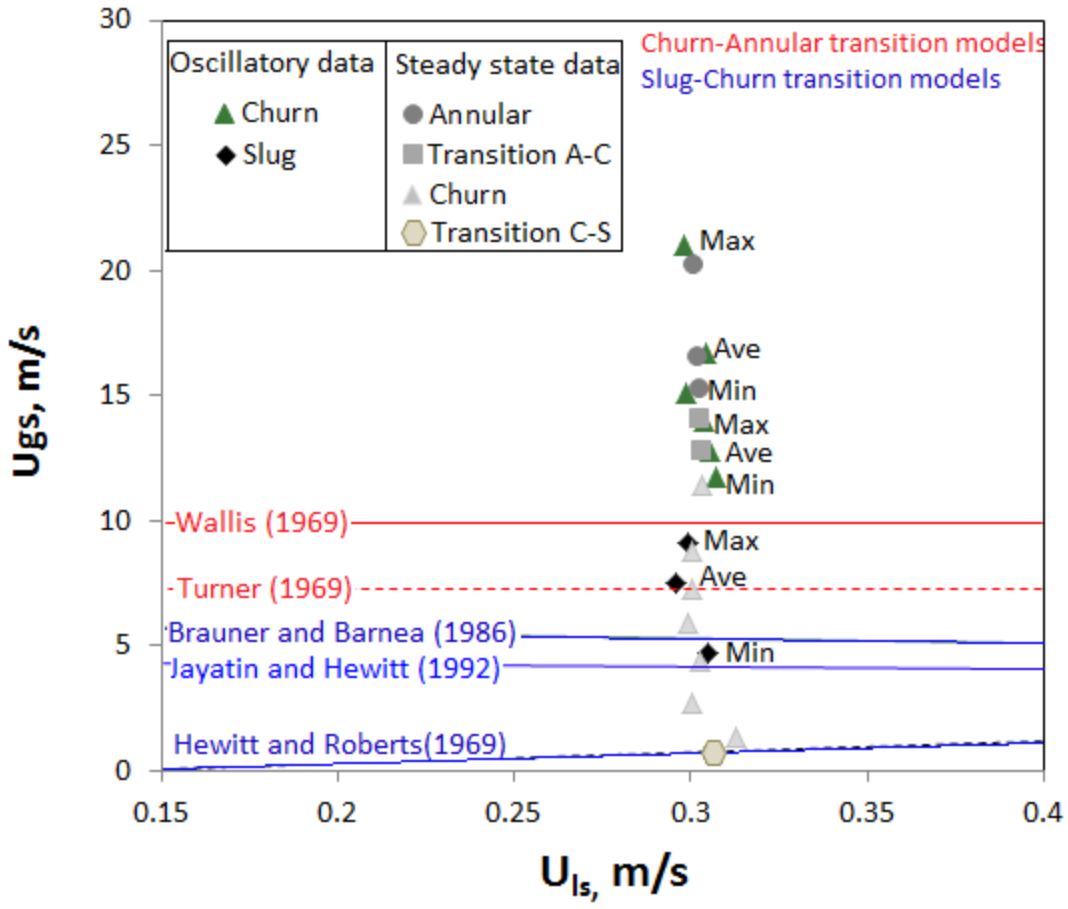

Figure 4.2 Flow regime comparison for steady-state, oscillatory data and transition models at 220 Kpa.

Figure 4.2 presents the comparison again between the characterization of the flow regimes under steady-state and oscillatory conditions. The superficial liquid velocity for both steady-state and oscillatory conditions was 0.3 m/s, and the average pressure was 220 Kpa. The range of local superficial gas velocities for steady conditions was 1-26 m/s and for oscillatory conditions the ranges were 4.5-9, 12.5-15, and 11.5-21 m/s, approximately. For Figure 4.2, the four previous flow regimes models were implemented, but for this case was also included the slug-to-churn transition model of Hewitt and Roberts (1969).

As can be seen from the figure, Hewitt and Roberts model was the only model which matched the steady-state experimental data. However, all models failed to capture the slug-to-churn flow regime transition for the oscillatory experimental data.

Considering only the experimental data in Figure 4.2, the oscillatory data shows that slug and churn flow were observed at much higher superficial gas velocities than commonly found in steady-state conditions. Additionally, annular flow was not visualized at oscillatory conditions.

The main conclusion from Figure 4.1 and Figure 3.1 is that gas flow oscillations have a significant impact of the two-phase flow regimes. Under oscillatory conditions it was possible to observe that much higher superficial gas velocities are necessary to experience the same flow regime when compared to steady-state conditions.

Since the formation and structure of liquid waves are an important characteristic of the flow regimes, the frequency of large liquid structures was analyzed in this study. These analysis have the objective of helping to explain the effect of gas flow oscillations on flow regime transitions, as observed in Figure 4.1 and Figure 4.2. To carry out this analysis, the wave frequency for both steady-state and oscillatory conditions was calculated and plotted as a function of dimensionless superficial gas velocity (U_{gs}^{*}), as presented in Figure 4.3

Waltrich et al 2013 studied the axial effect on the wave frequency fixing the superficial gas velocity at the inlet, and obtained the steady-state data shown in Figure 4.3. These authors concluded that the axial development of the flow did not have a significantly effect on the wave frequency for steady-state conditions.

The methodology used in that investigation was previously proposed by Hazuku et al. (2008), who investigated disturbance waves in annular flow. However, Waltrich et al. (2013) extended the analysis of the later authors to churn and annular flows. In the present study, the Waltrich et al. (2013) analysis was extended as presented Figure 4.3.

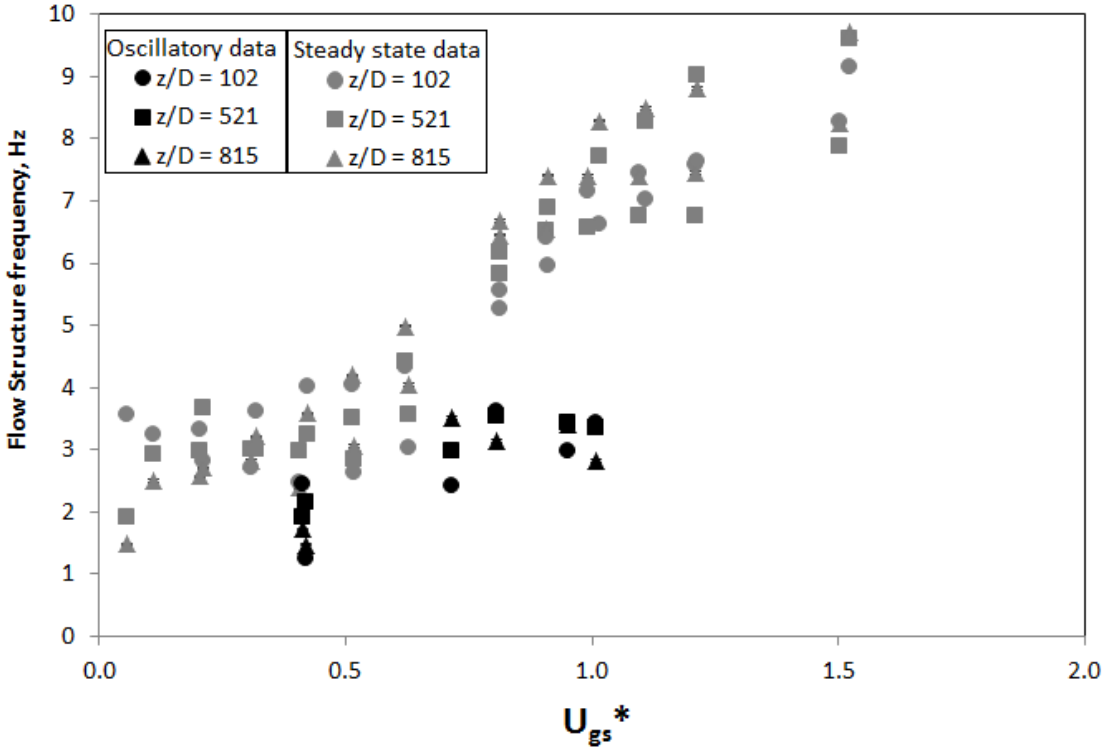

Figure 4.3 The effect of different axial positions in the wave frequency as a function of the inlet dimensionless superficial gas velocity (U_{gs}^{*})

Figure 4.4 shows a comparison between the oscillatory experimental data and three correlations used to predict the wave frequency including Hazuku (2008), Azzopardi (2006), and Sekoguchi (1985). The oscillatory vision label is referred to the visual characterization made through the videos in this investigation.

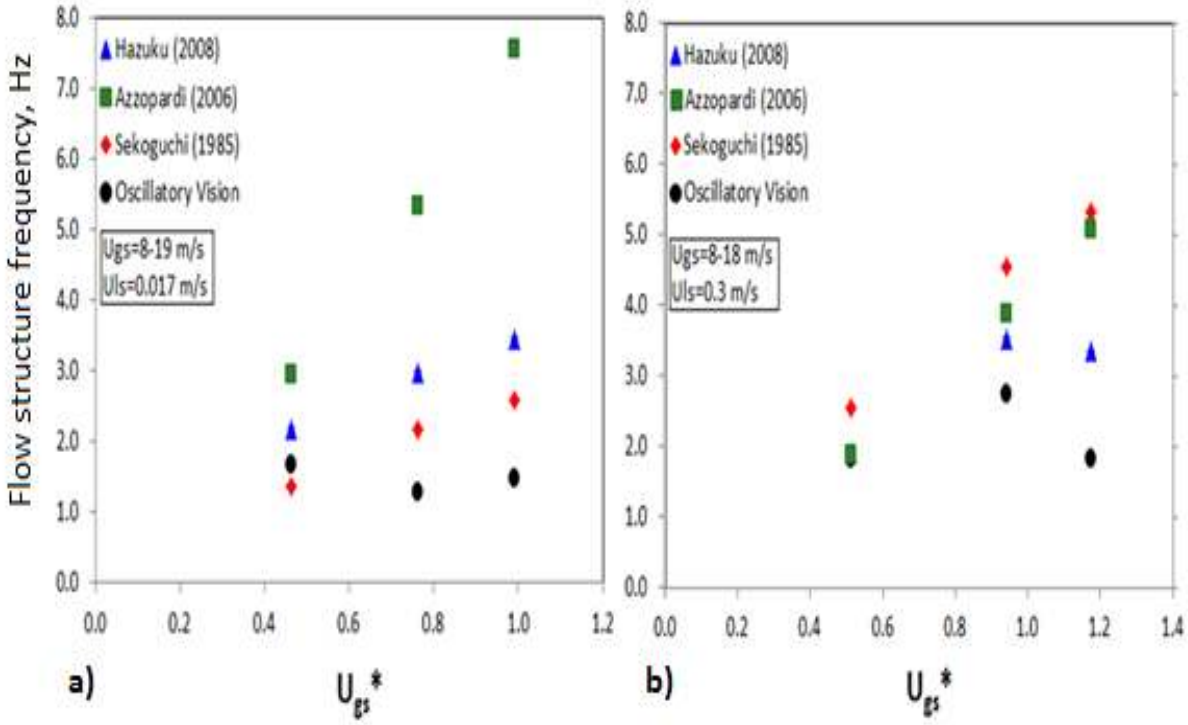

Figure 4.4 Comparison between the experimental observations of wave frequency under oscillatory conditions and models designed to predict wave frequency.

The equations used to implement these models were described in the literature review. After concluding that the axial development of the flow does not impact the wave frequency, the number of waves passing through the camera located at z/D=437 (see Figure 3.1) were counted for a period of 5 seconds obtaining the flow structure frequency. To calculate the wave frequency, each model used the average dimensionless superficial gas velocity at that point. In Figure 4.4 a, the range of superficial gas and liquid velocities were Ugs=8-19m/s and Usl = 0.017 m/s respectively while Figure 0.4 b were Ugs=8-18m/s and Usl=0.3m/s.

As can be seen from Figure 4.4 a, the frequency of the waves do not change significantly with increasing superficial gas velocity for the oscillatory data while the three steady-state models showed a linear growth. The increasing behavior of the wave frequency for higher gas velocities in steady-state is a consequence of the larger interfacial shear stress for larger gas

velocities. This high frequency is responsible for the pumping action that helps to transfer liquids against the gravity and friction forces (Fukano and Ousaka 1989) in annular flow, for example. Sekoguchi's model was previously used by Okawa et al. (2010) to study the wave frequency under annular oscillatory conditions, which in fact provided the closest results to the experimental data from the present work.

Figure 4.4 b, presents a similar analysis but for Uls = 0.3 m/s. The oscillatory data from the present work shows a concave shape. As a result, under oscillatory conditions the flow structure frequency reaches a maximum point and after that starts to decline. These results combined with the characterization of the flow regimes done above (Figure 4.2) showed that under oscillatory conditions annular flow was not present in the experiments. Annular flow is characterized by having a higher flow structure frequency which was not seen under Uls=0.3m/s. Hazuku et al. (2008) is the only model that captures the concave trend and a good agreement with respect to the experimental data, while the other two models still predict linear growth for Uls=0.3 m/s.

The large liquid structures frequency of the experimental oscillatory from this work was compared with the previously published steady-state data. This comparison used the gas Strouhal number as a function of the Lockhart-Martinelli parameter, as is presented in Figure 4.5.

$$St_g = \frac{fD}{U_{gs}} \tag{14}$$

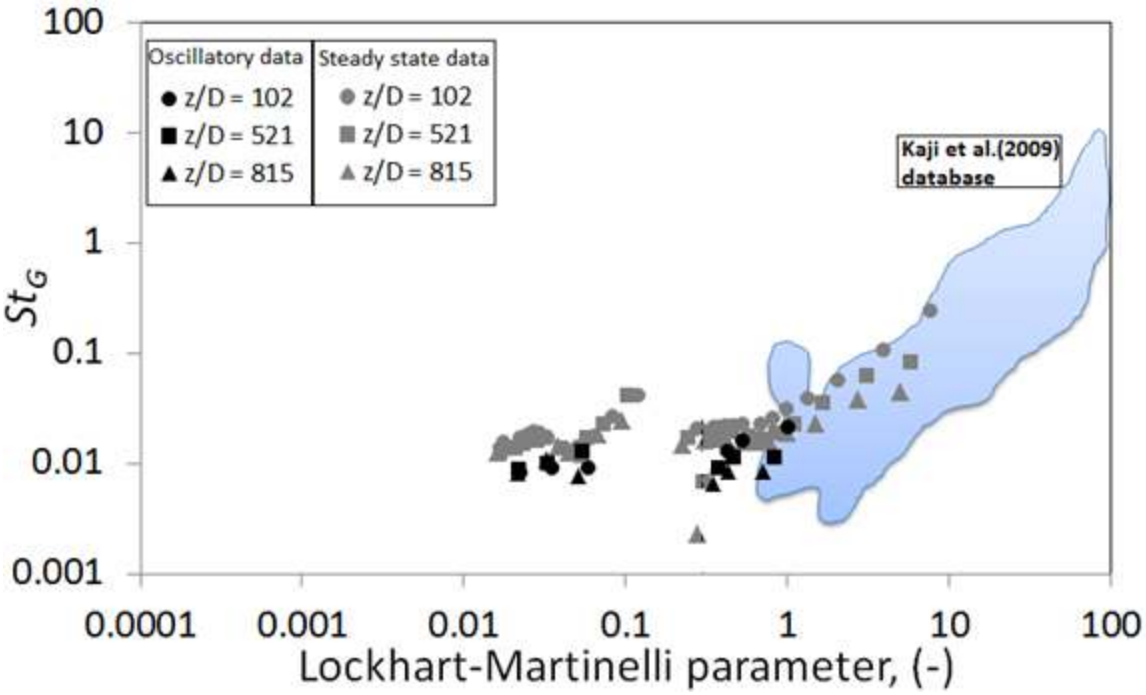

Figure 4.5 Liquid structure frequency comparison using the gas Strouhal number as a function of the Lockhart-Martinelli parameter between steady-state, oscillatory experimental data, and previous published data from Kahi et al. (2009).

The gas Strouhal number was calculated using equation 14, relating frequency with superficial gas velocity. The wave frequency for the steady-state data was not characterized visually. Therefore, the frequency value used for both steady-state and oscillatory experiments was obtained using Hazuku's method. This model has shown an acceptable agreement for both Uls=0.019 m/s and Uls=0.3 m/s on the work of Waltrich et al (2013). For the oscillatory parameters, the average of local measurements was used to calculate the superficial velocities and densities necessary to estimate the Strouhal number and Lockhart-Martinelli parameter.

Figure 0.5 illustrates the reported experimental data from Kaji et al. (2009), where only slug flow conditions were studied. Waltrich et al. (2013) used the analysis by Kaji and extended the analysis to include slug, churn and annular flow regimes. The current study uses this type of analysis to confirm the existence of slug flow under oscillatory conditions in the absences of the

Taylor bubble visualization. Both Waltrich et al.(2013) and Kahi et al. (2009) investigation covered slug flow in their experiments and analysis. The oscillatory data fell into the range of slug flow characterized under steady state conditions.

Liquid Holdup

A comparison between the variation of the liquid holdup with respect to the dimensionless axial position (z/D) for steady-state and oscillatory conditions is represented in Figure 4.6.

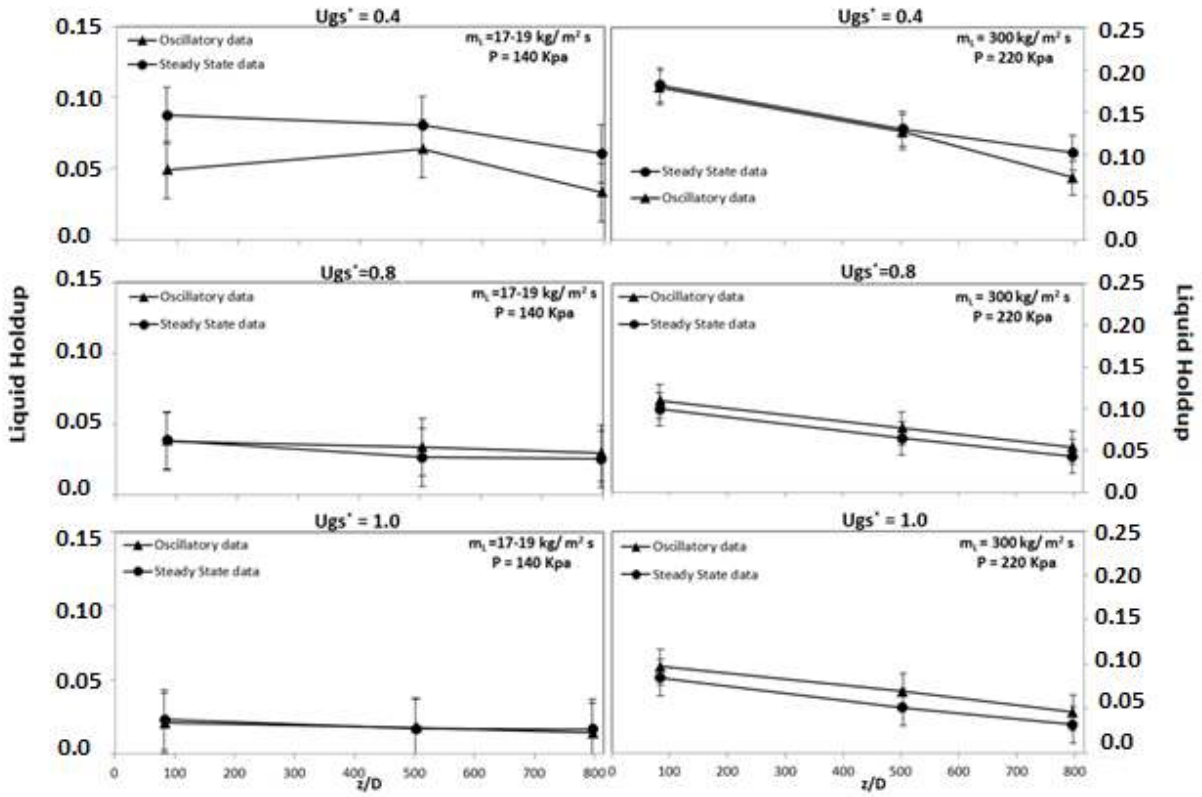

Figure 4.6 Comparison between steady-state and oscillatory liquid holdup behavior as a function of the axial position for three different dimensionless superficial gas velocities.

The time-averaged local liquid holdup was calculated for the oscillatory conditions for three axial locations: z/D = 102, 500 and 800. Three dimensionless superficial gas velocities (0.4, 0.8, and 1.0) were analyzed for Uls=0.017 m/s and Uls=0.3 m/s. The dimensionless superficial

gas velocities were calculated at the inlet to carry out the analysis under the same conditions as Waltrich et al. (2013). The later authors concluded in their investigation that for superficial liquid velocities of Usl =0.3 m/s the average liquid holdup varies considerably in the axial direction, while for Usl =0.019 m/s there was not a substantial variation. Figure 4.6 shows almost no differences in the liquid holdup behavior with respect to the axial position between steady-state and oscillatory conditions for all the dimensionless superficial gas velocities at Usl =0.3 m/s. The same trend is observed on the Usl =0.017 m/s for dimensionless superficial gas velocities of 0.8 and 1.0.

For dimensionless superficial gas velocity of 0.4 in Figure 4.6, the liquid holdup under oscillatory conditions showed a different behavior when compared to the steady-state data. Although the uncertainty bars are overlapping in the middle (z/D=521) and top positions (z/D=815) at Uls=0.017 m/s and U^*_{gs}=0.4, there is a trend of the liquid holdup to be significantly lower under oscillatory conditions than for steady-state at z/D=102. One of the reasons could be that the average superficial liquid velocity for oscillatory conditions is lower (Uls=0.017 m/s) than the steady-state (Uls=0.019 m/s). However, some results from this study indicates that the differences between the liquid holdups are more related to the influence of sinusoidal forced oscillation of the inlet gas flow rate, as can be seen from the pressure gradient results in Figure 4.11. The pressure gradient for oscillatory data is significantly lower than the steady-state data, particularly for lower dimensionless gas velocities at the tube inlet. Hence, the pressure gradient results also indicate that the average liquid holdup for oscillatory conditions is lower than for steady-state data.

Figure 4.7 and Figure 4.8 illustrate the liquid holdup as a function of the local dimensionless superficial gas velocity. Steady-state and oscillatory experimental results of the

liquid holdup are plotted for the three positions (102D, 521D, and 815D) and two different constant liquid flow rates. As reported by Waltrich et al. (2013), the liquid holdup follows an exponential decrease with respect to U^*_{gs} under steady-state conditions. Also, an increase in the liquid holdup is produced by an increment on the liquid flow rate. The authors' analysis was focused on understanding the behavior of the liquid holdup with respect to the axial position. Therefore, the U^*_{gs} used was calculated at the inlet for all the three length with position being the only source of variability.

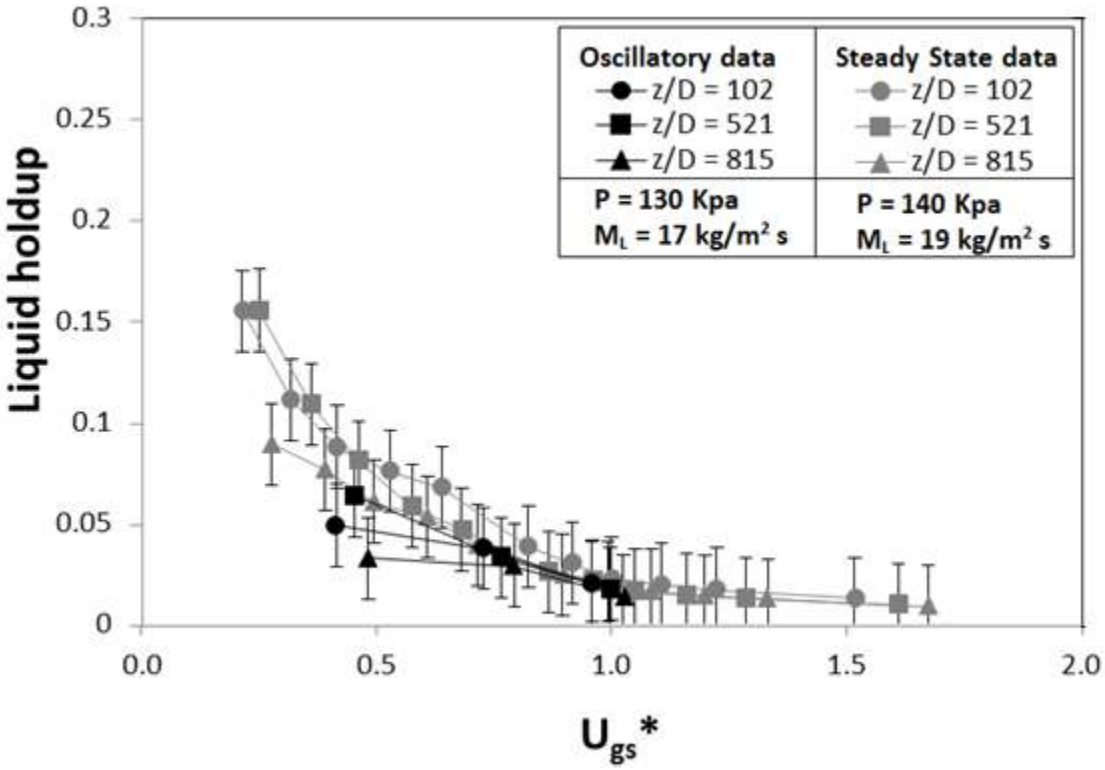

Figure 4.7 Liquid holdup as a function of U^*_{gs} for different positions under steady-state and oscillatory conditions for a constant low liquid flow rate.

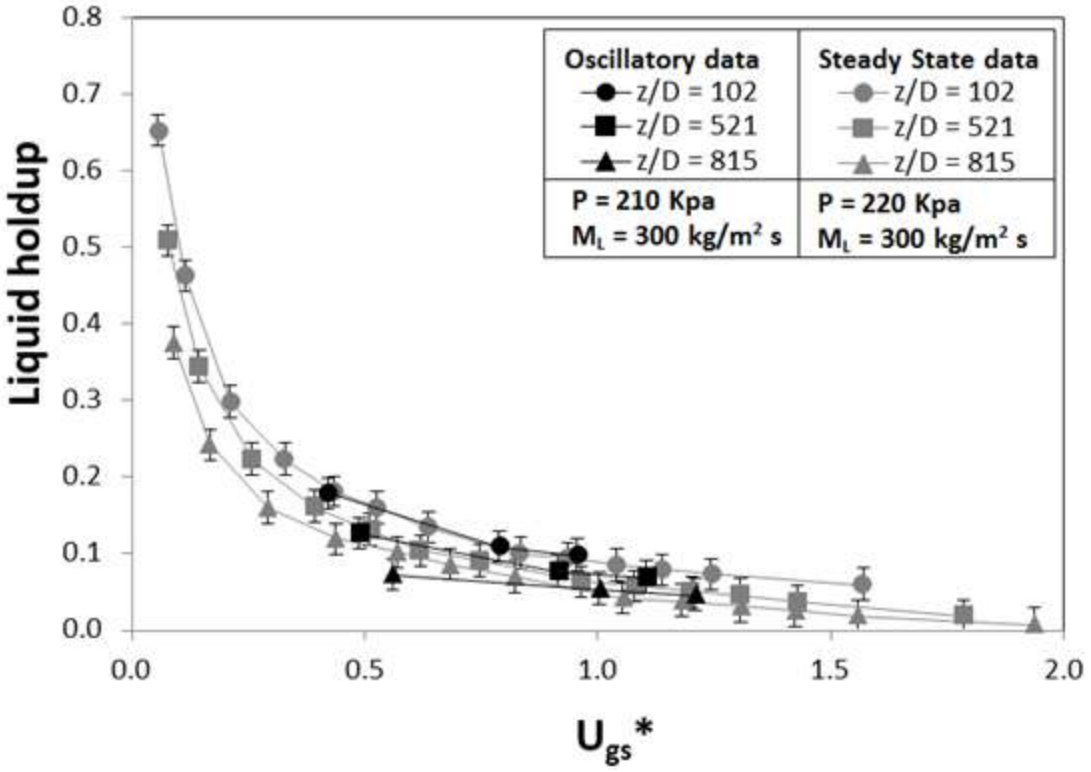

Figure 4.8 Liquid holdup as a function of U^*_{gs} for different positions under steady-state and oscillatory conditions for a constant high liquid flow rate.

The current investigation attempted to analyze the behavior of the liquid holdup taking into account the dimensionless superficial gas velocity for each axial position. Figure 0.7 shows that, for U^*_{gs} >0.3, Usl = 0.017 m/s and for steady-state and oscillatory conditions, the change of U^*_{gs} between 102D and 815D is 10% in average. However, for U^*_{gs} < 0.3 under steady-state conditions, the liquid holdup decreases 40% between 102D and 815D, for an increment of 30% in U^*_{gs}.

For oscillatory conditions, the liquid holdup behaves similar to steady-state conditions. No significant variation in the liquid holdup with axial position was observed for U^*_{gs} >0.3, and the liquid holdup decreases with an increase in the U^*_{gs}. Additionally, the liquid holdup showed very similar values for oscillatory and steady-state data, particularly for Usl = 0.3 m/s as presented in Figure 4.8. However, for Usl =0.017 m/s (Figure 4.7), the trend of liquid holdup for

oscillatory conditions is slightly different than for steady-state data, even though the error band between for data set overlap each other for all dimensionless gas velocities tested. The trend of liquid holdup for the oscillatory data suggests that lower levels of liquid holdup are expected when compared to steady-state conditions, particularly for Usl =0.017 m/s and $U^*_{gs} \leq 0.4$.

For Usl =0.3 m/s experiments, Figure 4.8 indicates that steady-state and oscillatory results behave similarly. For $U^*_{gs} > 0.6$ the liquid holdup does not change considerably with the axial position, even though the U^*_{gs} increases substantially with position. However, for $U^*_{gs} < 0.6$ the liquid holdup showed significant changes with respect to axial location for both steady-state and oscillatory conditions. The dimensionless superficial gas velocity increases 45% on average with axial position, while the liquid holdup variation ranges from 30 to 60%.

The behavior of the average standard deviation of the liquid holdup as a function of the local dimensionless superficial gas velocity for the steady-state and oscillatory experimental data was also investigated, which presented in Figure 4.9. The standard deviation of the holdup declines exponentially with an increase of $U^*_{gs,}$ and increases when the liquid content is incremented for both steady-state and oscillatory conditions. As shown in Figure 4.9, the axial position only has a minor influence on the standard deviation. The large values of the standard deviation represent the constant fluctuation of liquid under Usl =0.017 m/s induced by the nature of slug and churn flow regimes. The periodic forced oscillation of the inlet gas flow rate does not impact the high frequency response of the liquid holdup measurements.

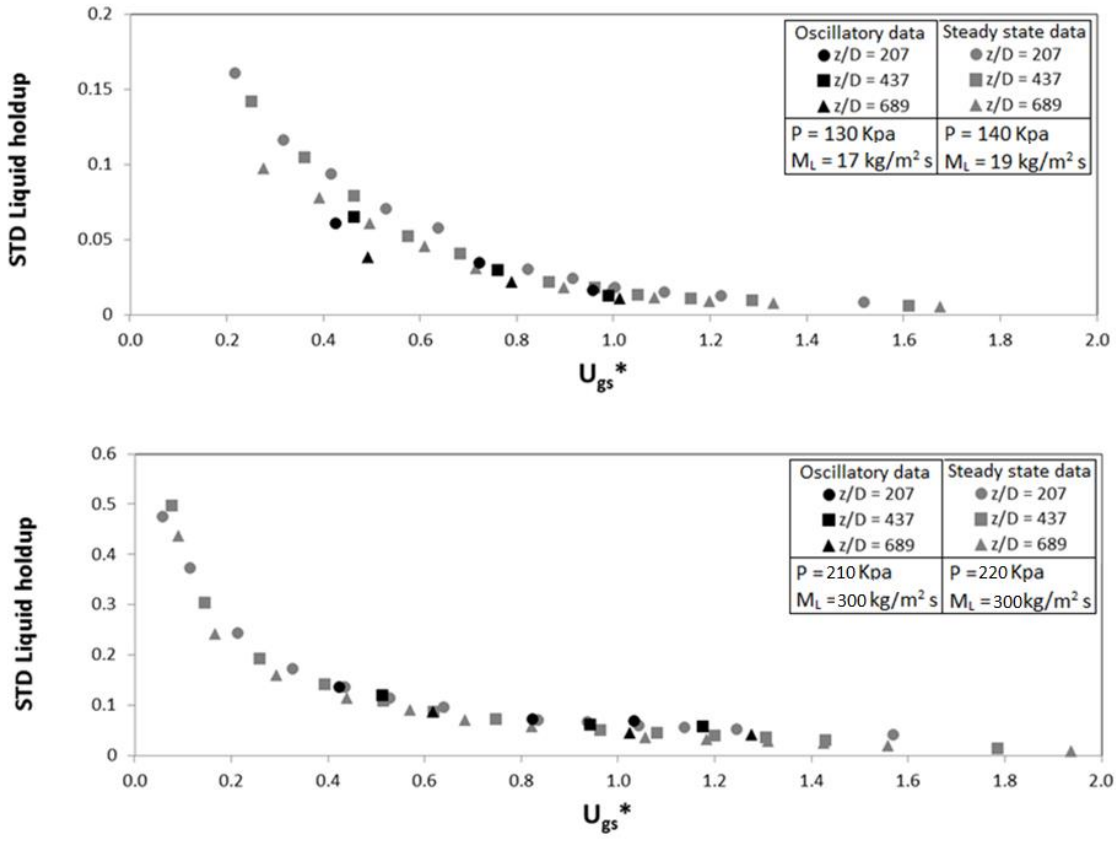

Figure 4.9 Standard deviation of liquid holdup fluctuation measured at three positions as a function of superficial gas velocity.

Pressure Gradient

A comparative study of the pressure gradient for steady-state and oscillatory conditions was investigate. Experimental data for pressure gradient as a function of different parameters such as the axial position, dimensionless superficial gas velocity, and superficial liquid velocity are discussed in this section.

The following procedure was used to calculate the pressure gradient and the other parameters:

- For steady-state, the U^*_{gs} was calculated either with the measurements obtained from the inlet or with local measurements depending on the type of analysis.

- For the oscillatory experiments, the only modification was that the total average of the local pressure measurements were determined beforehand, and then U^*_{gs} was calculated in based on the average pressure for all analyses.
- The pressure gradient was calculated following the same procedure used by Waltrich et al. (2013). Under steady-state conditions, the pressure gradient was obtained from the five local pressure measurements yielding a total of four different pressure gradients. The position z/D=18 was chosen as the reference point (origin). This length was subtracted to all the other lengths. Then, the difference of two consecutive pressure measurements was divided by the distance between these two positions to obtain the pressure gradient for that tube segment. Each pressure gradient was named with the top position of the pressure measurement used.
- Under oscillatory conditions, the procedure to calculate the pressure gradient was the same as the steady-state. However, the local average absolute pressure was first determined. The uncertainty of the pressure gradient was 0.06 Kpa/m and it is included in all the graphs in the form of error bars. For some figures, the error bars are not visible, since the error value under certain scenarios is smaller than the measurement points in the plots.

Figure 4.10 shows the variation of the pressure gradient as a function of the axial position for three different dimensionless superficial gas velocities (0.4, 0.8, and 1.0) and two liquid velocities under steady-state and oscillatory conditions. These specific superficial gas velocities were selected because they were the average of the gas variation ranges study in this investigation. The U^*_{gs} was calculated based on the inlet the pressure. In all cases, an increment in the liquid superficial velocity caused an increase in the pressure gradient.

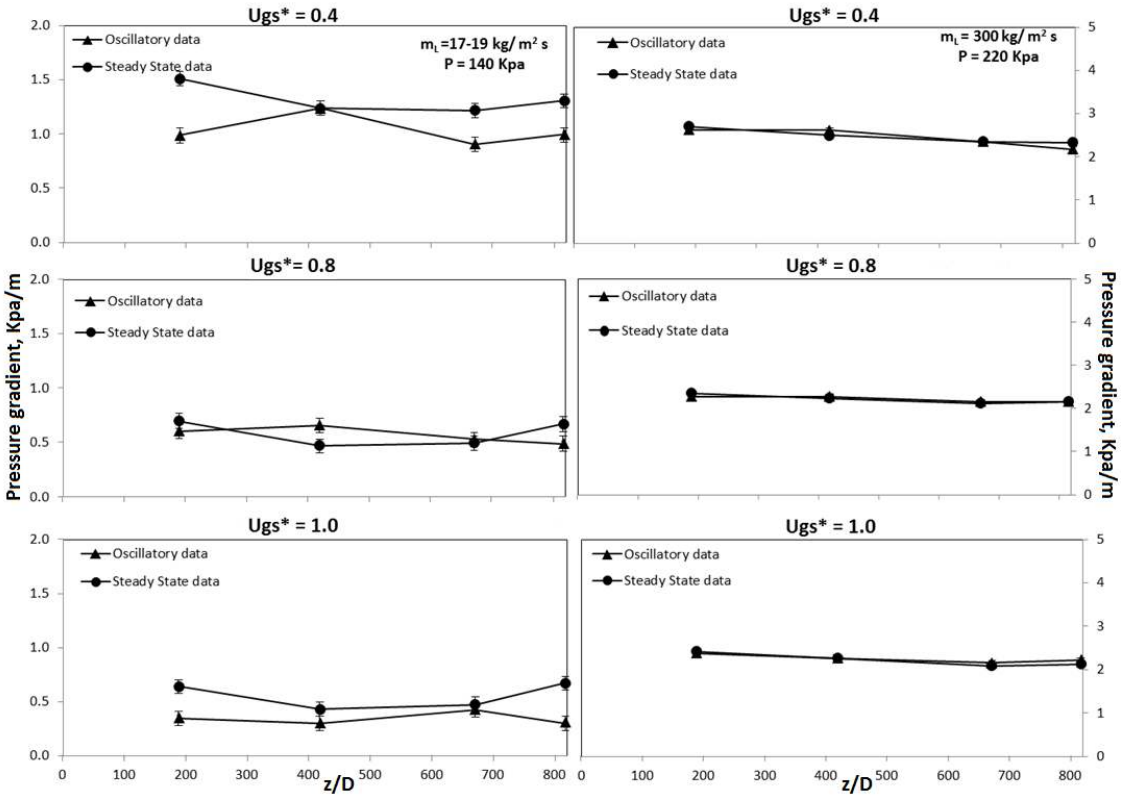

Figure 4.10 Comparison of the pressure gradient under steady-state and oscillatory conditions as a function of the axial position for three different U^*_{gs} for low (Q_L=109-124 kg/h) and high (Q_L=2003 kg/h) liquid flow rate.

The pressure gradient did not show different behavior between steady-state and oscillatory experimental data for Uls=0.3 m/s. Additionally, there was only a small variation in pressure gradient with respect to the axial position for any of the U^*_{gs} evaluated under Uls=0.3 m/s.

For U^*_{gs}=0.4 and Uls= 17-19 m/s the pressure gradient under oscillatory and steady-state conditions behaved different with respect to the position. The pressure gradient was significantly lower for oscillatory than for steady-state conditions in almost all the positions. This trend is supported by the results obtained from the analysis of the liquid holdup, where the liquid holdup was lower for oscillatory conditions than for steady-state at the first sensor (z/D=102).

Moreover, as shown in Figure 0.11for U^*_{gs}=0.4 and Uls= 17-19 m/s the pressure gradient is dominated by the gravitational component which varies considerably with liquid holdup. The pressure gradient variation was not relevant with the axial position for either steady-state or oscillatory experiments and behaved similarly to each other under U^*_{gs}=0.8 and Uls= 17-19m/s. Finally, for the last case of low liquid flow rate for U^*_{gs} = 1.0, the variation in pressure gradient with respect to axial position was not significant in either of the conditions. However, the pressure gradient was lower under oscillatory conditions than on steady-state.

A comparison between the steady-state and oscillatory variation of the local pressure gradient with respect to the local dimensionless superficial gas velocity is presented in Figure 4.11. In Figure 4.10, all the parameters were fixed to analyze the behavior of the pressure gradient with respect to the axial position. However, in Figure 4.11 U^*_{gs} were calculated from the local pressure measurements as the superficial gas velocity depends on the local density, which is a function of the local pressure. Waltrich et al. (2013) concluded that there was only a significant change in pressure gradient with position for U^*_{gs} <0.3. This investigation expand the range of U^*_{gs} where the pressure gradient vary with respect to the position being U^*_{gs} < 0.6. This conclusion is based on the result obtained from the steady-state and oscillatory experimental data. The main difference between the steady-state and oscillatory experimental data seen in Figure 4.11 was for U^*_{gs} =0.4 at z/D=835. The pressure gradient seemed to be significantly lower than the steady-state experiments. This result is correlated with the trend of the liquid holdup showed in Figure 4.7. An explanation of this outcome can be linked with the behavior of the liquid holdup under oscillatory conditions. The wave form at z/D=102 by the increment of gas at the inlet could be pushing the liquid that is accumulated in the bottom of the pipe.

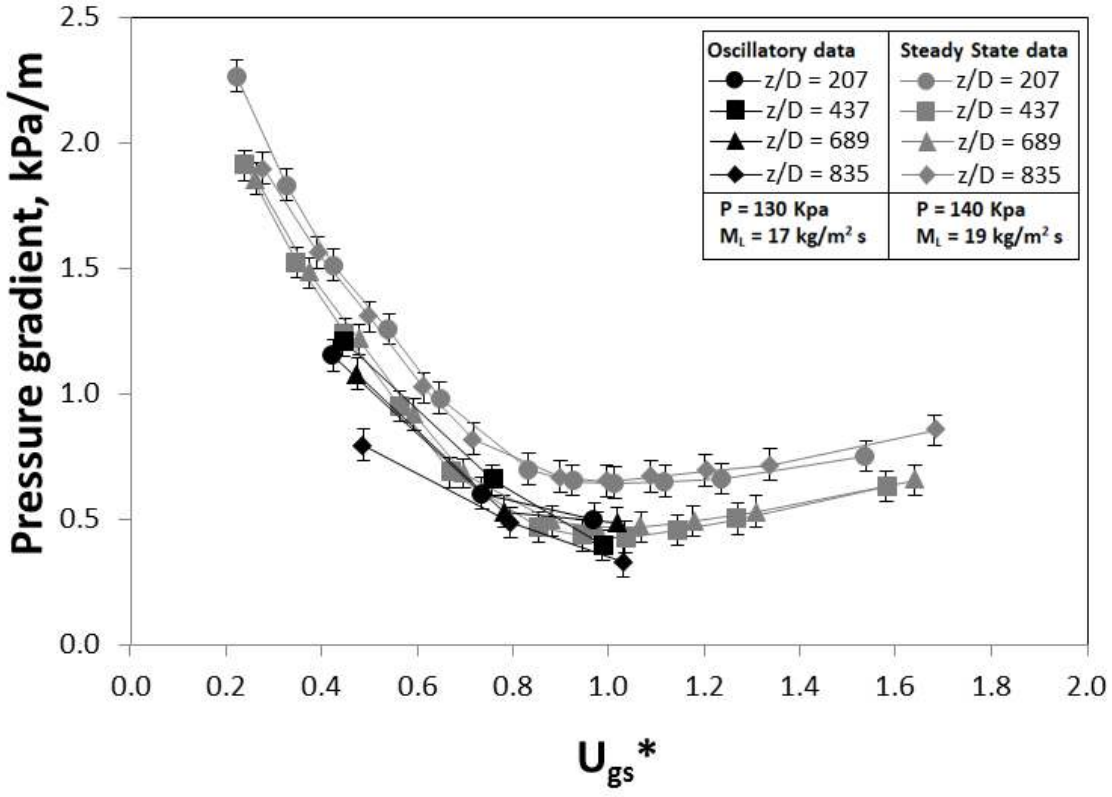

Figure 4.11 A comparison between steady-state and oscillatory result of the pressure gradient variation with respect to the local U^*_{gs} under Uls=0.017-0.019m/s

Figure 4.11 and Figure 4.12 show the total pressure gradient (ΔPt) calculated as a function of the U^*_{gs} for steady-state and oscillatory experiments. Both figures have the aim of discussing in more details the differences between oscillatory and steady-state data for the total pressure gradient, for different superficial liquid velocities.

Figure 4.11 illustrate the total pressure gradient (ΔPt) for Uls=0.017 m/s. The oscillatory results shows a lower pressure gradient for U^*_{gs} =0.48 than for steady-state. A possible explanation of this phenomenon is the effect of the creation of large liquid wave, as described in Figure 4.12. The formation of such wave may facilitate the liquid transport upwards, when the

flow would require less energy to lift liquid upwards, and consequently, decreasing the pressure gradient.

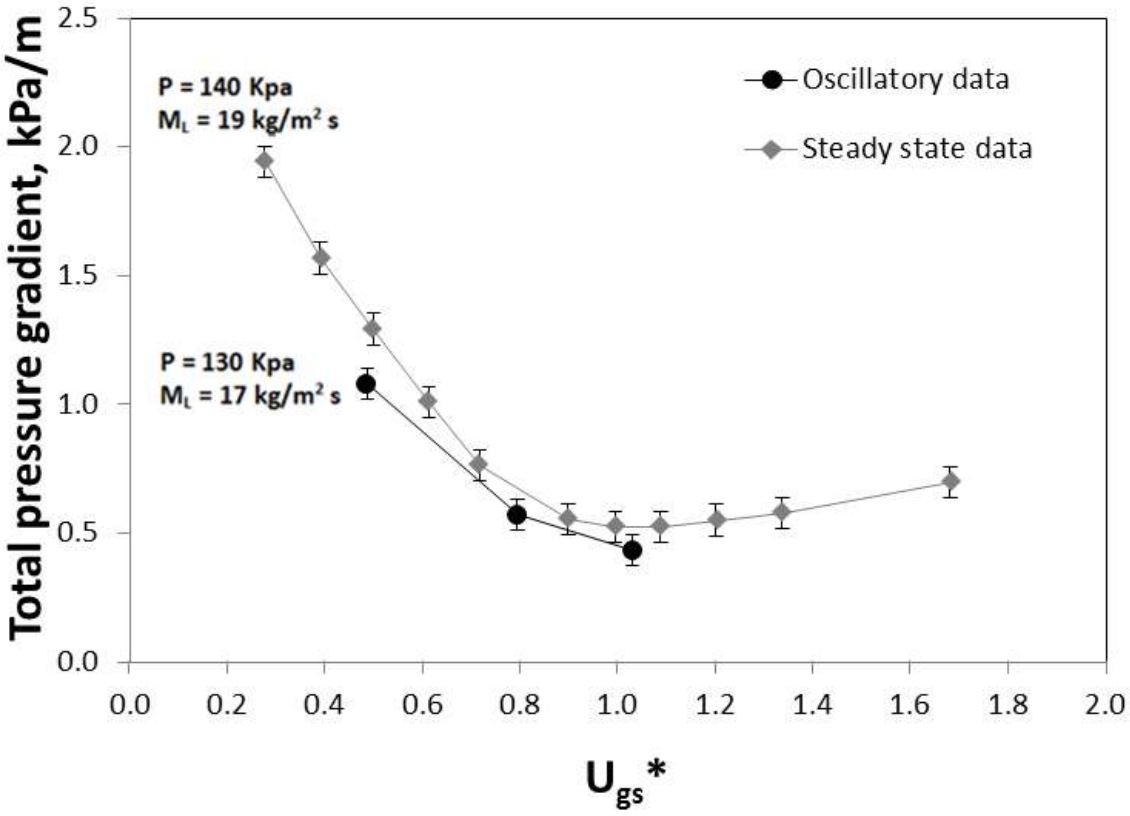

Figure 4.12 Total pressure gradient (ΔPt) as a function of U^*_{gs} for steady-state and oscillatory experiments, for Uls=0.017-0.019 m/s

As descried in Figure 4.8, for lower superficial liquid velocities under oscillatory conditions, a large liquid wave is formed in the bottom of the tube periodically with the gas velocity oscillation. As this wave is formed, the flowing cross-sectional are of gas is decreased, and consequently, the gas velocity will increase significantly. Larger gas velocities will consequently increase the interfacial friction factor, which will in turn provide a larger drag force to lift the liquid wave. After this increment in the drag force, the liquid wave will begin to accelerate as a consequence as a consequence of the larger upward force from the drag force. The liquid wave will then gain a large level of momentum, which facilitates the liquid transport

upwards. Since the liquid transport is facilitated, less energy would be required to lift the liquid upwards, which will in turn decrease the pressure gradient.

As can be seen in Figure 4.11, there is a larger difference for pressure gradient between oscillatory and steady-state data at z/D = 835 than for z/D = 102. This behavior corroborates the idea of large wave formation facilitating the liquid transport upwards, and then, decreasing the pressure gradient. As the large liquid wave is formed in the tube inlet for oscillatory conditions, the wave starts to gain momentum and less energy would be required to lift the liquid in pipe upstream to the point of the wave is formed.

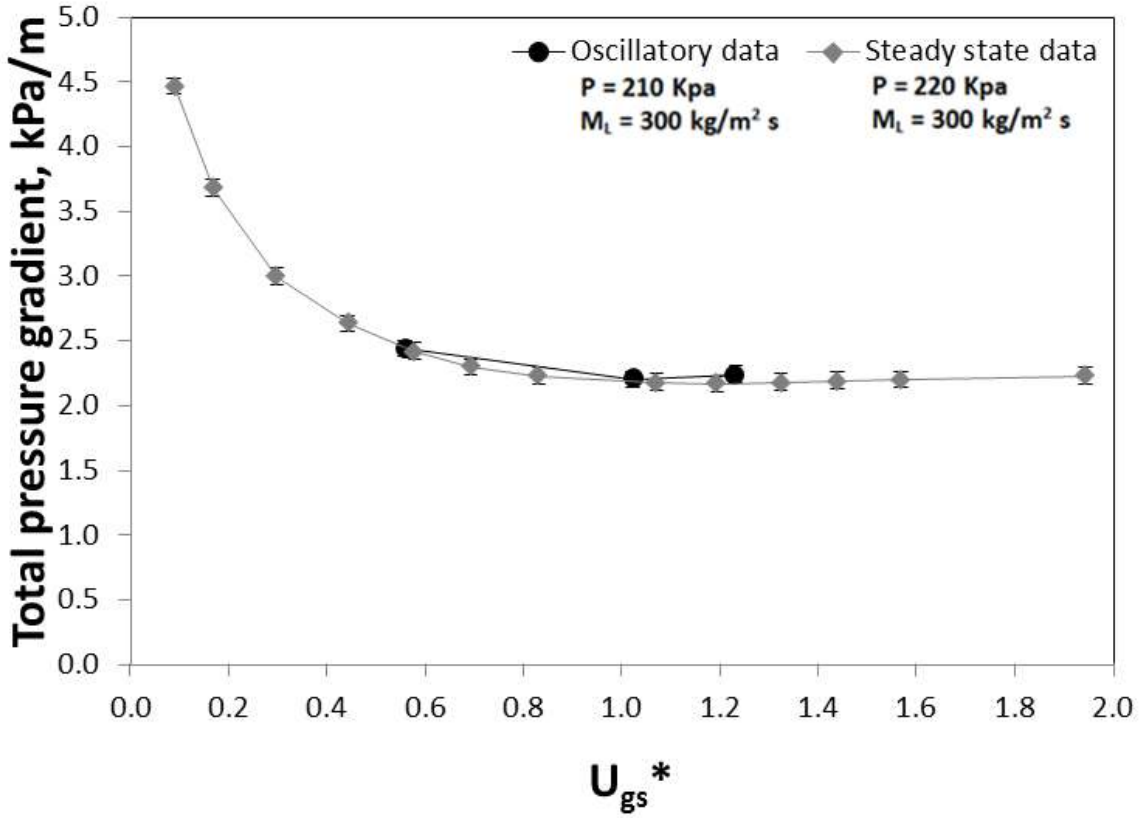

Figure 4.13 Total pressure gradient variation as a function of U^*_{gs} for steady-state and oscillatory experiments at Uls=0.3 m/s.

Figure 4.13 presents the total pressure gradient ΔPt/Δz for Uls=0.3 m/s. As can be seem in the figure, the experiments under steady-state and oscillatory conditions do not expose any difference in the total pressure gradient as a function of U^*_{gs}. One of the possible explanations is similar for the low superficial liquid velocities, as described above. For larger levels of liquid holdup, the cross-sectional area of the gas core is significantly smaller and the creation of a large liquid wave is not possible, since there is not enough space for the wave to grow. Therefore, the oscillation of the gas velocity would not affect the pressure gradient, as showed in Figure 4.13.

The standard deviation of the pressure gradient as a function of the local U^*_{gs} for the steady-state and oscillatory conditions is shown in Figure 4.14. The standard deviation of the pressure gradient decreased exponentially with an increase of U^*_{gs}, for steady-state measurements under Uls=0.017m/s. For Uls=0.3 m/s, the rate of change of the standard deviation with the Usg* is significantly lower. When the liquid velocity is incremented for both steady-state and oscillatory conditions, the standard deviation also increases. For oscillatory conditions and U^*_{gs} <0.6, the standard deviation changes drastically with respect to the axial position, while that for stedady-state there is not a considerable variation with the axial position. One more time, the wave formation at the inlet of the tube for oscillatory conditions can be used to explain the axial variation of the standard deviation of the pressure gradient. As can be seen from Figure 4.14, the standard deviation increased axially, particularly for high superficial liquid velocities and lower Usg*. As the liquid wave is formed at the tube inlet, is disturbs the liquid film and creates pressure disturbances, which can increase the standard deviation of the pressure measurements. As the wave moves upwards, it gains momentum and further disturbs the pressure upstream to the point of the wave formation. Also the constant change in density along the pipe due to the forced oscillation can generate an increment in the standard deviation.

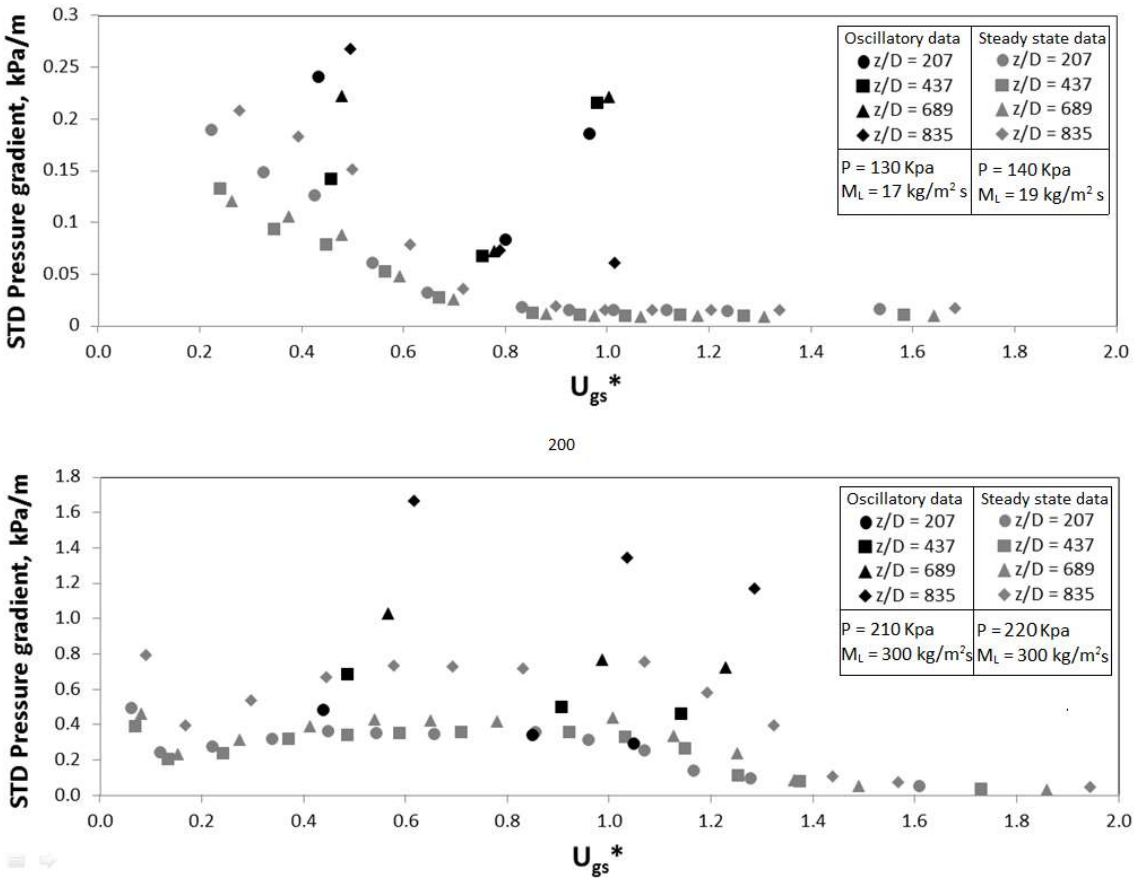

Figure 4.14 Standard deviation of pressure gradient variation determined at four positions as a function of U^*_{gs}.

4.3 Conclusions

Experimental data was obtained using a 42-m long, 0.04958 m ID tube system, under steady-state and oscillatory conditions. The experimental data was used to compared behavior of flow regimes, liquid holdup and pressure gradient for steady-state and oscillatory conditions. Based on the analysis of this comparison, the following conclusions can be draw from this study:

- The transition between gas-liquid two-phase flow regimes can be significantly affected by gas velocity oscillations. For lower pressures and oscillatory conditions, slug flow regime was observed at considerable larger superficial gas velocities than for steady-state flow. For higher pressures and oscillatory

conditions, churn flow regime was observed rather than annular flow regime for the same superficial gas and liquid velocities under steady-state flow conditions. The flow regime transition models available in the literature could only estimate the transition for low pressures, while none of these models predicted the transition reasonably for larger pressure under oscillatory flow conditions.

- The frequency of large-liquid structures as a function of axial position was visually characterized using high speed cameras. From the video recordings it was possible to concluded that the large-liquid structure frequency does not depend on the axial position, as previously observed by Waltrich et al (2013) for steady-state flow. However, the frequency of the large liquid structures is relatively smaller in oscillatory than in steady-state flow conditions, particularly for larger Usg*. Additionally, three different models were used to predict the wave frequency. The models of Sekoguchi et al. (1985) and Hazuku et al. (2008) presented the best agreement for low and high superficial liquid velocities, respectively.
- The total average liquid holdup was used to compare the oscillatory experiments with the steady-state ones as a function of the position. It was found that the liquid holdup under oscillatory conditions behave at the same manner than under steady-state conditions decreasing with position. However, for U^*_{gs} <0.6 and Uls=0.017 m/s, the rate of change of liquid holdup with U_{sg}^* is not as severe in oscillatory conditions as is in steady-state conditions.
- The pressure gradient under oscillatory conditions is significantly lower than in steady-state flow, particularly for lower superficial gas and liquid velocities and larger axial positions. The pressure gradient seems to be affected by the formation

of large liquid waves, which is a consequence of the forced gas flow rate oscillation.

CHAPTER 5: COMPARISON OF TWO-PHASE FLOW MODELS FOR STEADY-STATE AND OSCILLATORY FLOWS

5.1 Introduction

In the petroleum industry, when the production system is designed, engineers consider steady-state conditions under the assumption that the boundary conditions (flow rates, pressure) remain constant over certain fixed amount of time. When these parameters change due to natural oscillations of gas-liquid flows in pipes, or variations during operations, these assumptions can no longer be considered. Multiphase flow in pipes is a transient phenomenon in nature. Under certain conditions, steady-state assumptions have provided reasonable results, as shown in chapter 4 where the average of the oscillatory parameters shown that transient effects were not relevant. The prediction of liquid holdup and pressure gradient in two-phase flow has been widely studied under steady state conditions because of its relevance in the design and analysis of production systems. There are different steady state correlations/models available in the literature to calculate and predict liquid holdup and pressure gradient. However, the application of these standard models generates large uncertainty in the results when they are not applied to their specific range of conditions, which they were tested. Thus, the reliability of the production design usually depends on the choice of the right correlation.

In the first part of this chapter, a comparative study between different models for two-phase flow in pipes and experimental data from TowerLab can be found. This comparison was directed to evaluate the performance of the empirical correlations in estimating liquid holdup and pressure gradient.

Second, the oscillatory behavior of liquid holdup and pressure gradient were simulated from the steady state experimental data using their changes as a function of dimensionless

superficial gas velocity. From the analysis carried out in chapter 4, it is possible to conclude that the total average of the liquid holdup and pressure gradient under oscillatory conditions have a similar behavior that under steady-state in general. Some exceptions were seen especially under U_{gs}^{*}<0.4. In base of those results the question about if oil and gas two-phase flow correlations can be used to predict the average behavior of the oscillatory (transient) flows was formulated. The main purpose of this chapter is analyzed the performance of different models predicting the liquid holdup and pressure gradient for both steady-state and oscillatory conditions. The potential applicability of these correlations for the current conditions was studied. The use of these simple correlations to predict an average response of the parameters (liquid holdup and pressure gradient) can help to analyze systems when transient simulators are not available.

5.2 Characteristics of the Correlations and Models

Correlations

Although there are multiply correlations developed to predict liquid holdup and pressure gradient, no all of them are suitable for the current conditions. Three vertical (*H&B*-Hagedorn and Brown (1965), *D&R*-Duns and Ros (1963), and *GC*-Gray (1978)), and one vertical-horizontal (*B&B*-Beggs and Brill (1973)) multiphase flow correlations were selected to evaluated their performance in comparison to the current steady state and averaged oscillatory experimental data. The selection of these correlations was based on their acceptance in the oil and gas industry in addition to their main features described in details in the literature review. These models have been developed in facilities similar to the one used to obtain the current experimental data with a pipe length larger than 27 m, with ID range between 2.5-14 cm, some of them using same fluids and gas-liquid ratios.

Simulator

For the purpose of this research, a steady state model was used to simulate upward two-phase flow in a vertical pipe. This simulator is a research code based on different mechanistic model available in the literature. The following mechanistic models were implemented for this simulator:

- Slug Flow: model of de Cachard and Delhaye (1996)
- Churn Flow: model of Jayanti and Hewitt (1992)
- Annular Flow: model of Ahmad et al. (2013)

Combining flow regime maps and conservation equations of mass, energy, and momentum, this code can predict different parameters such as pressure gradient, entrained liquid fraction, film thickness, and void fraction at different positions adjusting multiple balance equations along the pipe. Oil-gas, air-water and steam-water flow systems can be evaluated with this model. A research code similar to this simulator has been validated against experimental data in previous studies (Ahmad et al. 2013, Waltrich 2012).

5.3 Results and Discussions

Steady-state

The experimental data used to evaluate the performance of the correlations and models covered the range of air –water superficial velocities described in chapter 3 for steady state and oscillatory conditions. The steady state liquid holdup data used in this study has been statistically analyzed in previous investigations to characterize flow regimes and the combination of the liquyid holdup and pressure gradient to assess the axial flow development (Waltrich 2012).

However, this is the first attempt to evaluate the performance of common correlations used in the petroleum industry by comparing them with the current steady state experimental data.

The empirical correlations selected in this study (*H&B*-Hagedorn and Brown (1965), *D&R*-Duns and Ros (1963), *GC*-Gray (1978), and *B&B*-Beggs and Brill (1973)) and the simulator have been compared with measured experimental data and evaluated graphically and statistically. In this investigation, all the chosen correlations are specifically pressure gradient models which have liquid holdup correlations implemented in the method to calculate the frictional, gravitational and acceleration component of the total pressure gradient. Excluding Hagedorn and Brown model, all the other models predict the liquid holdup based on the flow regimes. Additionally, a comparison between the measured and the predicted parameter was done through a statistical analysis using six statistical parameters that allowed calculating the relative performance factor for each correlation and model. This factor evaluates the accuracy of the correlation; the smaller the F_{RP} the better the model fit the experimental data in comparison with the other models. The statistical parameters used in this analysis are shown in (Shoham 2006).

Figure 5.1 shows the comparative results of the measured liquid holdup and the calculated values from each model at z/D=521 as a function of the local dimensionless superficial gas velocity. Previous investigations have categorized the churn-annular transition zone in the range of $0.9 < U_{gs}^{*} < 1.1$ for this type of pipe configuration and flow conditions (Waltrich 2012, Lumban-Gaol and Valkó 2014)

Beggs and Brill, Gray and the Simulator presented a good agreement predicting the liquid holdup for dimensionless superficial gas velocity higher than 0.9 which indicates that the models captured the liquid holdup behavior under transition and annular flow conditions.

The simulator was the only model capturing the exponential decrease tendency of the liquid holdup, but it overpredict this parameter under churn flow conditions, U_{gs}^{*}<0.9.

Hagedorn and Brown is the only model selected that does not consider the flow regime to predict the liquid holdup. The liquid holdup predicted by this correlation illustrated a constant trend with respect to the dimensionless superficial gas velocity. This behavior can be explained for the nature of the liquid holdup correlation used by Hagedorn and Brown's model where the liquid holdup is calculated based on a local pressure, the liquid properties and liquid flow rate. Under steady state conditions, the pressure and the liquid rate were kept constant. Therefore, the liquid holdup did not change significantly with respect to U_{gs}^{*}.

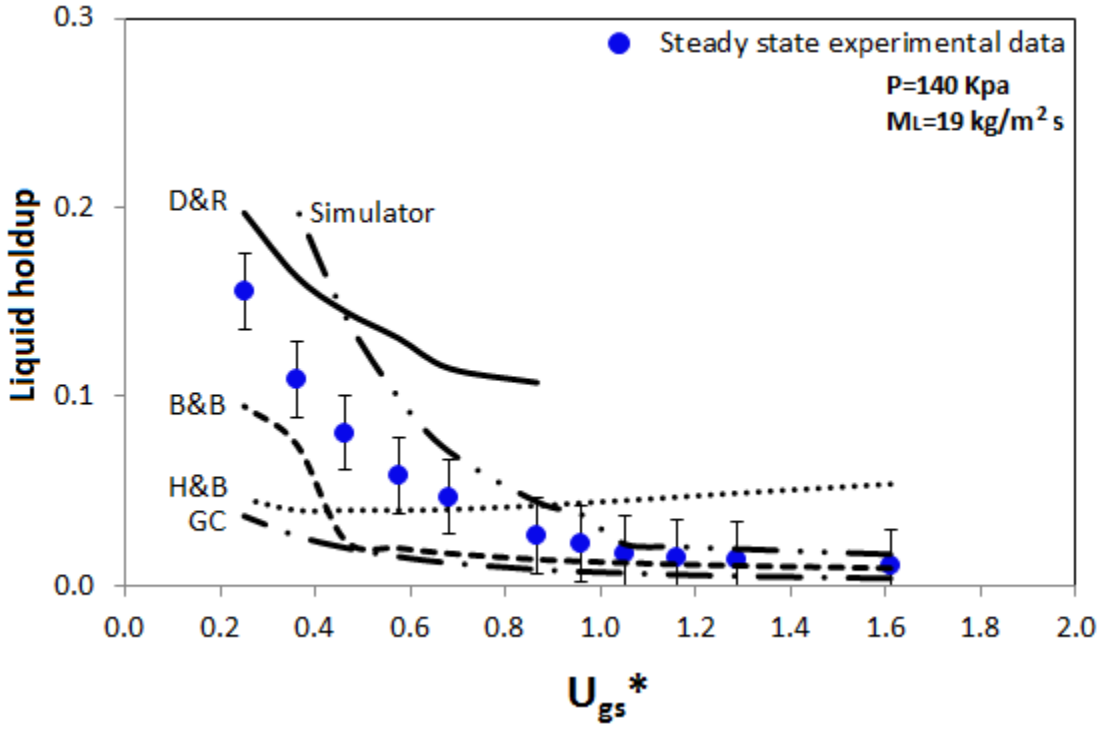

Figure 5.1 The comparison of the measured and the predicted local liquid holdup as a function of the dimensionless superficial gas velocity using five different models under constant liquid content (M_L=19 kg/m^2 s).

An evaluation was carried out based on the statistical analysis where the five models were compared with the experimental data. A relative performance factor was calculated, F_{RP}, that integrates the minimum and maximum of each statistical parameter. Six statistical parameters are used to estimate F_{PR}. The parameters Ɛ1, Ɛ2, Ɛ3 are based on percentage error and are more appropriate to analyze small changes in values, while the actual errors are represented by Ɛ4, Ɛ5, Ɛ6 and they can be used to evaluate larger changes of values. The Ɛ1 is the average percentage error and Ɛ4 is the average error; however, Ɛ2 that is the absolute average percent error and Ɛ5 absolute average error are considered more relevant parameters because the sign of the error does not influence the two parameters. The scatter of errors are represented by Ɛ3 and Ɛ6 being the percentage standard deviation and the standard deviation respectively with respect to their equivalent average percentage error Ɛ1 and average error Ɛ4 (Shoham 2006).

Table 5.1 presents the statistical analysis results for the performance evaluation of the two-phase flow modes and correlations for the liquid holdup. As can be seen from the table, Beggs and Brill's correlation was the best fit for the experimental data with respect to the other models with F_{RP}=-1.62.

Table 5.1 Statistical analysis results of the selected models for the liquid holdup prediction

Model/Correlation	Ɛ1	Ɛ2	Ɛ3	Ɛ4	Ɛ5	Ɛ6	F_{RP}
	(%)						
Hagedorn & Brown (1965)	92.5	134.3	457.1	0.006	0.038	0.135	2.38
Beggs & Brill (1973)	-39.4	39.4	56.8	0.023	0.023	0.066	-1.62
Duns & Ros (1963)	21.4	112.4	384.0	-0.028	0.042	0.137	1.71
Gray (1978)	-68.0	68.0	22.0	0.037	0.037	0.100	2.51
Simulator	46.1	64.2	105.2	-0.011	0.039	0.118	-0.70

In addition, Beggs and Brill's model had the lowest absolute average percentage 39.4 % and absolute average error 0.023 followed by the simulator and Gray's correlation with 64.2% and 68% respectively. Beggs and Brill and Gray models underestimated the liquid holdup for the entire range of dimensionless superficial gas velocity. This behavior could be seen in figure 36 and represented by the negative sign of the average percentage error. Even though Gray's correlation showed an acceptable performance predicting the liquid holdup, the model did not calculate accurately the liquid holdup for low superficial gas velocities. This discrepancy might be explained by the limitations of the correlation where the water ratio cannot exceed 141584 m^3/d.

Duns and Ros correlation did not predict the liquid holdup for U_{gs}^{*}>0.9. The analysis of this model was carried out assuming zero the no predicted values. A deeper analysis of why this correlation did not predict the liquid holdup was not possible. The liquid holdup is calculated in base on the flow regimes. Each flow regime has its own graph that combines the dimensionless numbers and what they call non-dimensional functions obtained experimentally for a range of viscosities and diameters.

Figure 5.2 illustrates a comparative analysis of the experimental pressure gradient variation with respect to inlet dimensionless superficial gas velocity and the predicted pressure gradient from the models mentioned previously.

The evaluation of each method was based on the comparison between the total pressure gradient calculated from the measurements and the performance of each model predicting such parameter. In this investigation, only the gravitational and frictional components of the total pressure gradient were considered, neglecting the acceleration component. In two-phase vertical flow, except when annular flow is present in the pipe, the major contributor to the total pressure

gradient is the gravitational component, which provides approximately 80% of the total pressure gradient. The gravitational pressure has been directly related to the in situ volume fraction. A reduction in the liquid holdup (in situ volume fraction) causes a decrease in the hydrostatic pressure. Figure 5.1 and Figure 5.2 illustrates a parallel variation between the experimental liquid holdup and the experimental gravitational pressure loss. This behavior is captured by the correlations, which predict the pressure gradient according to their own prediction of the liquid holdup including Hagedorn and Brown's model. That is why it is important to estimate the liquid holdup accurately.

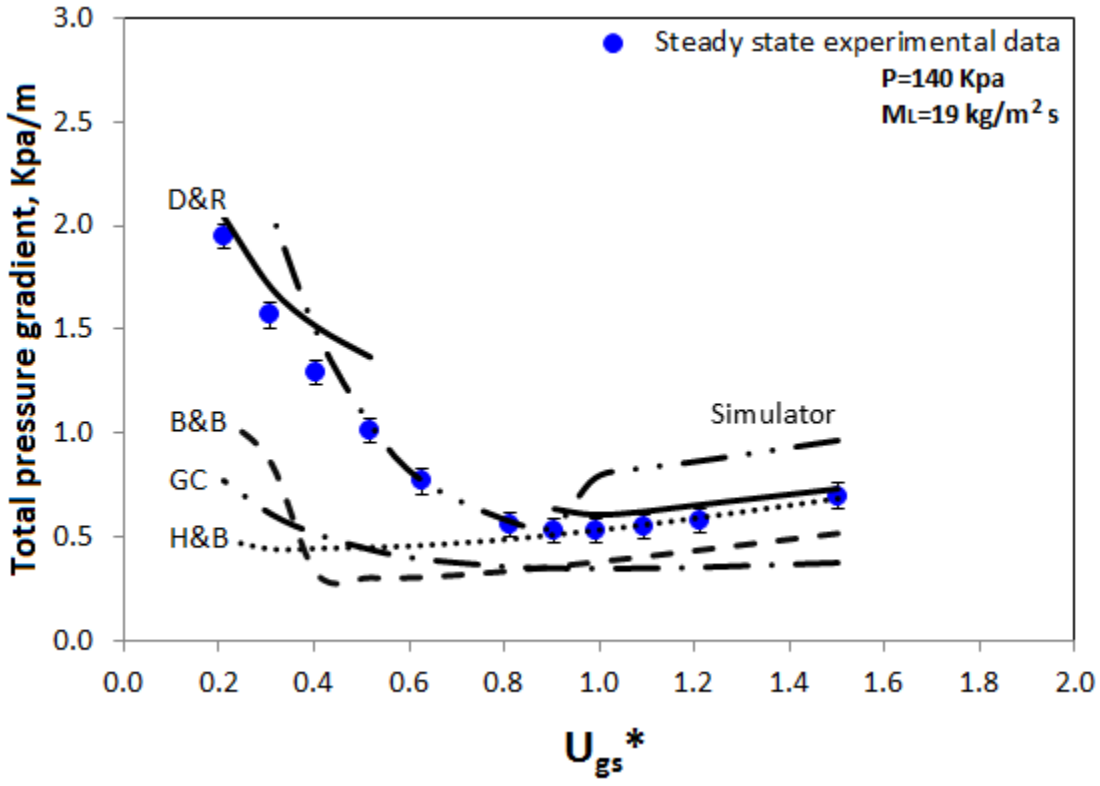

Figure 5.2 Comparison between the experimental pressure gradient as a function of the inlet dimensionless superficial gas and the predicted pressure gradient from five models.

For U_{gs}^{*}>0.9, all the models showed a good agreement with respect to the experimental pressure gradient. The overall statistical evaluation of the different models against the experimental data is shown in Table 5.2

Table 5.2 Statistical analysis results of the selected models for the pressure gradient prediction

Model/Correlation	Ɛ1	Ɛ2	Ɛ3	Ɛ4	Ɛ5	Ɛ6	F_{RP}
	(%)			(Kpa/m)			
Hagedorn & Brown (1965)	-28.9	42.8	26.8	0.396	0.402	1.518	4.62
Beggs & Brill (1973)	-42.8	12.2	34.4	0.428	0.428	0.992	3.32
Duns & Ros (1963)	12.2	46.4	98.3	0.013	0.228	0.822	1.05
Gray (1978)	-46.4	31.6	34.4	0.468	0.468	1.014	3.38
Simulator	13.4	102.9	98.3	0.007	0.347	1.226	3.58

As it is illustrated on the table, the Beggs and Brill's correlation had the smallest absolute percentage error Ɛ2=12.2%, followed by Gray and Hagedorn and Brown's correlation with 31.6 % and 42.8% respectively. These three correlations had negative values for the average percentage error Ɛ1, which indicates that they underpredicted the total pressure gradient in comparison with the measured data. The positives values register for Duns and Ros's correlation and the simulator meant that they overpredicted this parameter with respect to the experimental data. Finally the performance relative factor F_{RP} was calculated to evaluate the best model for this set of data. As a result, it was obtained that Duns and Ros model was the best fit for this type of conditions with a F_{RP} =1.05. Even though, in Figure 5.2. Duns and Ros's curve showed a discontinuity due to the lack of performance in this range of conditions, this correlation captured the behavior and predicted the pressure gradient more accurate. The Beggs and Brill and Gray's correlations and the simulator had a similar performance with respect to each other obtaining a F_{RP} of 3.32, 3.38, and 3.58 respectively.

The following conclusion can be made from the overall evaluation. For Hagedorn and Brown, Beggs and Brill and Gray's correlations is notorious the influence of the liquid holdup on the gravitational component. The miscalculation of liquid holdup highly affected the pressure gradient especially under low gas velocities. On the other hand, the simulator that had a good agreement predicting the liquid holdup showed a jump and increment on the frictional component prediction. This discrepancy was also observed by Waltrich (2012) and concluded that the liquid film velocity used by the simulator is relatively high in comparison with another simulators. Higher liquid film velocity produces higher values of wall friction.

Similar analysis was carried out for Uls = 0.3 m/s where the liquid holdup and total pressure gradient were studied and compared with the same models. Figure 5.3 shows the comparison between the experimental liquid holdup variation at z/D=521 with respect to the local dimensionless superficial gas velocity and the predicted buildup from the models. As an overall, all the models captured the exponential decay behavior of the liquid holdup with an increase in the dimensionless superficial gas velocity. In addition, the models had good performance in the estimation of the liquid holdup in general. The model with the larger discrepancy with respect to the measured liquid holdup was Hagedorn and Brown's correlation. This model presented again a similar behavior as the seen in the low liquid content case where it predicted a constant liquid holdup for a large range of dimensionless superficial gas velocity. The liquid holdup predicted by Hagedorn and Brown's model increased with a decrease in gas content especially for U_{gs}^{*}<0.2. This behavior should be mainly related to an increase in the inlet pressure due to the amount of liquid compared with the gas.

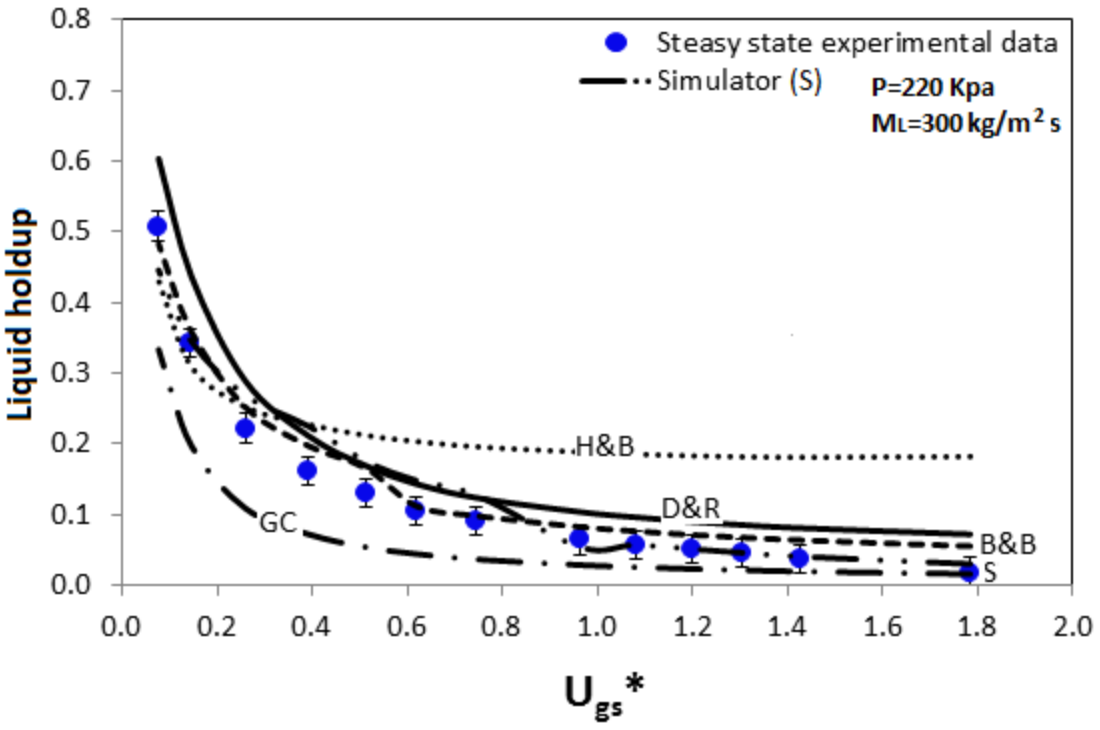

Figure 5.3 The comparison of the measured and the predicted local liquid holdup as a function of the dimensionless superficial gas velocity using five different models under constant liquid content (M_L=300 kg/m^2 s).

A general statistical evaluation of the models against the experimental liquid holdup data is shown in Table 5.3. The simulator had the smallest absolute average percentage error, Ɛ2=22% followed by Beggs and Brill with a Ɛ2=39.4% in comparison to the other models analyzed. In addition, the relative performance factor for all the correlations was calculated giving as a result Duns and Ros the best model for the prediction of the experimental liquid holdup with a F_{RP} =2.59. Finally, the only model that underpredited the buildup was Gray's correlation. The behavior is represented in Figure 0.3, and confirmed by the negative value of the average percentage error, Ɛ1.

Table 5.3 Statistical analysis results of the selected models for the liquid holdup prediction

Model/ Correlation	Ɛ1	Ɛ2	Ɛ3	Ɛ4	Ɛ5	Ɛ6	F_{RP}
	(%)						
Hagedorn & Brown (1965)	195.8	199.6	615.5	-0.085	0.102	0.205	5.98
Beggs & Brill (1973)	38.6	39.4	118.6	-0.020	0.023	0.042	3.15
Duns & Ros (1963)	70.3	70.3	168.0	-0.052	0.052	0.060	2.59
Gray (1978)	-48.7	48.7	33.6	0.065	0.065	0.156	2.97
Simulator	17.5	22.0	79.7	-0.014	0.025	0.097	3.92

Under Uls=0.3 m/s, Waltrich (2012) characterized this set of the steady state conditions under churn flow mainly. Annular flow was characterized for U_{gs}^{*}>1.1. Therefore, the gravitational pressure gradient contributed to approximately 80% of the total pressure gradient, for the majority of the experiments. As it has been expressed before, the liquid holdup is the fundamental parameter in the forecast of the gravitational component thus of the total pressure gradient in this scenario.

Figure 5.4 shows the comparison between the prediction of the models and the experimental variation of the total pressure gradient with respect to the dimensionless superficial gas velocity at the inlet for Uls=0.3 m/s. The results obtained by the different models studied under these conditions showed a much better fit than the ones obtained for the low liquid content. The absolute percentage average error range was 4.7-49.8%. Hagedorn and Brown, Beggs and Brill and Duns and Ros show a reasonable good performance with an absolute average percentage error of 4.7%, 10.6 % and 24.6% respectively.

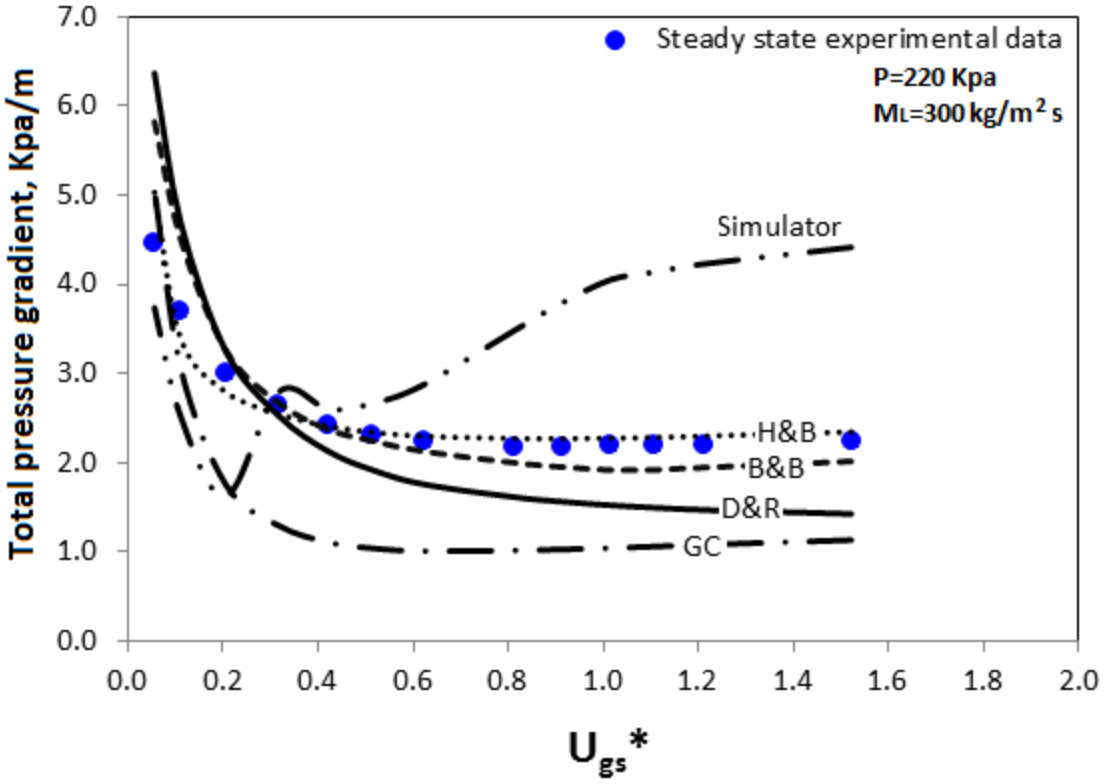

Figure 5.4 Comparison between the experimental pressure gradient as a function of the inlet dimensionless superficial gas and the predicted pressure gradient from the five models selected.

Considering the different amount of factors that are involved on the estimation of the pressure gradient under multiphase flow conditions, average errors lower than 25% have been widely accepted in the oil and gas industry. This acceptable performance can be explained by the capability of the models to predict the liquid holdup more accurate. The correlations selected have a range of application similar to the conditions of the experiments analyzed in Figure 5.4 with the exception of Gray correlation. That can explain the improvement of the performance of the correlations. The overall statistical analysis is shown in Table 5.4 and categorized Hagedorn and Brown models as the best fit for the high liquid content scenario with a F_{RP} =2.96. This is a surprising result considering that H&B results for the liquid holdup analysis was the worse among all the models. The exceptional performance of this correlation can be only associated to

the different modifications implemented in the model to improve it and the considerable amount of experimental data used to develop it.

Table 5.4 Statistical analysis results of the selected models for the pressure gradient prediction

Model/Correlation	Ɛ1	Ɛ2	Ɛ3	Ɛ4	Ɛ5	Ɛ6	FRP
	(%)			(Kpa/m)			
Hagedorn & Brown (1965)	1.7	4.7	15.4	-0.05	0.14	0.47	2.96
Beggs & Brill (1973)	-1.0	10.6	38.2	-0.06	0.32	1.30	3.79
Duns & Ros (1963)	-12.5	24.6	71.8	0.17	0.66	2.15	3.88
Gray (1978)	-44.0	46.0	50.1	1.02	1.11	1.16	3.27
Simulator	35.4	49.8	164.6	-0.69	1.19	3.92	5.00

On the other hand, the biggest discrepancy between the measured and the predicted pressure gradient was obtained from the simulator results, as can be seen in Figure 5.4 and Table 5.4. The pressure gradient curve had a different trend compared with the experimental data and the prediction of the other models. Two drastic changes were presented in the curve when the transition occurred from one flow regime to another according to the model boundaries. The most remarkable change was experienced in the transition from slug to churn flow at approximately U_{gs}^{*}=0.25. The other change was made in the transition from churn to annular flow at U_{gs}^{*}=0.9. However the last variation was smoother and related to the slope of the curve instead of the trend. The reason to see this type of behavior is still not well understood. The simulator was the model with the lowest absolute average percentage error Ɛ2=22 % for the liquid holdup prediction but with the highest for the pressure gradient Ɛ2=49.8 %. This implies the simulator miscalculations with respect to the pressure gradient are not mainly related to the liquid holdup prediction.

Oscillatory

A comparative study between five different multiphase flow correlations (Hagedorn and Brown, Duns and Ros, Gray, Beggs and Brill, and the simulator) and the oscillatory experimental data was carried out graphically and statically. The minimum, average and maximum values of the inlet gas flow rate were considered to get the liquid holdup and pressure gradient correlated to the specific condition. This procedure was done for the three ranges of gas variations for each of the two liquid content scenarios. Figure 5.5 illustrates the variation of the inlet gas flow rate with respect to time and the corresponding values of liquid holdup and pressure gradient at the same time and an example of how the values were obtained from the oscillatory experimental data.

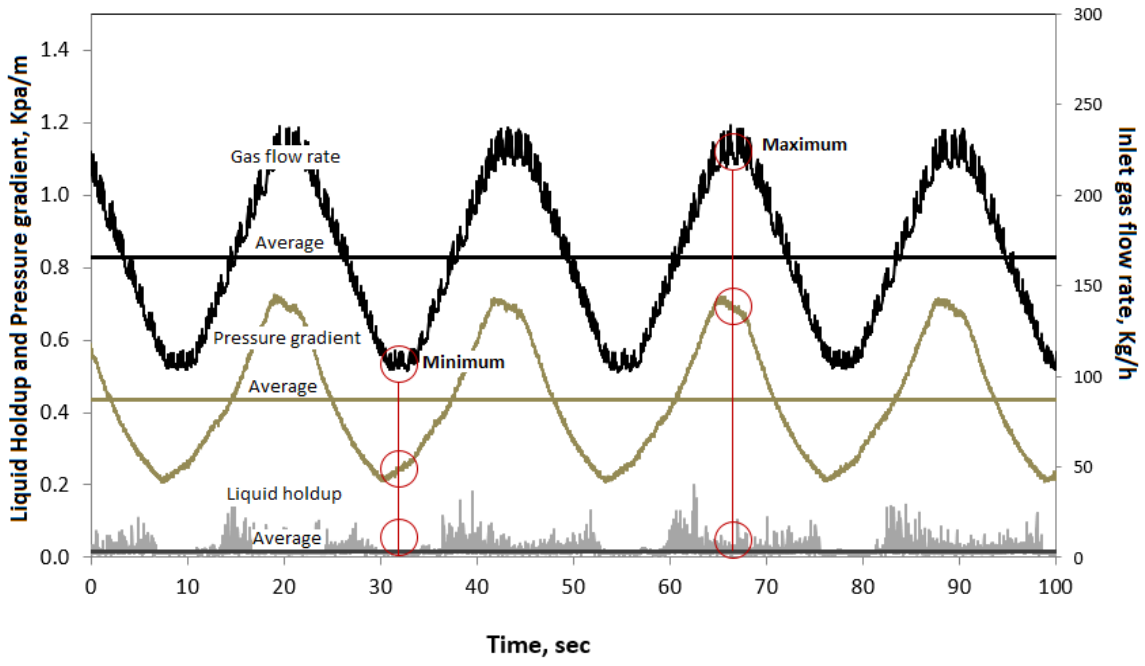

Figure 5.5 Characterization of the minimum and maximum values used for liquid holdup and pressure gradient at the highest and lowest values of the inlet gas flow rate with respect to time. The average of each parameter is also indicated.

Here for the minimum and maximum values, the moving average of two seconds was applied to the liquid holdup and pressure gradient experimental data to capture a wider behavior of these points of interest. The average value was calculated taking into account all the oscillatory experimental data of each case. Through this process, the necessary boundary conditions for the models were found. A total of nine different gas flow rate were implemented in each correlation to get the prediction of the liquid holdup and pressure gradient behavior keeping constant the liquid flow rate.

The multiphase flow models selected in this comparative analysis were design to be used under steady state conditions. Thus, the performance of the correlations on the prediction of oscillatory flow conditions was investigated. The minimum, average, and maximum gas flow rate were selected as points of interest in order to have a larger amount of experimental data to compare with the predictions from the models. For this last type of analysis was also included the prediction of the oscillatory data from the steady state curves for liquid holdup and pressure gradient variation with respect to the dimensionless superficial gas velocity presented in *chapter 4*. The nine points selected were considered to execute the statistical analysis for each constant liquid rate in the studied of liquid holdup and pressure gradient.

Figure 5.6 illustrates the comparison of the measured liquid holdup and the predicted values from the models on two ranges of errors ±20% and ±50%. The graphs on the left of this figure represented the liquid velocity U_{sl}=0.017m/s while the right side evaluated the liquid velocity U_{sl}=0.3 m/s. For each range of gas flow rate variation, the minimum (min), average (ave), and maximum (max) values were evaluated and located in ascendant form from the top to the bottom in Figure 5.6

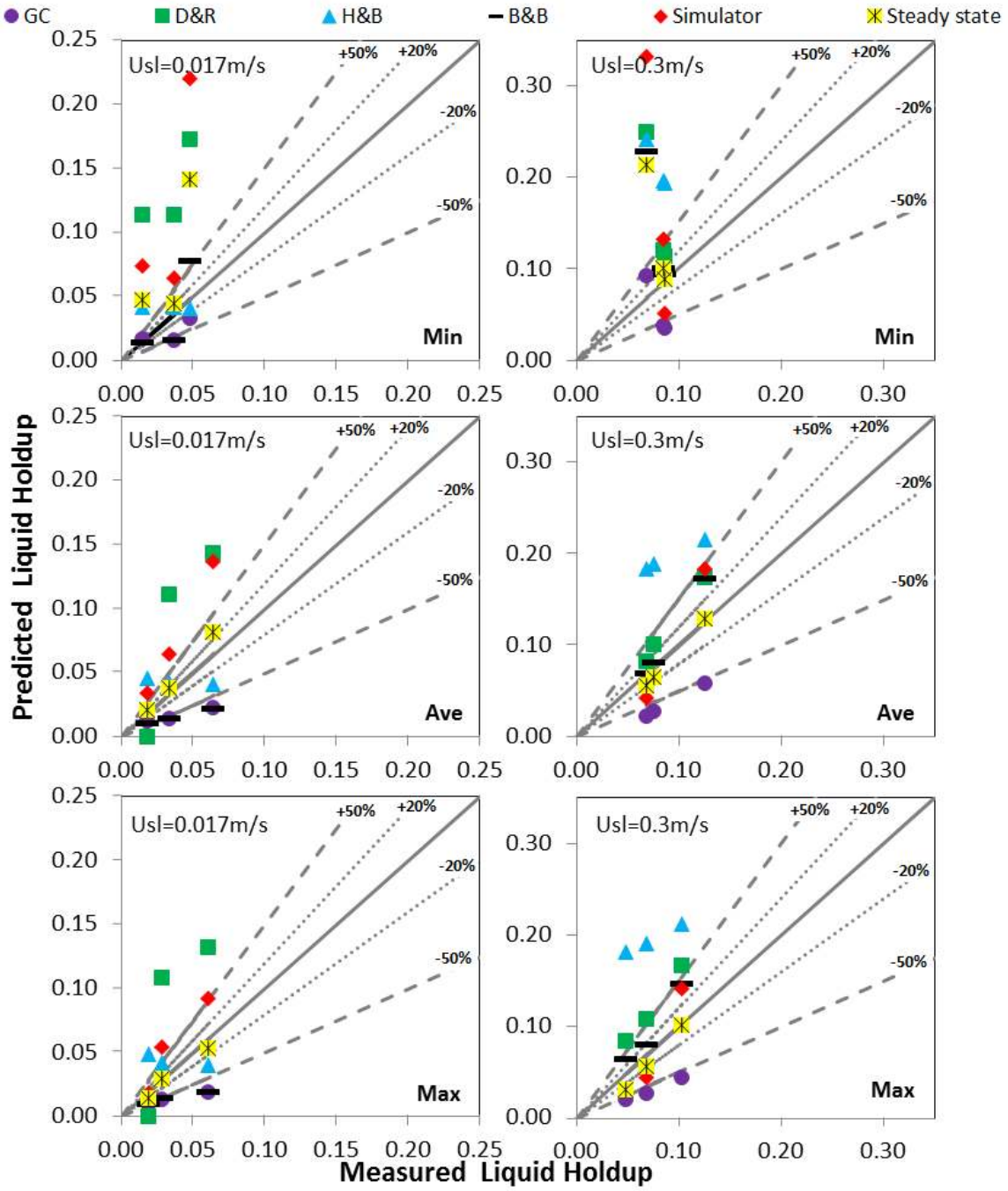

Figure 5.6 The comparison of the measured and predicted liquid holdup using different models for gas flow rate variation at the minimum, average and maximum rates of each experiment U_{sl}=0.017 m/s and U_{sl}=0.3 m/s.

The results showed that Gray and Beggs and Brill and the steady state correlations had the best performance predicting this parameter with an overall absolute percentage error of 47.4%, 49.5%, and 57.3% respectively for U_{sl}=0.017m/s. For U_{sl}=0.3 m/s, the models that had a good agreement with the oscillatory data were steady state, Gray and Duns and Ros correlations with an absolute average error of 35.9%, 56.8% and 67% correspondingly. Under both scenarios the relative performance factor F_{RP} pointed out Gray model as the most appropriated methods to predict the liquid holdup in comparison with the other correlations. The steady state model seemed to have an acceptable performance when it was predicting the average and maximum values. This meant that it was good predicting under high gas flow rate conditions within of range of 20 % error as can be seen in Figure 5.6. The biggest discrepancies found in this analysis were when the models had to predict the minimum condition for both liquid velocities which meant they did not perform well under $U_{gs}^{*} < 0.75$. The overall statistical evaluation of the models is presented in Table 0.5 for U_{sl}=0.017 m/s and Table 5.5 for U_{sl}=0.3 m/s.

Table 5.5 Statistical evaluation results of the different models for the liquid holdup prediction using the minimum, average, and maximum oscillatory experimental data for U_{sl}=0.017 m/s.

Model/Correlation	Ɛ1	Ɛ2	Ɛ3	Ɛ4	Ɛ5	Ɛ6	F_{RP}
	%						
Hagedorn & Brown (1965)	190.7	190.7	432.9	-0.04	0.04	0.05	3.7
Beggs & Brill (1973)	-33.6	49.5	96.5	0.01	0.02	0.05	1.4
Duns & Ros (1963)	190.3	234.7	509.0	-0.06	0.07	0.12	5.0
Gray (1978)	-43.8	47.4	59.5	0.02	0.02	0.03	1.0
Simulator	136.7	137.9	302.0	-0.05	0.05	0.11	3.4
Steady state	48.9	57.3	212.8	-0.02	0.02	0.06	1.9

Table 5.6 Statistical evaluation results of the different models for the liquid holdup prediction using the minimum, average, and maximum oscillatory experimental data for U_{sl}=0.3 m/s.

Model/Correlation	Ɛ1	Ɛ2	Ɛ3	Ɛ4	Ɛ5	Ɛ6	F_{RP}
	%						
Hagedorn & Brown (1965)	116.4	116.4	145.0	-0.08	0.08	0.06	3.4
Beggs & Brill (1973)	82.6	82.6	135.7	-0.06	0.06	0.10	2.9
Duns & Ros (1963)	67.0	67.0	139.5	-0.05	0.05	0.10	2.6
Gray (1978)	-49.4	56.8	58.4	0.04	0.05	0.05	1.6
Simulator	35.1	78.5	262.2	-0.03	0.06	0.21	4.2
Steady state	14.5	35.9	136.9	-0.01	0.02	0.10	1.8

The comparison of the predicted pressure gradient from several models and the measured pressure gradient is depicted in Figure 5.7 with ±20% and ±50% error ranges indicated. The type of analysis applied for the pressure gradient was similar to the liquid holdup where the minimum (min), average (ave), and maximum (max) gas flow rate variation were studied for both left figures U_{sl}=0.017m/ as indicated in Figure 5.7. For U_{sl}=0.017m/s, the most satisfactory results in the prediction of the total pressure gradient were given by Hagedorn and Brown, Beggs and Brill, and Gray correlations with 40.7%, 40.7%, and 42.2% of error correspondingly. However, The statistical analysis gave as a result that the most appropriate model to forecast this parameter was the steady state model with a F_{RP}=-5.9 and an absolute average percentage error of 45.3%. The steady state model showed a good performance when it was predicting the pressure gradient for the total average and maximum gas flow rates. Therefore its high absolute average percentage error was associated to the poor performance of the model predicting under churn flow conditions $U_{gs}^{*} < 0.7$. Table 5.7 showed the complete statistical analysis carried out for the pressure gradient under liquid velocity of 0.017 m/s.

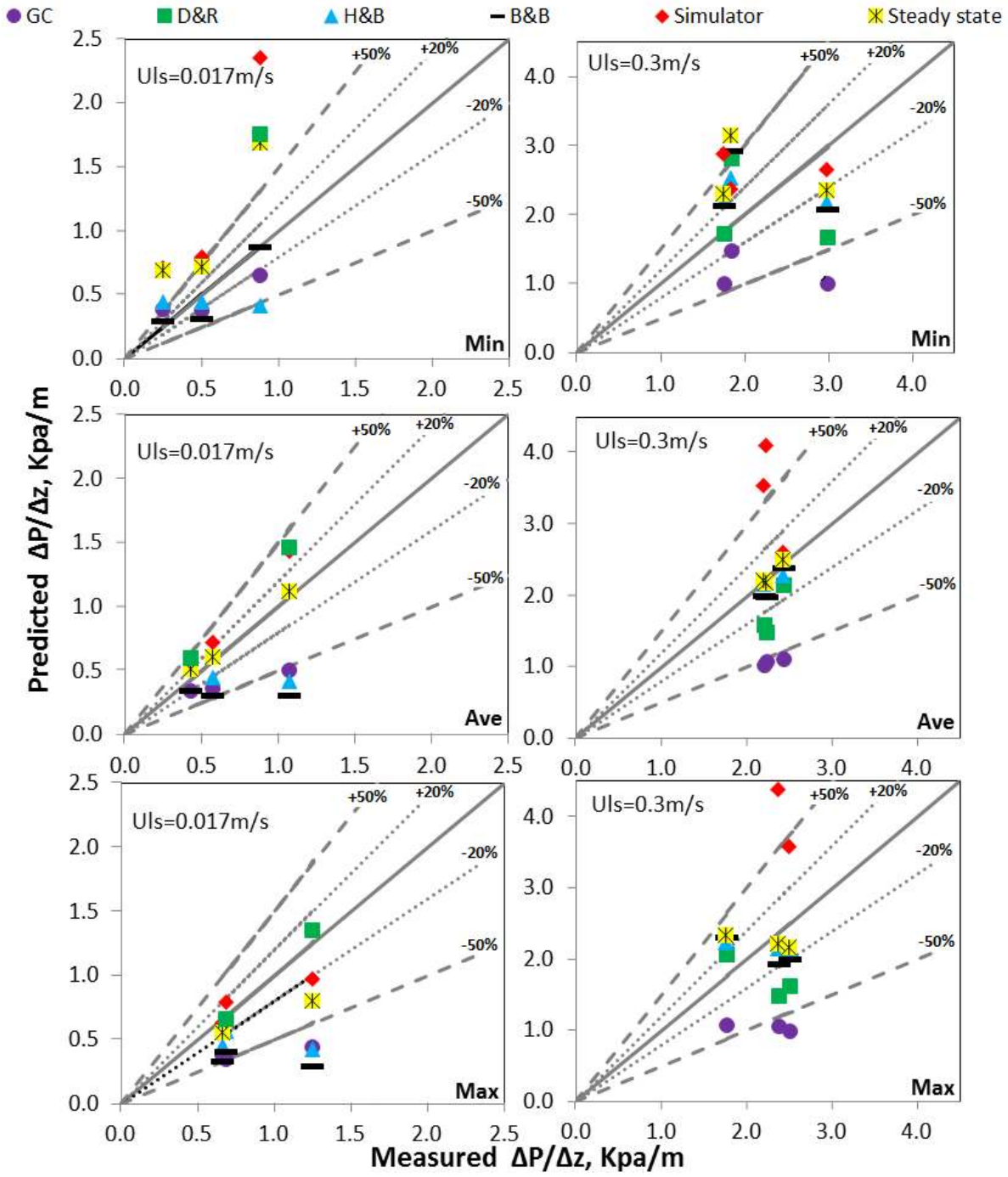

Figure 5.7 The comparison of the measured and predicted total pressure gradient using five different models for minimum, average and maximum gas flow rate of each experiment.

Figure 5.7 also included the study of the pressure gradient for U_{sl}=0.3 m/s. For this case, it can be seen that most of the points fell on the 50% range of error. This behavior implied that there was not a better performance of the models predicting any of the range of flow rates evaluated under these conditions.

The most accurate model forecasting the liquid holdup was Hagedorn and Brown with a 16.8% of absolute average percentage error and F_{RP}=1.18 and followed by the steady state model and Beggs and Brill with 19.9% and 22.6 % respectively. The complete statistical evaluation is presented in Table 5.8. The total pressure gradient was underpredicted Uls=0.017 m/s and Uls=0.3 m/s by Gray model as it is illustrated in Figure 5.7. The total pressure gradient was underpredicted for Gray correlation and indicated by the average percent error Ɛ1 with the negative sign. These results can be explained by the fact that Gray correlation allows the liquid film create at the wall a pseudo wall roughness that helps to reduce the friction factor which affects substantially the pressure gradient under high gas velocities. This assumption can cause the underprediction of the parameter studied.

Tbale 5.7 Statistical evaluation results of the different models for the pressure gradient prediction using the minimum, average, and maximum oscillatory experimental data for U_{sl}=0.017 m/s.

Model/Correlation	Ɛ1	Ɛ2	Ɛ3	Ɛ4	Ɛ5	Ɛ6	F_{RP}
	%			Kpa/m			
Hagedorn & Brown (1965)	-18.9	40.7	592.8	0.25	0.31	0.86	-0.90
Beggs & Brill (1973)	-37.0	40.7	79.9	0.32	0.33	0.79	1.85
Duns & Ros (1963)	-25.1	65.0	696.4	0.06	0.39	1.24	-4.79
Gray (1978)	-29.6	42.2	66.9	0.28	0.32	0.63	-0.18
Simulator	54.7	60.8	348.6	-0.29	0.36	0.98	3.64
Steady state	31.7	45.3	156.9	-0.11	0.25	0.80	-5.90

Tbale 5.8 Statistical evaluation results of the different models for the pressure gradient prediction using the minimum, average, and maximum oscillatory experimental data for U_{sl}=0.3 m/s.

Model/Correlation	Ɛ1	Ɛ2	Ɛ3	Ɛ4	Ɛ5	Ɛ6	F_{RP}
	%			Kpa/m			
Hagedorn & Brown (1965)	2.1	16.8	55.6	0.02	0.37	1.14	1.18
Beggs & Brill (1973)	1.5	22.6	73.5	0.05	0.49	1.50	1.96
Duns & Ros (1963)	-13.9	29.2	77.9	0.40	0.68	1.78	2.70
Gray (1978)	-49.7	49.7	32.8	1.15	1.15	1.15	2.92
Simulator	28.1	52.9	134.0	-0.65	1.12	2.88	4.96
Steady state	9.5	19.9	71.9	-0.13	0.41	1.40	1.50

After the statistical and graphic analysis of the performance of common multiphase flow correlations used in the oil and gas industry under steady state and oscillatory conditions. In general, the models reached a better agreement when they were applied to steady state conditions. This behavior was expected and agreed with the nature of the models. The performance of the models predicting the liquid holdup and pressure gradient under steady state was much better than for oscillatory conditions having a much lower absolute average percentage error for similar conditions. The only correlation that showed certain improvement in error was the simulator predicting the pressure gradient for Usl=0.017m/s under oscillatory conditions. However, Hagedorn and Brown and Beggs and Brill were highly affected by the prediction of the oscillatory pressure gradient under liquid velocity of 0.3 m/s. doubling the error. The relative performance factor only remained constant under Usl=0.3 m/s predicting the pressure gradient and pointing the superiority of Hagedorn and Brown model for both steady state and oscillatory conditions. Neither for the liquid velocity of 0.017 m/s nor both cases of liquid holdup the F_{RP} showed an agreement in just one model predicting the parameters. This meant that the models had difficulties capturing the behavior of the parameters under oscillatory conditions in addition to their own inconvenient predicting under steady state conditions.

This chapter showed the importance of knowing the range of applicability and limitations of the models when selecting the best option to predict liquid holdup and pressure gradient. The models did not perform on the same way even for the same type of facility, which confirms that the interaction between phases is the most important aspect to obtain a reliable model.

5.4 Conclusions

An extensive evaluation of some of the multiphase flow correlations commonly used in the petroleum industry predicting pressure gradient and liquid holdup was carried out through a comparison between their estimations and the measured experimental data under steady state and oscillatory conditions. In base on this investigation the following conclusions were postulated.

- In the comparison between the models and the experimental data under steady state conditions was found there was a notorious lack of performance predicting the pressure gradient by the models for dimensionless superficial gas velocities lower than 0.7 under liquid velocity of 0.017 m/s. This behavior was correlated to the miscalculation of the liquid holdup by the models. The liquid holdup has been directly related to the gravitational component of the total pressure gradient. Beggs and Brill correlation was suggested as the most indicated model to predict both the liquid loading and the pressure gradient under these conditions by the relative performance factor.
- The contrast made between the steady state experimental data and the models for liquid velocity of 0.3 m/s presented a good agreement with the simulator when predicting the liquid holdup with an absolute average percentage error of 22%. When the pressure gradient was analyzed the Hagedorn and Brown model showed

an excellent match with respect to the experimental data with a difference of 4.7%.

- The performance of the different multiphase flow models was better for the steady state than for oscillatory conditions obtaining lower absolute average percentage error for the steady state prediction. These results were in concordance with the nature of the models.

CHAPTER 6: CONCLUSIONS AND FUTURE WORK

6.1 Conclusions

An experimental investigation was carried out to evaluate the effect of periodic forced oscillations of the inlet gas flow rate on gas-liquid two-phase flow in a vertical pipe system. The major conclusions of this investigation are the following:

- Slug, churn, and annular two-phase flow regimes flow were characterized under oscillatory condition through video recordings located at four axial positions (z/D = 100, 375, 480, and 820). The observations of flow regimes under oscillatory conditions showed significant difference than the ones expect under the same conditions but in steady-state flow.

- The transition between gas-liquid two-phase flow regimes can be significantly affected by gas velocity oscillations. For lower pressures and oscillatory conditions, slug flow regime was observed at considerable larger superficial gas velocities than for steady-state flow. For higher pressures and oscillatory conditions, churn flow regime was observed rather than annular flow regime for the same superficial gas and liquid velocities under steady-state flow conditions. The flow regime transition models available in the literature could only estimate the transition for low pressures, while none of these models predicted the transition reasonably for larger pressure under oscillatory flow conditions.

- For the range of conditions tested, it is possible to conclude that the axial variation of the liquid holdup is directly affected by the periodic forced oscillations of the inlet gas flow rate. Depending in the superficial liquid velocity, the liquid holdup have different responses at the z/D=102. For Uls=0.017 m/s, the liquid holdup oscillated at the same period that

the gas flow rate, while for Uls=0.3 m/s the liquid holdup oscillated with a significant phase delay for the period of the forced oscillated gas flow rate.

- The tubing pressure oscillated sinusoidally at the same period that the forced oscillated gas flow rate. It was also found that the pressure decreased and experienced a phase delay with the axial position.

- For the experimental data under oscillatory conditions, the large-liquid structure frequency does not depend on the axial position, as previously observed by Waltrich et al (2013) for steady-state flow. However, the frequency of the large liquid structures is relatively lower in oscillatory than in steady-state flow conditions, particularly for larger Usg*. Additionally, three different models were used to predict the wave frequency. The models of Sekoguchi et al. (1985) and Hazuku et al. (2008) presented the best agreement for Uls=0.017m/s and Uls=0.3m/s, respectively.

- The total average liquid holdup was used to compare the oscillatory experiments with the steady-state ones as a function of the position. It was found that the liquid holdup under oscillatory conditions behave at the same manner than under steady-state conditions decreasing with position. However, for U_{gs}^{*} <0.6 and Uls=0.017 m/s, the rate of change of liquid holdup with U_{sg}^{*} is not as severe in oscillatory conditions as is in steady-state conditions.

- For superficial gas velocities between 4.0 and 9.0 m/s and superficial liquid velocity of 0.017 m/s, the pressure gradient was considerable lower under oscillatory flow when compared to steady state data. This behavior was correlated to the influence of the forced oscillated gas flow rate on the liquid holdup under those conditions.

- The results from the experiments under steady-state and oscillatory conditions were compared to evaluate the performance of different two-phase flow models. Beggs and Brill (1973) correlation was found to be the best fit for the steady state conditions tested.

- The models were also used to predict the liquid holdup and pressure gradient for the oscillatory experiments. The empirical correlation developed in this study (which was obtained from the steady-state experiments) showed an acceptable agreement with respect to the average of the oscillatory experiments for liquid holdup and pressure gradient.

- The comparison of the two-phase flow models with the steady-state and oscillatory experimental data showed that these models could be used with a reasonable agreement to predict the average of the liquid holdup and pressure gradient for the oscillatory experiments.

6.2 Recommendations for Future Work

One of the main contributions of this investigation is the characterization of the influence of periodic forced oscillations of the inlet gas flow rate in parameters such as liquid holdup, pressure gradient and flow regimes. Based on the literature review, this is the first attempt to systematically experimentally characterized flow instabilities (dynamic instabilities) that are present in two-phase flow in vertical tubes. However, to extend this study to a wider range of conditions and to enhance the understating of oscillations in two-phase flow in vertical pipes, the following recommendations are made for future work:

- Based on the experimental results, it seems to be necessary to expand the experimental data base to include lower superficial gas velocities. The results of this

investigation have shown that for both superficial liquid and gas velocities there is a significant change in the liquid holdup and pressure gradient with respect to the position.

- Obtain experimental data for larger pipe diameters, which since two-phase flow in vertical pipes com significantly change for different pipes diameters.

- The implementation of liquid and gas mass flow rate sensors at the end of the experimental setup can help to understand the interaction of the gas and liquid under oscillatory conditions through material balance calculations.

- The implementation of transient simulators such as OLGA and CFD that can be an important contribution to this investigation. The performance of these models can be evaluated with the experimental data.

REFERENCES

Abili, Nimi, Fuat Kara, Ifeanyi J. Ohanyere. 2014. Reassessment of Multiphase Pump on Field-Case Studies for Marginal-Deepwater-Field Devolopments (in.

Ahmad, M, DK Chandraker, GF Hewitt, PK Vijayan, SP Walker. 2013. Phenomenological modeling of critical heat flux: The GRAMP code and its validation (in *Nuclear Engineering and Design* **254**: 280-290.

Alhanati, F. J. S., Zelimir Schmidt, D. R. Doty, D. D. Lagerlef. 1993. Continuous Gas-Lift Instability: Diagnosis, Criteria, and Solutions. Proc.

Ali, Shazia Farman. 2009. Two-phase flow in a large diameter vertical riser (in.

Aziz, Khalid, George W Govier. 1972. Pressure drop in wells producing oil and gas (in *Journal of Canadian Petroleum Technology* **11** (03).

Azzopardi, Barry J. 2006. *Gas-liquid flows*, Begell house New York (Reprint).

Azzopardi, BJ, E Wren. 2004. What is entrainment in vertical two-phase churn flow? (in *International journal of multiphase flow* **30** (1): 89-103.

Baker, Ovid. 1953. Design of Pipelines for the Simultaneous Flow of Oil and Gas. Proc.

Barbosa Jr, J. R., G. F. Hewitt, G. König, S. M. Richardson. 2002. Liquid entrainment, droplet concentration and pressure gradient at the onset of annular flow in a vertical pipe (in *International Journal of Multiphase Flow* **28** (6): 943-961. http://www.sciencedirect.com/science/article/pii/S0301932202000034.

Beggs, Dale H, James P Brill. 1973. A study of two-phase flow in inclined pipes (in *Journal of Petroleum technology* **25** (05): 607-617.

Beggs, Howard Dale. 1991. *Production Optimization: using NODAL analysis*, OGCI publications (Reprint).

Bendiksen, Kjell H, Dag Maines, Randi Moe, Sven Nuland. 1991. The dynamic two-fluid model OLGA: Theory and application (in *SPE production engineering* **6** (02): 171-180.

Berna, C, A Escrivá, JL Muñoz-Cobo, LE Herranz. 2014. Review of droplet entrainment in annular flow: Interfacial waves and onset of entrainment (in *Progress in Nuclear Energy* **74**: 14-43.

Bin, Hu, Michael Golan. 2003. Gas-lift Instability Resulted Production Loss and Its Remedy by Feedback Control: Dynamical Simulation Results. Proc.

Brauner, Neima, Dvora Barnea. 1986. Slug/churn transition in upward gas-liquid flow (in *Chemical engineering science* **41** (1): 159-163.

Brennen, Christopher E. 2005. *Fundamentals of multiphase flow*, Cambridge University Press (Reprint).

Brill, J.P., H.K. Mukherjee. 1999. *Multiphase Flow in Wells*, Henry L. Doherty Memorial Fund of AIME, Society of Petroleum Engineers Incorporated (Reprint). http://books.google.com/books?id=oo4KAQAAMAAJ.

Choi, Jinho, Eduardo Pereyra, Cem Sarica, Hoyoung Lee, Il Sik Jang, JooMyoung Kang. 2013. Development of a fast transient simulator for gas–liquid two-phase flow in pipes (in *Journal of Petroleum Science and Engineering* **102**: 27-35.

Clegg, Joe Dunn. 1988. High-rate artificial lift (in *Journal of petroleum technology* **40** (03): 277-282.

Dalsmo, M., E. Halvorsen, O. Slupphaug. 2002. Active Feedback Control of Unstable Wells at the Brage Field. Proc.

de Cachard, F., Delhaye, J.M., 1996, A slug-churn flow model for small-diameter airlift pumps. Int. J. Multiphase Flow 22(4), 627-649.

Duns, H., Jr., N. C. J. Ros. 1963. Vertical flow of gas and liquid mixtures in wells. Proc.
Economides, M.J., A.D. Hill, C. Ehlig-Economides. 1994. *Petroleum Production Systems*, PTR Prentice Hall (Reprint). http://books.google.com/books?id=UrVTAAAAMAAJ.

Eikrem, Gisle O, Ole M Aamo, Bjarne A Foss. 2008. On instability in gas lift wells and schemes for stabilization by automatic control (in *SPE Production & Operations* **23** (02): 268-279.

Elperin, T, M Klochko. 2002. Flow regime identification in a two-phase flow using wavelet transform (in *Experiments in fluids* **32** (6): 674-682.

Fairuzov, YV, I Guerrero-Sarabia, C Calva-Morales, R Carmona-Diaz, T Cervantes-Baza, N Miguel-Hernandez, A Rojas-Figueroa. Stability maps for continuous gas-lift wells: a new approach to solving an old problem. Society of Petroleum Engineers.

Fernandez, Juan J, Gioia Falcone, Catalin Teodoriu. 2010. Design of a High-Pressure Research Flow Loop for the Experimental Investigation of Liquid Loading in Gas Wells (in *SPE Projects Facilities & Construction* **5** (02): 76-88.

Fukano, T., A. Ousaka. 1989. Prediction of the circumferential distribution of film thickness in horizontal and near-horizontal gas-liquid annular flows (in *International Journal of Multiphase Flow* **15** (3): 403-419. http://www.sciencedirect.com/science/article/pii/0301932289900104.

Fukuda, K, T Kobori. Two-phase flow instability in parallel channels.

Govan, A. H., G. F. Hewitt, H. J. Richter, A. Scott. 1991. Flooding and churn flow in vertical pipes (in *International Journal of Multiphase Flow* **17** (1): 27-44. http://www.sciencedirect.com/science/article/pii/030193229190068E.

Gray, HE. 1974. Vertical flow correlation in gas wells (in *User manual for API14B, Subsurface Controlled Safety Valve Sizing Computer Program*.

Hagedorn, Alton R., Kermit E. Brown. 1965. Experimental Study of Pressure Gradients Occurring During Continuous Two-Phase Flow in Small-Diameter Vertical Conduits (in **17**.

Han, Huawei, Zhenfeng Zhu, Kamiel Gabriel. 2006. A study on the effect of gas flow rate on the wave characteristics in two-phase gas–liquid annular flow (in *Nuclear engineering and design* **236** (24): 2580-2588.

Hazuku, Tatsuya, Tomoji Takamasa, Yoichiro Matsumoto. 2008. Experimental study on axial development of liquid film in vertical upward annular two-phase flow (in *International Journal of Multiphase Flow* **34** (2): 111-127. http://www.sciencedirect.com/science/article/pii/S0301932207001565.

Hewitt, Geoffrey Frederick, DN Roberts. 1969. Studies of two-phase flow patterns by simultaneous X-ray and flash photography, DTIC Document.

Holowach, MJ, LE Hochreiter, FB Cheung. 2002. A model for droplet entrainment in heated annular flow (in *International journal of heat and fluid flow* **23** (6): 807-822.

Hu, Bin. 2005. Characterization of gas-lift instabilities .

Hu, Bin, Cornelis A. M. Veeken, Rahel Yusuf, Havard Holmas. 2010. Use of Wellbore-Reservoir Coupled Dynamic Simulation to Evaluate the Cycling Capability of Liquid-Loaded Gas Wells. Proc.

Jahanshahi, Esmaeel, karim salahshoor, Riyaz Kharrat, Hamid Rahnema. 2008. Modeling and Simulation of Instabilities in Gas-lifted Oil Wells. Proc.

Jayanti, S, GF Hewitt. 1992. Prediction of the slug-to-churn flow transition in vertical two-phase flow (in *International Journal of Multiphase Flow* **18** (6): 847-860.

Kaji, R., B. J. Azzopardi, D. Lucas. 2009. Investigation of flow development of co-current gas–liquid vertical slug flow (in *International Journal of Multiphase Flow* **35** (4): 335-348. http://www.sciencedirect.com/science/article/pii/S0301932209000081.

Kakac, Sadik. 2009. Investigation of two-phase flow dynamic instabilities in vertical and horizontal in-tube boiling systems (in *ICHMT DIGITAL LIBRARY ONLINE*.

Lea, James F, Henry V Nickens, Mike Wells. 2011. *Gas well deliquification*, Gulf Professional Publishing (Reprint).

Lozada, Miguel Angel, Eduardo Poblano, Ivan Guerrero, Yuri V. Fairuzov. 2011. Flow Instabilities in Gas-Lift Wells with Water Coning. Proc.

Lumban-Gaol, Ardhi, Peter P. Valkó. 2014. Liquid holdup correlation for conditions affected by partial flow reversal (in *International Journal of Multiphase Flow* (0). http://www.sciencedirect.com/science/article/pii/S0301932214001621.

March-Leuba, J. 1992. Density-wave instabilities in boiling water reactors, Nuclear Regulatory Commission, Washington, DC (United States). Div. of Systems Technology.

Kaasa, Glenn-Ole, Vidar Alstad, Jing Zhou, and Ole Morten Aamo. "Nonlinear model-based control of unstable wells." *Modeling, Identification and Control* 28, no. 3 (2007): 69-79.

Minami, Kazuioshi, Ovadia Shoham. 1995. Pigging dynamics in two-phase flow pipelines: experiment and modeling (in *SPE production & Facilities* **10** (04): 225-232.

NI, Kolev. 2007. *Multiphase Flow Dynamics, Vol. 2 Thermal and mechanical interactions*, Springer, Berlin, New York, Tokyo (Reprint).

Nosseir, MA, TA Darwich, MH Sayyouh, M El Sallaly. 2000. A new approach for accurate prediction of loading in gas wells under different flowing conditions (in *SPE Production & Facilities* **15** (04): 241-246.

Okawa, Tomio, Taisuke Goto, Yosuke Yamagoe. 2010. Liquid film behavior in annular two-phase flow under flow oscillation conditions (in *International Journal of Heat and Mass Transfer* **53** (5–6): 962-971. http://www.sciencedirect.com/science/article/pii/S0017931009006243.

Okawa, Tomio, Tsuyoshi Kitahara, Kenji Yoshida, Tadayoshi Matsumoto, Isao Kataoka. 2002. New entrainment rate correlation in annular two-phase flow applicable to wide range of flow condition (in *International Journal of Heat and Mass Transfer* **45** (1): 87-98.

Papini, Davide, Antonio Cammi, Marco Colombo, Marco E Ricotti. 2011. On Density Wave Instability Phenomena–Modelling and Experimental Investigation (in *Two Phase Flow, Phase Change and Numerical Modeling*: 257-284.

Pierre, Benjamin. 2010. Pressure waves in pipelines and impulse pumping: physical principles, model development and numerical simulation (in.

Pickering, P. F., G. F. Hewitt, M. J. Watson, and C. P. Hale. "The prediction of flows in production risers-truth & myth." In *IIR Conference*, vol. 10. 2001

Prayitno, Sigit, R. A. Santoso, Deendarlianto, Thomas Höhne, Dirk Lucas. 2012. Counter Current Flow Limitation of Gas-Liquid Two-Phase Flow in Nearly Horizontal Pipe (in *Science and Technology of Nuclear Installations* **2012**: 9. 513809. http://dx.doi.org/10.1155/2012/513809.

Sagen, Jan, Monica Ostenstad, Bin Hu, Kjell Eirik Irgens Henanger, Siv Kari Lien, Zheng-gang Xu, Steinar Groland, Terje Sira. A Dynamic Model for Simulation of Integrated Reservoir Well and Pipeline System. Society of Petroleum Engineers.

Schoppa, Wade, George J Zabaras, Raghu Menon, Moye Wicks. Gaps and Advancements for Deepwater Production and Remote Processing: Large Diameter Riser Laboratory Gas-Lift Tests. Offshore Technology Conference.

Seim, J. E., V. L. van Beusekom, R. A. W. M. Henkes, O. J. Nydal. 2011. Experiments and Modelling for the Control of Riser Instabilities with Gas Lift. Proc.

Sekoguchi, K, M Takeishi, T Ishimatsu. 1985. Interfacial structure in vertical upward annular flow (in *PhysicoChemical Hydrodynamics* **6** (1/2): 239-255.

Shoham, Ovadia. 2006. *Mechanistic modeling of gas-liquid two-phase flow in pipes*, Richardson, TX: Society of Petroleum Engineers (Reprint).

Silva, Luciana Loureiro, Jos Luiz Arias Vidal, Paulo Correia Monteiro, Theodoro Antonum Netto. 2013. Study of Slugs Control Techniques in Pipeline Systems (in *OTC Brasil*.

Taitel, Yehuda, Dvora Bornea, AE Dukler. 1980. Modelling flow pattern transitions for steady upward gas-liquid flow in vertical tubes (in *AIChE Journal* **26** (3): 345-354.

Taitel, Yemada, AE Dukler. 1976. A model for predicting flow regime transitions in horizontal and near horizontal gas-liquid flow (in *AIChE Journal* **22** (1): 47-55.

Thais McComb, Brian F. Towler. 2013. How to Tackle the Challenge of Mature Field Development (in **9**: 18-20. http://www.spe.org/twa/print/archives/2013/2013v9n3/11_TechLeaders_v9n3_FINAL.pdf.

Torre, AJ, Z Schmidt, RN Blais, DR Doty, JP Brill. 1987. Casing heading in flowing oil wells (in *SPE Production Engineering* **2** (04): 297-304.

Turner, RG, MG Hubbard, AE Dukler. 1969. Analysis and prediction of minimum flow rate for the continuous removal of liquids from gas wells (in *Journal of Petroleum Technology* **21** (11): 1475-1482.

Van't Westende, Jozef Marinus Cyril. 2008. Droplets in annular-dispersed gas-liquid pipe-flows (in.

Vijayan, M., S. Jayanti, A. R. Balakrishnan. 2001. Effect of tube diameter on flooding (in *International Journal of Multiphase Flow* **27** (5): 797-816. http://www.sciencedirect.com/science/article/pii/S0301932200000458.

Wallis, Graham B, John E Dodson. 1973. The onset of slugging in horizontal stratified air-water flow (in *International Journal of Multiphase Flow* **1** (1): 173-193.

Waltrich, Paulo. 2012. *Onset and Subsequent Transient Phenomena of Liquid Loading in Gas Wells: Experimental Investigation Using a Large Scale Flow Loop*, Texas A&M University (Reprint).

Waltrich, Paulo J, Gioia Falcone, Jader R Barbosa Jr. 2013. Axial development of annular, churn and slug flows in a long vertical tube (in *International Journal of Multiphase Flow* **57**: 38-48.

Wang, Ke, Bofeng Bai, Jiahuan Cui, Weimin Ma. 2012. A physical model for huge wave movement in gas–liquid churn flow (in *Chemical Engineering Science* **79** (0): 19-28. http://www.sciencedirect.com/science/article/pii/S0009250912002850.

Wang, Ke, Bofeng Bai, Weimin Ma. 2013a. Huge wave and drop entrainment mechanism in gas–liquid churn flow (in *Chemical Engineering Science* **104** (0): 638-646. http://www.sciencedirect.com/science/article/pii/S0009250913006350.

Wang, Ke, Bofeng Bai, Weimin Ma. 2013b. A model for droplet entrainment in churn flow (in *Chemical Engineering Science* **104** (0): 1045-1055. http://www.sciencedirect.com/science/article/pii/S000925091300715X.

Weisman, J. 1983. Two-phase flow patterns (in *Handbook of fluids in motion*: 409-425.

Xu, ZG, M Golan. 1989. Criteria for operation stability of gas-lift wells (in.

Yüncü, H, S Kakaç. 1988. Fundamentals of two-phase flow instabilities. In *Two-Phase Flow Heat Exchangers*, 375-406. Springer.

Zabaras, G, AE Dukler, D Moalem-Maron. 1986. Vertical upward cocurrent gas-liquid annular flow (in *AIChE journal* **32** (5): 829-843.

Zuber, Novak, JAa Findlay. 1965. Average volumetric concentration in two-phase flow systems (in *Journal of Heat Transfer* **87** (4): 453-468.

VITA

Catalina Posada was born in Los Angeles, California January 1986. She obtained her Bachelor of Science in Chemical Engineering from the University of Los Andes, Colombia in 2010. She was accepted to be part of the graduated school at Louisiana State University where she is pursuing her Masters of Science degree in Petroleum Engineering. Her research interest includes multiphase flow in pipes, artificial lift systems, and production optimization.